

UNIVERSITÀ DEGLI STUDI DI NAPOLI

FEDERICO II



PHD IN CHEMICAL SCIENCES

XXVII Cycle (2012-2015)

**G-quadruplexes: design, synthesis and
characterization of new modified ODNs
and natural ligands**

Valeria Romanucci

Tutor

Prof. Giovanni Di Fabio

Index

Publications.....	<i>ii</i>
Long abstract.....	<i>vii</i>
CHAPTER 1.....	1
Biological interest of non canonical DNA structures:	
"G-quadruplexes"	1
1.1 General introduction on the G-quadruplexes.....	1
1.2 Topologies of G-quadruplex structures.....	4
1.2.1 Grooves and metal ion coordination.....	6
1.3 Quadruplexes in telomeres or quadruplexes everywhere?	8
1.3.1 G-Quadruplex-binding ligands as anticancer drug	11
1.4 G-quadruplexes: new class of aptamers.....	14
1.5 G-quadruplexes against HIV infection	16
1.6 Aim of research work	20
References	25
CHAPTER 2.....	34
Discovery of novel anti-HIV active G-quadruplex-forming	
oligonucleotides.....	34
2.1. Synthesis, biophysical characterization and anti-HIV activity	
of d(TGGGAG) Quadruplexes bearing hydrophobic tails at the 5'-	
end	36
2.1.2 Experimental Session	46
2.2 Hairpin oligonucleotides forming G-quadruplexes: New	
aptamers with anti-HIV activity.....	56
2.2.1 Experimental Session	66
2.3 General Conclusions and Perspective.....	69
References	72

CHAPTER 3	76
Improvement of Solid Phase Synthetic Approach	76
3.1 Aim of research work	76
3.2 Results and Discussion	78
3.3 Conclusions and Perspective	82
3.4 Experimental Session	83
References	89
CHAPTER 4	92
Kinetic study of G-quadruplex formation by ESI-MS	92
4.1 ESI-MS to detect nucleic acids	94
4.2 Aim of research work	96
4.3 Results and Discussion	98
4.3.1 Native PolyAcrilamide Gel Electrophoresis	103
4.3.2 Ion Mobility Spectrometry for the detection of high order structures.....	104
4.4 Conclusions and Prespective	106
4.5 Experiment Session	107
References	110
CHAPTER 5	114
Silibinin: biomolecule as potential G-quadruplex-ligand	114
5.1 Aim of research work	118
5.2 A rapid and simple chromatographic separation of diastereomers of silibinin and their oxidation to produce 2,3- dehydrosilybin enantiomers in an optically pure form.	120
5.2.1 Experimental Session	123
5.3 Microwave-assisted oxidation of Silibinin: a simple and preparative method for the synthesis of improved radical scavengers	128
5.3.1 Experimental Session	133

5.4 Conclusions and Prespective	134
5.5 New silibinin analogues with improved bioavailability	135
5.5.1 Synthesis of new silybins and evaluation of their antioxidant properties	136
5.5.1.1 Experimental Session	139
5.5.2 New silibinin scaffold for chemical diversification: synthesis of novel 9"-silibinin conjugates	148
5.5.2.2 Experimental Session	150
5.5.3 New silibinin glyco-conjugates: Synthesis and evaluation of antioxidant properties.....	154
5.5.3.1 Experimental Session	157
5.5.4 General Conclusions	159
References	162

Abbreviations

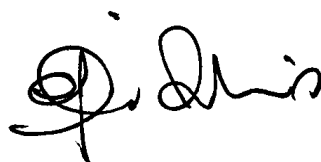
Preface

PhD project of Dr. Valeria Romanucci concerned the synthesis, purification and structural characterization of several biomolecules, such as DNA aptamers (anti-HIV) based on G-quadruplex structures and modified flavonolignans as potential G-quadruplex-ligands. In her project, Valeria mainly applied the classic organic synthesis techniques to obtain new biomolecules in good yields. The purification and structural characterization were followed by some HPLC and spectroscopic techniques (UV, CD and NMR), respectively. The thermodynamic and kinetic studies as well as biological assays were done in collaboration with different European research groups. In particular the thermodynamic studies were done in collaboration with Dr. *Danilo Milardi* of the Institute of Biostructures and Bioimage, UOS-CNR, Catania (Italy). Biological assays were conducted in collaboration with different research groups: Prof. *Jan Balzarini* of Rega Institute for Medical Research, Catholic University of Leuven (Belgium); Prof. *Carmela Loguercio* of the Department of Clinical and Experimental Medicine, Second University of Naples, (Italy).

During her third year, she started a new abroad collaboration with Dr. *Valérie Gabelica* (U869 ARNA - Inserm/Univ. Bordeaux), in order to explore the kinetic aspects of G-quadruplex-forming oligonucleotides endowed with strong anti-HIV activity using ESI-MS technique.

Tutor

Dr. *Giovanni Di Fabio*



Overall results will be discussed in the forthcoming chapters, and have been published in the papers listed below:

- 1 Armando Zarrelli, **Valeria Romanucci**, Marina Della Greca, Lorenzo De Napoli, Lucio Previtiera and Giovanni Di Fabio. “New Silybin Scaffold for Chemical Diversification: Synthesis of Novel 23-Phosphodiester Silybin Conjugates” *Synlett* 24, no. 01 (December 04, **2013**): 45–48, doi:10.1055/s-0032-1317688.

Abstract: Silybin is the major component (ca. 30%) of the silymarin complex extracted from the seeds of *Silybum marianum*, with multiple biological activities operating at various cell levels. As an ongoing effort toward the exploitation of natural products as scaffolds for chemical diversification at readily accessible positions, we present here an efficient synthetic procedure to obtain new 23-phosphodiester silybin conjugates with different labels. A key point in our approach is the new 3,5,7,20-tetra-O-acetylsilybin-23-phosphoramidite, useful for a variety of derivatizations following a reliable and well-known chemistry. The feasibility of the procedure has been demonstrated by preparing new 23-silybin conjugates, exploiting standard phosphoramidite chemistry.

- 2 Giovanni Di Fabio, **Valeria Romanucci**, Cinzia Di Marino, Lorenzo De Napoli and Armando Zarrelli. “A Rapid and Simple Chromatographic Separation of Diastereomers of Silibinin and Their Oxidation to Produce 2,3-Dehydrosilybin Enantiomers in an Optically Pure Form” *Planta Medica* 79, no. 12 (August **2013**): 1077–80, doi:10.1055/s-0032-1328703.

Abstract: Silybin A and B were separated from commercial silibinin using the preparative HPLC method. The described method is rapid and effective in obtaining gram-scale amounts of two diastereoisomers with minimal effort. In our approach, silibinin was dissolved in THF (solubility greater than 100mg/mL), an alternative solvent to H₂O or MeOH in which silibinin has a very low solubility (ca 0.05–1.5mg/mL), and then separated into its two components using preparative RP-HPLC. By starting with purified diastereoisomers, it was possible to obtain the two enantiomers of 2,3-dehydrosilybin in good yields and optically pure using an efficient oxidation procedure. All of the purified products were fully characterised using NMR (1H, 13C), CD, [α]_D, and ESI-MS analyses. The purities of the products, which were evaluated using analytical HPLC, were greater than 98% in all cases.

- 3 Giovanni Di Fabio, **Valeria Romanucci**, Mauro De Nisco, Silvana Pedatella, Cinzia Di Marino and Armando Zarrelli. "Microwave-Assisted Oxidation of Silibinin: A Simple and Preparative Method for the Synthesis of Improved Radical Scavengers" *Tetrahedron Letters* 54, no. 46 (November 2013): 6279–82, doi:10.1016/j.tetlet.2013.09.035.

Abstract: A new and preparative oxidation of silibinin has been developed to give access to two different silibinin derivatives known for their enhanced antioxidant properties. Conventional heating methods were compared with results obtained from microwave (MW) heating. The base-catalysed oxidation of silibinin under MW heating is a very efficient method for the preparation of 2,3-dehydrosilybin and a related silybin rearrangement product. This latter compound shows enhanced radical scavenging properties. Optimised conditions were used to prepare 2,3-dehydrosilybins A and B from optically pure silybins A and B. An efficient, preparative purification method was also developed to enable isolation of different products in high purity.

- 4 **Valeria Romanucci**, Armando Zarrelli, Lorenzo De Napoli, Cinzia Di Marino, and Giovanni Di Fabio. "Synthesis of Oligonucleotide Conjugates and Phosphorylated Nucleotide Analogues: An Improvement to a Solid Phase Synthetic Approach" *Journal of Chemistry*, 2013, doi:10.1155/2013/469470.

Abstract: An improvement to our solid phase strategy to generate pharmacologically interesting molecule libraries is proposed here. The synthesis of new σ -chlorophenol-functionalised solid supports with very high loading (0.18–0.22meq/g for control pore glass (CPG) and 0.25–0.50meq/g for TG) is reported. To test the efficiency of these supports, we prepared nucleotide and oligonucleotide models, and their coupling yields and the purity of the crude detached materials were comparable to previously available results. These supports allow the facile and high yield preparation of highly pure phosphodiester and phosphoramidate monoester nucleosides, conjugated oligonucleotides, and other yet unexplored classes of phosphodiester and phosphoramidate molecules.

- 5 Maria Gaglione, Nicoletta Potenza, Giovanni Di Fabio, **Valeria Romanucci**, Nicola Mosca, Aniello Russo, Ettore Novellino, Sandro Cosconati and Anna Messere. "Tuning RNA Interference by Enhancing siRNA/PAZ Recognition" *ACS Medicinal Chemistry Letters* 4, no. 1 (January 10, 2013): 75–78, doi:10.1021/ml300284b.

Abstract: Chemically modified siRNAs were synthesized to enhance siRNA/PAZ interactions. These modifications allowed obtaining siRNAs endowed with high silencing potential, long persistence and better serum resistance. Theoretical data allowed correlating the observed siRNAs interfering performance with the peculiar interactions with PAZ.

- 6 **Valeria Romanucci**, Danilo Milardi, Tiziana Campagna, Maria Gaglione, Anna Messere, Alessandro D'Urso, Emanuela Crisafi, Carmelo La Rosa, Armando Zarrelli, Jan Balzarini and Giovanni Di Fabio. "Synthesis, Biophysical Characterization and Anti-HIV Activity of d(TG₃AG) Quadruplexes Bearing Hydrophobic Tails at the 5'-End" *Bioorganic & Medicinal Chemistry* 22, no. 3 (February 01, 2014): 960–66, doi:10.1016/j.bmc.2013.12.051.

Abstract: Novel conjugated G-quadruplex-forming d(TG₃AG) oligonucleotides, linked to hydrophobic groups through phosphodiester bonds at 5'-end, have been synthesized as potential anti-HIV aptamers, via a fully automated, online phosphoramidite-based solid-phase strategy. Conjugated quadruplexes showed pronounced anti-HIV activity with some preference for HIV-1, with inhibitory activity invariably in the low micromolar range. The CD and DSC monitored thermal denaturation studies on the resulting quadruplexes, indicated the insertion of lipophilic residue at the 5'-end, conferring always improved stability to the quadruplex complex (20 ΔT_m <math>< 40^\circ\text{C}</math>). The data suggest no direct functional relationship between the thermal stability and anti-HIV activity of the folded conjugated G-quartets. It would appear that the nature of the residue at 5' end of the d(TG₃AG) quadruplexes plays an important role in the thermodynamic stabilization but a minor influence on the anti-HIV activity. Moreover, a detailed CD and DSC analyses indicate a monophasic behaviour for sequences **I** and **V**, while for ODNs (**II–IV**) clearly show that these quadruplex structures deviate from simple two-state melting, supporting the hypothesis that inter- mediate states along the dissociation pathway may exist.

- 7 Armando Zarrelli, **Valeria Romanucci**, Concetta Tuccillo, Alessandro Federico, Carmela Loguercio, Raffaele Gravante and Giovanni Di Fabio. "New Silibinin Glyco-Conjugates: Synthesis and Evaluation of Antioxidant Properties" *Bioorganic & Medicinal Chemistry Letters* 24, no. 22 (2014): 5147–49, doi:10.1016/j.bmcl.2014.10.023.

Abstract: New silibinin glyco-conjugates have been synthesized by efficient method and in short time. Exploiting our solution phase strategy, several structurally diverse silibinin glyco-conjugates (gluco, manno,

galacto, and lacto-) were successfully realized in very good yields and in short time. In preliminary study to evaluate their antioxidant and neuroprotective activities new derivatives were subjected to DPPH free radical scavenging assay and the Xanthine oxidase (XO) inhibition models assay. Irrespective of the sugar moiety examined, new glyco-conjugates are more than 50 times water-soluble of silibinin. In the other hand they exhibit a radical scavenging activities slightly higher than to silibinin and XO inhibition at least as silibinin.

- 8 Armando Zarrelli, **Valeria Romanucci**, Lorenzo De Napoli, Lucio Previtiera and Giovanni Di Fabio. "Synthesis of New Silybin Derivatives and Evaluation of Their Antioxidant Properties" *Helvetica Chimica Acta* 98 (2015): 399–409, doi:10.1002/hlca.201400282.

Abstract: Silibinin, the major flavonolignan of silymarin, displays a broad spectrum of biological features that are generally ascribed to its antioxidant properties. Silibinin occurs in two diastereoisomeric forms, i.e., silybins A and B, in a ratio of ca. 1:1. With a simple and robust purification method, it is now possible to obtain silybins A and B in pure forms, in g-scale amounts, and within a short period of time. Herein, we describe an efficient synthesis strategy to obtain a variety of new and more H₂O-soluble derivatives from the single silybins in which the 9"-OH group was converted to a sulfate, N₃, phosphodiester, or NH₂ group via a solution-phase approach. Thus, eight new compounds have been synthesized, purified by HPLC analysis, and characterized by NMR and MS analyses. To conduct experiments to clarify the many biological properties of pure silibinin diastereoisomers and their derivatives, the synthetic compounds were tested by using the DPPH assay to evaluate their antioxidant activities. The results, even if only for a small number of derivatives, revealed that some of these compounds are much more active than their parent compounds. It is also interesting to consider the synergetic effects.

- 9 **Valeria Romanucci**, Maria Gaglione, Anna Messere, Nicoletta Potenza, Armando Zarrelli, Sam Noppen, Sandra Liekens, Jan Balzarini and Giovanni Di Fabio "Hairpin Oligonucleotides Forming G-Quadruplexes: New Aptamers with Anti-HIV Activity" *European Journal of Medicinal Chemistry* 99 (2015): 51–58, doi:10.1016/j.ejmech.2014.10.030.

Abstract: We describe the facile syntheses of new modified oligonucleotides based on d(TG₃AG) that form bimolecular G-quadruplexes and possess a HEG loop as an inversion of polarity site 3'-3' or 5'-5' and aromatic residues conjugated to the 5'-end through

phosphodiester bonds. The conjugated hairpin G-quadruplexes exhibited parallel orientation, high thermal stability, elevated resistance in human serum and high or moderate anti-HIV-1 activity with low cytotoxicity. Further, these molecules showed significant binding to HIV envelope glycoproteins gp120, gp41 and HSA, as revealed by SPR assays. As a result, these conjugated hairpins represent the first active anti-HIV-1 bimolecular G-quadruplexes based on the d(TG₃AG) sequence.

During the three years of PhD, Valeria is committed on issues concerning the isolation and characterization of natural products. The list of the papers published in this field, which will not be discussed in the forthcoming chapters of the thesis, is reported below:

1. Giovanni Di Fabio, **Valeria Romanucci**, Mauro Zarrelli, Michele Giordano and Armando Zarrelli, “C-4 Gem-Dimethylated Oleanes of *Gymnema Sylvestre* and Their Pharmacological Activities” *Molecules*, **2013**, doi:10.3390/molecules181214892.
2. Giovanni Di Fabio, **Valeria Romanucci**, Anna De Marco and Armando Zarrelli “Triterpenoids from *Gymnema Sylvestre* and Their Pharmacological Activities” *Molecules (Basel, Switzerland)* 19, no. 8 (2014): 10956–81, doi:10.3390/molecules190810956.
3. Armando Zarrelli, **Valeria Romanucci**, Raffaele Gravante, Cinzia Di Marino and Giovanni Di Fabio “History of Gymnemic Acid, a Molecule That Does Not Exist” *Natural Product Communications* 9, no. 10 (October 2014): 1429–32, <http://www.ncbi.nlm.nih.gov/pubmed/25522530>.
4. Giovanni Di Fabio, **Valeria Romanucci**, Cinzia Di Marino, Antonio Pisanti and Armando Zarrelli “*Gymnema Sylvestre* R. Br., an Indian Medicinal Herb: Traditional Uses, Chemical Composition, and Biological Activity” *Current Pharmaceutical Biotechnology* 16, no. 6 (2015).

Long Abstract

DNA G-quadruplexes are very appealing structures for their variety of pharmacological applications. G-quadruplex structures are involved as targets in antitumour therapies¹ and as scaffolds of oligonucleotides (ONs) able to specifically inhibit proteins (aptamers). In the last 30 years, there has been growing interest in the potentiality of G-quadruplexes as novel aptamers².

In '90s, Hotoda et al. identified a variety of tetramolecular G-quadruplexes based on the sequence d(TGGGAG), targeting the glycoprotein of HIV-1, gp120^{3,4}. This sequence d(TGGGAG), showed a high anti-HIV-1 activity only with conjugated with an aromatic group at the 5'-end. Structure-activity relationship analysis on Hotoda modified sequences, indicated that G-quadruplex formation, as well as the presence of large aromatic groups at the 5'-end, were both essential for the antiviral activity^{5,6}. In 2011 Di Fabio et al. reported the synthesis and characterization of a new mini-library of d(TGGGAG) ODNs carrying aryl groups at the 5'-end⁷. The results obtained, showed that all 5'-end-modified sequences formed G-quadruplexes with strongly increased thermal stability and are endowed with high anti-HIV activity. As is it known both thermodynamic and kinetic aspects are relevant into G-quadruplex folding, so it is necessary to explore both of them to get a more complete picture of structure-activity relationship⁸.

In my PhD project, we focused our attention on the synthesis and biophysically and biologically characterization of a new mini-library of d(TGGGAG) oligomers as potential anti-HIV⁹. In addition, in order to have more information on the G-quadruplex folding depending on the modifications at 5'-end of d(TGGGAG), we are started kinetic

studies of G-quadruplex formation by ESI-MS with the precious collaboration of *Valérie Gabelica*, Research Director in Inserm/Univ. Bordeaux, (France), pioneer of the study of non-covalent DNA complexes by ESI-MS^{10–12}. In the first part of my PhD project, we developed an efficient procedure to synthesize a new mini-library of d(TGGGAG) oligomers carrying hydrophobic and aromatic groups at the 5'-end by a phosphodiester bond (*Fig. 1*). The choice of conjugated groups aim to improve cellular uptake, to extend the half-life of these molecules in plasma and especially to stabilize DNA structures by hydrophobic interactions.

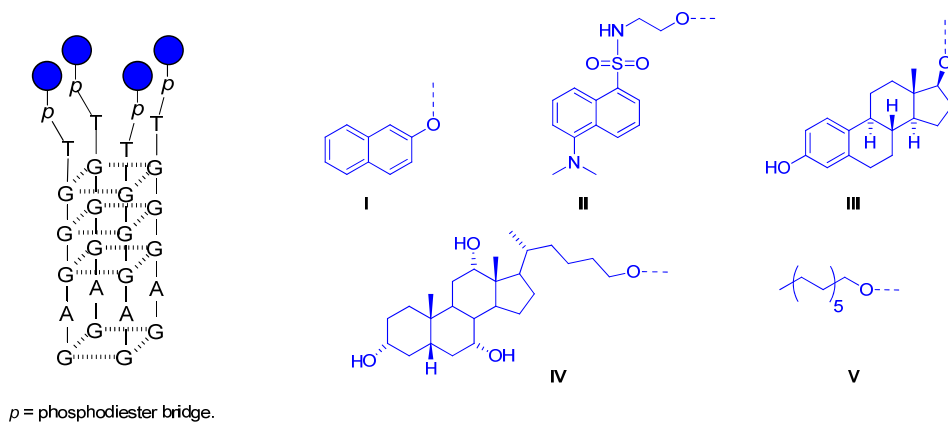


Figure 1

CD analysis was undertaken on oligomers **I–V** in comparison with the corresponding unmodified d(TGGGAG). Thermal denaturation studies on the resulting G-quadruplexes, suggested that the insertion of lipophilic residue at the 5'-end, involves always, in stability enhancement of G-quadruplex complexes ($20 < \Delta T_m < 40^\circ\text{C}$).

Moreover, detailed CD and DSC analysis indicated a monophasic behaviour for sequences **I** and **V**, while **II–IV** deviated from simple two-state melting, supporting the hypothesis that intermediate states along the dissociation pathway may exist. All heating runs were fully

irreversible. Therefore, neither an extrapolation of the thermodynamic parameters ΔG and ΔS from the melting curves nor a deconvolution of the Cp curves by statistical mechanic methods were possible. Consequently, in these non-equilibrium conditions only the enthalpy change relative to the G-quadruplex dissociation process may be directly obtained¹³.

In the second part of PhD project, aiming to improve the kinetic of G-quadruplex formation using d(TGGGAG) as a lead sequence, and therefore to enhance the anti-HIV activity of these aptamers, we designed and synthesized, for the first time, bimolecular G-quadruplex based on d(TGGGAG) sequence containing a HEG loop as a 3'-3' or 5'-5' inversion of polarity site (*Fig 2*)¹⁴.

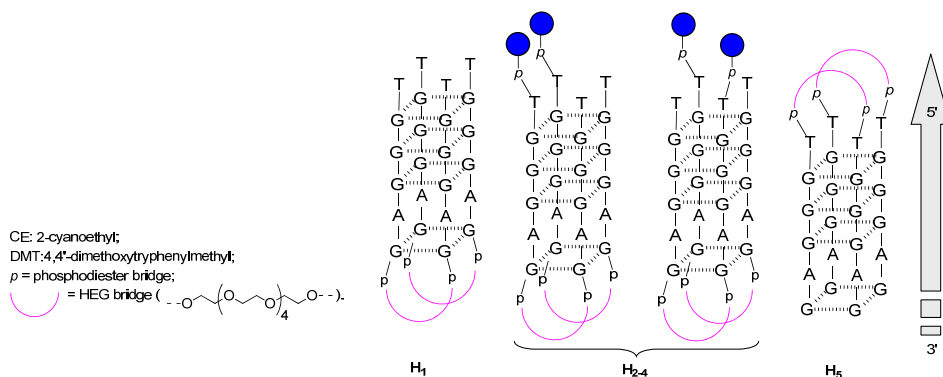


Figure 2

CD studies assessed that the introduction of a HEG loop, produces an improvement of the thermal stability of **H₁-H₅** ODNs compared to d(TGGGAG) tetramolecular G-quadruplexes and that this insertion has no effect on the original parallel folding of the G-quadruplex structure. This thermal stabilization was further increased, once more time, by introduction of different aromatic residues at the 5'-end of oligonucleotides **H₂₋₄**. Moreover, only compounds **H₂₋₄**, have proven

to exhibit significant anti-HIV activity in cell culture. Besides the moderate anti-HIV activity, the conjugated hairpin G-quadruplexes exhibited interesting properties in terms of slight cytotoxicity, favorable CC_{50}/EC_{50} (selectivity index) ratio and increased stability in human serum. Finally, the good affinity of the synthetic conjugated G-quadruplexes **H₂₋₄** for HSA is an interesting result due to the increased use of albumin as a versatile drug carrier in anti- HIV strategy.

In attempt to investigate if there is an influence of the end conjugated moiety on the kinetics of G4 formation and also to have more details about the G-quadruplex formed; ESI-MS studies are conducted on more active 5'-end modified ODNs in comparison with unmodified sequence d(TGGGAG). By ESI-MS experiments, it is possible to have information about the number of strands, and the cations inside each structure, moreover it is possible to detect all possible intermediate complexes (*Fig.3*) and to determine equilibrium binding constants of non-covalent complexes^{10,15}.

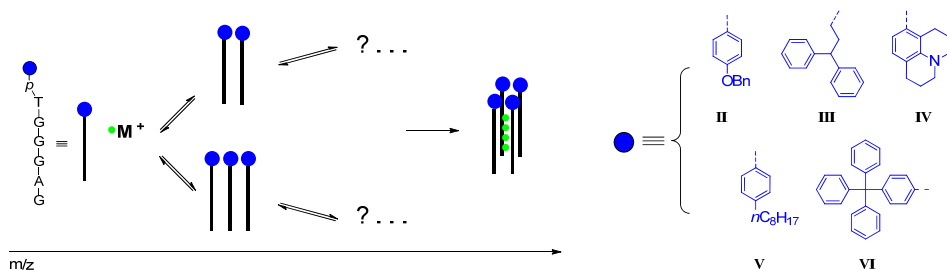


Figure 3

To study the kinetic of G-quadruplex formation, we recorded ESI-MS spectra as a function of the time after addition of cation in the ODN solutions, at room temperature. All modified sequences shown the same spectra profile, in terms of distribution of complexes and relative charge states. Overall data, reported a rapid conversion of the

single strand into dimer and trimer species, in agreement with the association pathways proposed by Stefl et al.¹⁶, then the tetramer begins to form quite quickly and continues to increase up to 14 days but more slowly. An unexpected result is the detection of an octameric specie, the formation of this begins simultaneously to tetramer, but their concentration remains, in all cases, lower than that of tetramer.

In over years, some G-rich DNA sequences, potentially G-quadruplex structures, are found at the chromosomal extremities (telomeres) and also in several important oncogenes^{17,18}. Last year, the research group of Prof. S. Balasubramanian, has published an interesting article, describing a method for the quantitative visualization of G-quadruplexes *in vivo*, direct evidence of their natural formation in the human genome¹⁹. Many antitumor strategies have been developed on the inhibition of telomerase activity (enzyme overexpressed in cancer cells), as consequence of decrease in length of telomeric DNA²⁰. In this frame, there is a huge interest against of a variety of small organic molecules, capable to induce the formation of G-quadruplex in G-rich sequences found in telomeres²¹.

The main important characteristics of ligands are an aromatic core that favours stacking interactions with the G-tetrads and basic side chains that interact with DNA grooves²². A class of molecules that displays these features are flavonoids.

Over the years, flavonoids has reported a variety of therapeutic activities against cancers, tumors, AIDS, etc²³⁻²⁵. Many examples of telomerase inhibitors within the family of flavonoids (silibinin, epigallocatechin gallate and apigenin) have been also reported^{26,27}.

In this frame, my PhD project is focused on the study of silibinin, a flavonolignan isolated from the fruits of the milk thistle *Silybum marianum*, as potential anti-telomerase drug. silibinin is the major flavonolignan found in silymarin, isolated from the fruits of the milk thistle *Silybum marianum*²⁸. Structurally silibinin is a diastereoisomeric mixture of two flavonolignans, namely silybin A and silybin B in a ratio of approximately 1:1, hardly separable (*Fig. 4*).

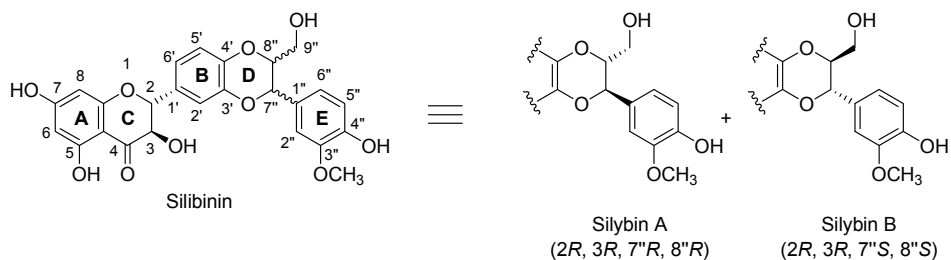


Figure 4

Recently, this metabolite has received attention due to its anticancer and chemopreventive actions^{29,30}, as well as hypocholesterolemic, cardioprotective, and neuroprotective activities³¹. In addition to the activity of silibinin, other constituents of silymarin such as isosilybin, silychristin and 2,3-dehydrosilybin, have been shown an attractive pharmacological properties. In particular, the oxidized form of silibinin, the 2,3- dehydrosilybin (DHS), displays major antioxidant and anticancer properties than silibinin suggesting that DHS may be useful therapeutically³².

In an effort to investigate the ability of silibinin and DHS to induce inter- and intramolecular G-quadruplex structures, the stereochemistry of these metabolites may play an extremely important role with interesting structural implications. For this reason we firstly, performed a new HPLC preparative method to

separate diastereoisomers of silibinin, with minimal effort and in a short time³³. Because of the low content of DHS in its natural state (silymarin extract), this compound was practically neglected in studies on the biological activity of silymarin. Therefore in order to obtain a large amount of DHS useful to test as therapeutics agent, a base-catalyzed oxidation of silybins A and B is carried out using microwave (MW). Moreover by starting with each diastereoisomer, silybin A and B, have been produced two enantiomers of DHS in an optically pure form; the use of microwaves has facilitated the reaction time (few minutes) and the yields³⁴.

While remaining within of chemistry of silininin, during my PhD, we also dealt with the low water solubility of silibinin that dramatically limits its pharmacological use. In this frame, in order to overcome these drawbacks, we developed a synthetic strategy to obtain new silibinin derivatives linking suitable chemical modifications able to improve its applications in biomedicine and biochemistry³⁵⁻³⁷.

References

- (1) Neidle, S. (2010) Human telomeric G-quadruplex: the current status of telomeric G-quadruplexes as therapeutic targets in human cancer. *The FEBS journal* 277, 1118–25.
- (2) Keefe, A. D., Pai, S., and Ellington, A. (2010) Aptamers as therapeutics. *Nature reviews. Drug discovery* 9, 537–50.
- (3) Koizumi, M., Koga, R., Hotoda, H., Momota, K., Ohmine, T., Furukawa, H., Agatsuma, T., Nishigaki, T., Abe, K., Kosaka, T., Tsutsumi, S., Sone, J., Kaneko, M., Kimura, S., and Shimada, K. (1997) Biologically active oligodeoxyribonucleotides-IX. Synthesis and anti-HIV-1 activity of hexadeoxyribonucleotides, TGGGAG, bearing 3'- and 5'-end-modification. *Bioorganic and Medicinal Chemistry* 5, 2235–2243.

- (4) Hotoda, H., Koizumi, M., Koga, R., Kaneko, M., Momota, K., and Ohmine, T. (1998) d (TGGGAG) Possesses Anti-Human Immunodeficiency Virus Type 1 Activity by Forming a G-Quadruplex Structure. *journal medicinal chemistry* 41, 3655–3663.
- (5) Furukawa, H., Momota, K., Agatsuma, T., Yamamoto, I., Kimura, S., and Shimada, K. (1997) Identification of a Phosphodiester Hexanucleotide That Inhibits HIV-1 Infection In Vitro on Covalent Linkage of Its 5'-End with a Dimethoxytrityl Residue. *Antisense and Nucleic Acid Drug Development* 7, 167–175.
- (6) Agatsuma, T., Abe, K., Furukawa, H., Koga, R., Koizumi, M., Hotoda, H., and Kaneko, M. (1997) Protection of hu-PBL-SCID/beige mice from HIV-1 infection by a 6-mer modified oligonucleotide, R-95288. *Antiviral Research* 34, 121–130.
- (7) Di Fabio, G., D'Onofrio, J., Chiapparelli, M., Hoorelbeke, B., Montesarchio, D., Balzarini, J., and De Napoli, L. (2011) Discovery of novel anti-HIV active G-quadruplex-forming oligonucleotides. *Chemical communications (Cambridge, England)* 47, 2363–2365.
- (8) Tran, P. L. T., De Cian, A., Gros, J., Moriyama, R., and Mergny, J.-L. (2013) Tetramolecular quadruplex stability and assembly. *Topics in current chemistry* 330, 243–73.
- (9) Romanucci, V., Milardi, D., Campagna, T., Gaglione, M., Messere, A., D'Urso, A., Crisafi, E., La Rosa, C., Zarrelli, A., Balzarini, J., and Di Fabio, G. (2014) Synthesis, biophysical characterization and anti-HIV activity of d(TG3AG) Quadruplexes bearing hydrophobic tails at the 5'-end. *Bioorganic & medicinal chemistry* 22, 960–6.
- (10) Rosu, F., Gabelica, V., Poncelet, H., and De Pauw, E. (2010) Tetramolecular G-quadruplex formation pathways studied by electrospray mass spectrometry. *Nucleic acids research* 38, 5217–25.
- (11) Ferreira, R., Marchand, A., and Gabelica, V. (2012) Mass spectrometry and ion mobility spectrometry of G-quadruplexes. A study of solvent effects on dimer formation and structural transitions in the telomeric DNA sequence d(TAGGGTTAGGGT). *Methods (San Diego, Calif.)* 57, 56–63.
- (12) Chemistry, P. (2014) *Nucleic Acids in the Gas Phase* (Gabelica, V., Ed.). Springer Berlin Heidelberg, Berlin, Heidelberg.
- (13) Pagano, B., Randazzo, A., Fotticchia, I., Novellino, E., Petraccone, L., and Giancola, C. (2013) Differential scanning calorimetry to investigate G-quadruplexes structural stability. *Methods (San Diego, Calif.)* 64, 43–51.
- (14) Romanucci, V., Gaglione, M., Messere, A., Potenza, N., Zarrelli, A., Noppen, S., Liekens, S., Balzarini, J., and Di Fabio, G. (2015) Hairpin oligonucleotides forming G-quadruplexes: New aptamers with anti-HIV activity. *European Journal of Medicinal Chemistry* 89, 51–58.
- (15) Marchand, A., Granzhan, A., Iida, K., Tsushima, Y., Ma, Y., Nagasawa, K., Teulade-Fichou, M.-P., and Gabelica, V. (2015) Ligand-Induced Conformational

Changes with Cation Ejection upon Binding to Human Telomeric DNA G-Quadruplexes. *Journal of the American Chemical Society* 137, 750–756.

(16) Stefl, R., Cheatham, T. E., Spacková, N., Fadrná, E., Berger, I., Koca, J., and Sponer, J. (2003) Formation pathways of a guanine-quadruplex DNA revealed by molecular dynamics and thermodynamic analysis of the substates. *Biophysical journal* 85, 1787–1804.

(17) Lipps, H. J., and Rhodes, D. (2009) G-quadruplex structures: in vivo evidence and function. *Trends in Cell Biology* 19, 414–422.

(18) Shankar, Hurley, L. H., and Neidle, S. (2011) Targeting G-quadruplexes in gene promoters: a novel anticancer strategy? *Nature reviews. Drug discovery* 10, 261–275.

(19) Biffi, G., Tannahill, D., McCafferty, J., and Balasubramanian, S. (2013) Quantitative visualization of DNA G-quadruplex structures in human cells. *Nature chemistry* 5, 182–6.

(20) Moorhouse, A. D., Haider, S., Gunaratnam, M., Munnur, D., Neidle, S., and Moses, J. E. (2008) Targeting telomerase and telomeres: a click chemistry approach towards highly selective G-quadruplex ligands. *Molecular bioSystems* 4, 629–42.

(21) Monchaud, D., and Teulade-Fichou, M.-P. (2008) A hitchhiker's guide to G-quadruplex ligands. *Organic & biomolecular chemistry* 6, 627–36.

(22) Murat, P., Singh, Y., and Defrancq, E. (2011) Methods for investigating G-quadruplex DNA/ligand interactions. *Chemical Society reviews* 40, 5293–307.

(23) Newman, D. J., and Cragg, G. M. (2012) Natural products as sources of new drugs over the 30 years from 1981 to 2010. *Journal of Natural Products* 75, 311–335.

(24) Chen, J. L.-Y., Sperry, J., Ip, N. Y., and Brimble, M. a. (2011) Natural products targeting telomere maintenance. *Medicinal Chemistry Communications* 2, 229.

(25) Ginnari-Satriani, L., Casagrande, V., Bianco, A., Ortaggi, G., and Franceschin, M. (2009) A hydrophilic three side-chained triazatruxene as a new strong and selective G-quadruplex ligand. *Organic & biomolecular chemistry* 7, 2513–6.

(26) Thelen, P., Wuttke, W., Jarry, H., Grzmił, M., and Ringert, R.-H. (2004) Inhibition of telomerase activity and secretion of prostate specific antigen by silibinin in prostate cancer cells. *The Journal of urology* 171, 1934–1938.

(27) Menichincheri, M., Ballinari, D., Bargiotti, A., Bonomini, L., Ceccarelli, W., D'Alessio, R., Fretta, A., Moll, J., Polucci, P., Soncini, C., Tibolla, M., Trosset, J. Y., and Vanotti, E. (2004) Catecholic flavonoids acting as telomerase inhibitors. *Journal of Medicinal Chemistry* 47, 6466–6475.

(28) Gazák, R., Walterová, D., and Kren, V. (2007) Silybin and silymarin—new and emerging applications in medicine. *Current medicinal chemistry* 14, 315–38.

- (29) Hogan, F. S., Krishnegowda, N. K., Mikhailova, M., and Kahlenberg, M. S. (2007) Flavonoid, silibinin, inhibits proliferation and promotes cell-cycle arrest of human colon cancer. *The Journal of surgical research* 143, 58–65.
- (30) Sharma, G., Singh, R. P., Chan, D. C., and Agarwal, R. (2003) Silibinin induces growth inhibition and apoptotic cell death in human lung carcinoma cells. *Anticancer research* 23, 2649–55.
- (31) Zhao, H., Brandt, G. E., Galam, L., Matts, R. L., and Blagg, B. S. J. (2011) Identification and initial SAR of silybin: an Hsp90 inhibitor. *Bioorganic & medicinal chemistry letters* 21, 2659–64.
- (32) Huber, A., Thongphasuk, P., Erben, G., Lehmann, W. D., Tuma, S., Stremmel, W., and Chamulitrat, W. (2008) Significantly greater antioxidant anticancer activities of 2,3-dehydrosilybin than silybin. *Biochimica et Biophysica Acta* 1780, 837–847.
- (33) Di Fabio, G., Romanucci, V., Di Marino, C., De Napoli, L., and Zarrelli, A. (2013) A rapid and simple chromatographic separation of diastereomers of silibinin and their oxidation to produce 2,3-dehydrosilybin enantiomers in an optically pure form. *Planta medica* 79, 1077–80.
- (34) Di Fabio, G., Romanucci, V., De Nisco, M., Pedatella, S., Di Marino, C., and Zarrelli, A. (2013) Microwave-assisted oxidation of silibinin: a simple and preparative method for the synthesis of improved radical scavengers. *Tetrahedron Letters* 54, 6279–6282.
- (35) Zarrelli, A., Romanucci, V., Greca, M., De Napoli, L., Previtera, L., and Di Fabio, G. (2013) New Silybin Scaffold for Chemical Diversification: Synthesis of Novel 23-Phosphodiester Silybin Conjugates. *Synlett* 24, 45–48.
- (36) Zarrelli, A., Romanucci, V., Tuccillo, C., Federico, A., Loguercio, C., Gravante, R., and Di Fabio, G. (2014) New silibinin glyco-conjugates: Synthesis and evaluation of antioxidant properties. *Bioorganic & Medicinal Chemistry Letters* 24, 5147–5149.
- (37) Zarrelli, A., Romanucci, V., De Napoli, L., Previtera, L., and Di Fabio, G. (2015) Synthesis of New Silybin Derivatives and Evaluation of Their Antioxidant Properties. *Helvetica Chimica Acta* 98, 399–409.

CHAPTER 1

Biological interest of non canonical DNA structures: "G-quadruplexes"

1.1 General introduction on the G-quadruplexes

A few years ago, Alexander Rich wrote: ‘DNA comes in many forms’¹. Since many years we have learned that Nucleic Acids are highly flexible molecules that can adopt a wide range of structures in addition to the major double-helical conformation. One of the most attractive “unusual” DNA structures are the G-quadruplex^{2,3}. G-quadruplexes are a polymorphic class of secondary DNA structures formed from G-rich sequences. They are characterized by the stacking of units, known as G-tetrads⁴.

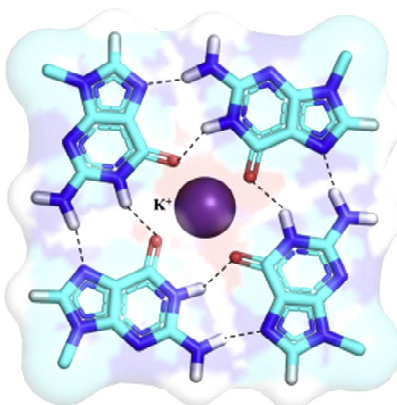


Figure 1. Representation of a G-tetrad stabilized by K^+ cation.

The G-tetrads are formed by a planar arrangement of four guanines that are stabilized by Hoogsteen hydrogen bonds and from the coordination of monovalent cations, preferentially Na^+ and K^+ (**Figure 1**). From many years the DNA G-quadruplex structures have

been studied because they are involved in genome function including transcription, recombination and replication⁵ (**Figure 2**).

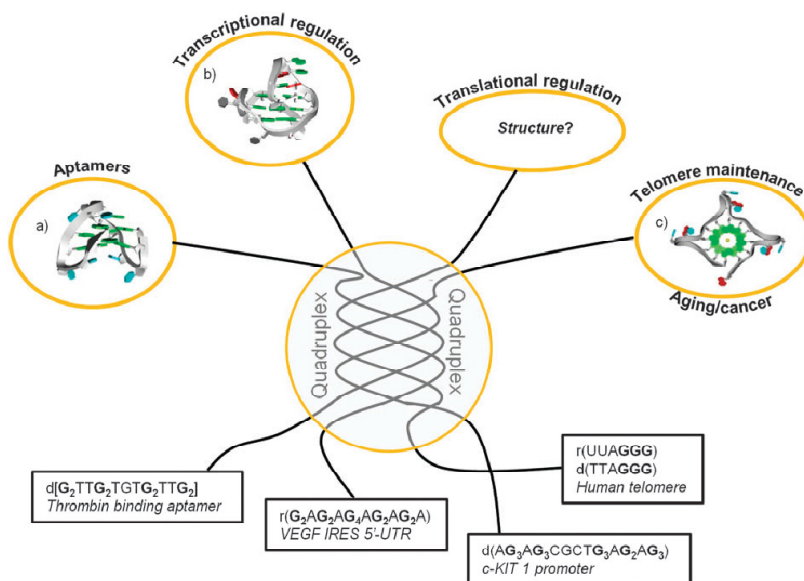


Figure 2. Current 3D structural understanding of G-quadruplexes and their possible biological role in human diseases. (a) Thrombin binding aptamer (PDB Id 148D), (b) DNA G-quadruplex formed from a sequence located in the c-KIT1 promoter region (PDB Id 2O3M), (c) human telomeric intramolecular G-quadruplex (PDB Id 1KF1). Colour scheme: adenine, red; thymine, cyan; guanine, green; cytosine, beige; phosphate backbone, grey ribbon.

Moreover, some G-rich DNA sequences, potentially G-quadruplex structures, are found at the chromosomal extremities (the telomeres) and also in several important oncogenes⁶ (**Figure 2**). In this regard, last year, the research group of Prof. S. Balasubramanian and G. Biffi, published an interesting paper describing a method for the quantitative visualization of G-quadruplexes in vivo, providing a direct evidence of their natural formation in the human genome⁷. The scientific interest in G4 structures has increased also for their biophysical properties among which, their high thermodynamic stability.

DNA quadruplex structures are very appealing from a pharmacological point of view, both as targets in antitumour therapies^{8,9} and as scaffolds of oligonucleotides (ONs) able to specifically inhibit proteins (aptamers). In the last 30 years, there has been growing interest in the potentiality of G-quadruplexes as novel aptamers, able to bind and recognize specific targets, ranging from small molecules (amino acids, antibiotics) to proteins or nucleic acid structures^{10,11}. The best known example of aptamer is the thrombin-binding aptamer (TBA), a single-stranded 15-mer DNA that was found to be a potent inhibitor of thrombin, the key enzyme of coagulation cascade^{12,13}. Furthermore, G-quadruplex have resulted to be potent inhibitors of the HIV-infection. In this way, the G-quadruplex structures may have important applications in medicinal chemistry research, in which they can be used as building blocks for the development of new DNA-based therapeutic agents.

In the last few years, a new field for the applications of nucleic acids is growing very quickly: the nanotechnologies by DNA. Nucleic acids can be optimal building blocks for their capacity to form predictable bidimensional and tridimensional structures. The first example of nanostructures by DNA are reported and called “DNA origamis,” by Paul Rothemund in 2006. Next, several groups investigating in this field reported many potential applications as sensors, electrical transportators and cellular carriers^{14,15}. In this context, some examples of G-quadruplexes used for the construction of DNA-based nanostructures are the G-wires, Frayed wires and Synapses (**Figure 3**).

G-wires are obtained by the stacking of tetramolecular G-quadruplex formed by telomeric sequence of some ciliates ($(d-G_4T_2G_4)^{16}$) or by poly-dG sequences¹⁷.

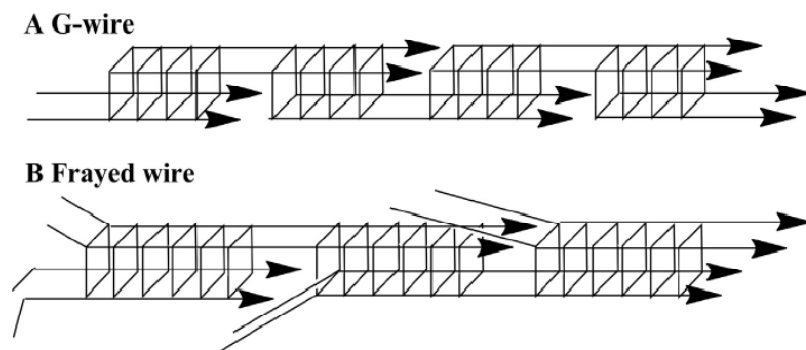


Figure 3. Models of G-wires and Frayed wires.

MacGregor and co-workers first identified the structure of frayed wires formed by $d-A_{15}G_{15}$ or $d-T_{15}G_{15}$ sequences¹⁸. These frayed wires are distinguished from G-wires by their flexible A_{15}/T_{15} tails that radiate from a guanine core. “Synapsable” DNA was described by Sen and co-workers in 1996¹⁹. It results from the interaction between two DNA duplexes containing mismatched regions of repeating G–G base pairs. The repeating G–G mismatches facilitate the formation of G-quartets that leads to the dimerization of the duplex.

1.2 Topologies of G-quadruplex structures

The G-quadruplexes display a fascinating array of polymorphic structures that contain a number of common variables (**Figure 4**): orientation and length of the loops (lateral, diagonal or external), geometry and sequence, number of quartets, relative orientation of strands (parallel, antiparallel), and glycosidic bond angles (*anti* or *syn*)²⁰ (**Figure 5d**).

In function of these variables, we can classify G-quadruplexes as intramolecular (one strand), bimolecular (two strands), or tetramolecular (four strands), in which the strands may run in a parallel (*anti* guanosine's conformation) or in antiparallel (*syn* and *anti* guanosine's conformations) direction^{21,22} (Figure 4 and 5).

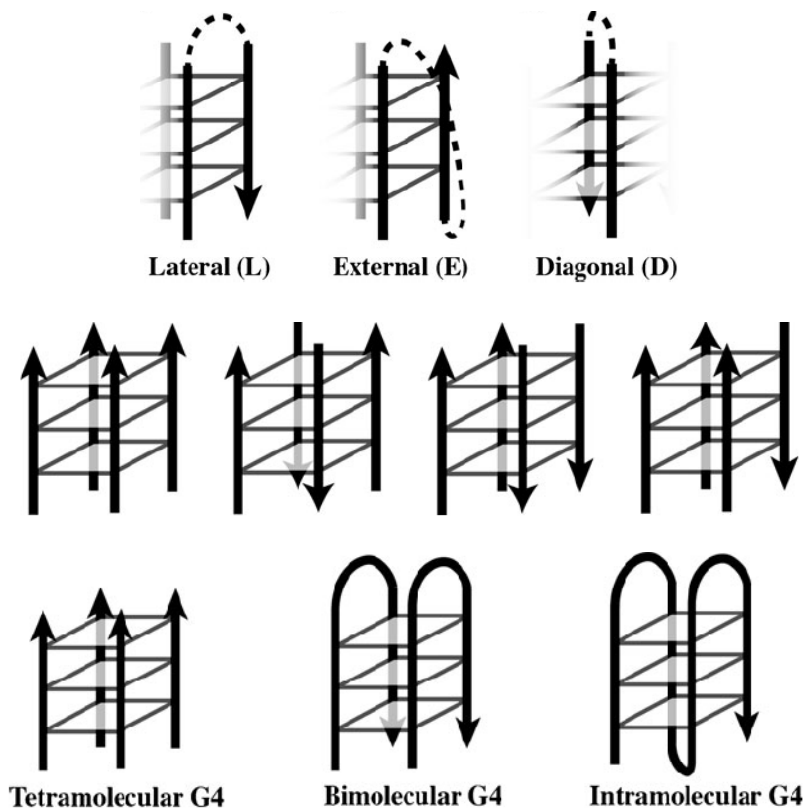


Figure 4. Schematic diagram shows three different side loops: lateral side loop (L); external side loop (E) and diagonal side loop (D). Orientation of strands: parallel, alternating anti-parallel strands, two groups of adjacent parallel strands and three parallel strands and one anti-parallel strand. Tetramolecular G4 (four strands), bimolecular G4 (two strands), and intramolecular G4 (one strand). Arrows indicate 5'–3' direction of DNA molecule.

Generally, tetramolecular G-quadruplexes adopt a well-defined structure, in which all strands are parallel with anti-conformation of bases²³; indeed intramolecular G-quadruplexes formed by single DNA

strand, form faster and are more complex, showing a wide conformational diversity²⁴. In addition, G-quadruplex can also multimerize by non-covalent stacking with the quartets or with base-pairing of flanking. The elevate structural polymorphism of G-quadruplex structures depends strongly on sequence but they can be also regulated or modulated by experimental conditions, such as the nature and concentration of cations, temperature, and pH. Fortunately, these structures can be studied with different techniques because they exhibit a specific profile; in particular, they show an unusual mobility under gel electrophoresis conditions, a characteristic CD spectrum, a signature cation-dependent stability to thermal denaturation, and distinctive imino resonances in the ¹H-NMR spectrum²⁴.

1.2.1 Grooves and metal ion coordination

The G-quadruplex structures are not stacked linearly, but adopt a right-handed helix in which are defined the internal grooves. The variation of groove-widths of the G-quadruplex is related to the conformation of base glycosidic torsion angles (**Figure 5d**) and so to the type of G-quadruplex. In a parallel four-stranded G-quadruplex with *anti* conformation of guanine, the grooves have medium width²³. On the other hand, in a monomolecular structure, *syn-anti-syn-anti* guanosine's conformation, will resulting in grooves of alternating wide-small-wide-small widths. Each groove, lined with the guanine O6 carbonyl oxygens, forms a specific binding site for metal ions. The order of cation ability to stabilize and/or to induce G-quadruplex structures is as follows : K⁺> NH₄⁺> Rb⁺> Na⁺> Cs⁺> Li⁺ for monovalent cations²⁵ and Sr²⁺> Ba²⁺> Ca²⁺> Mg²⁺ for divalent cations²⁶. The coordination of potassium, sodium, and strontium all

provide both thermodynamic and kinetic stability to the G-quadruplex structure.

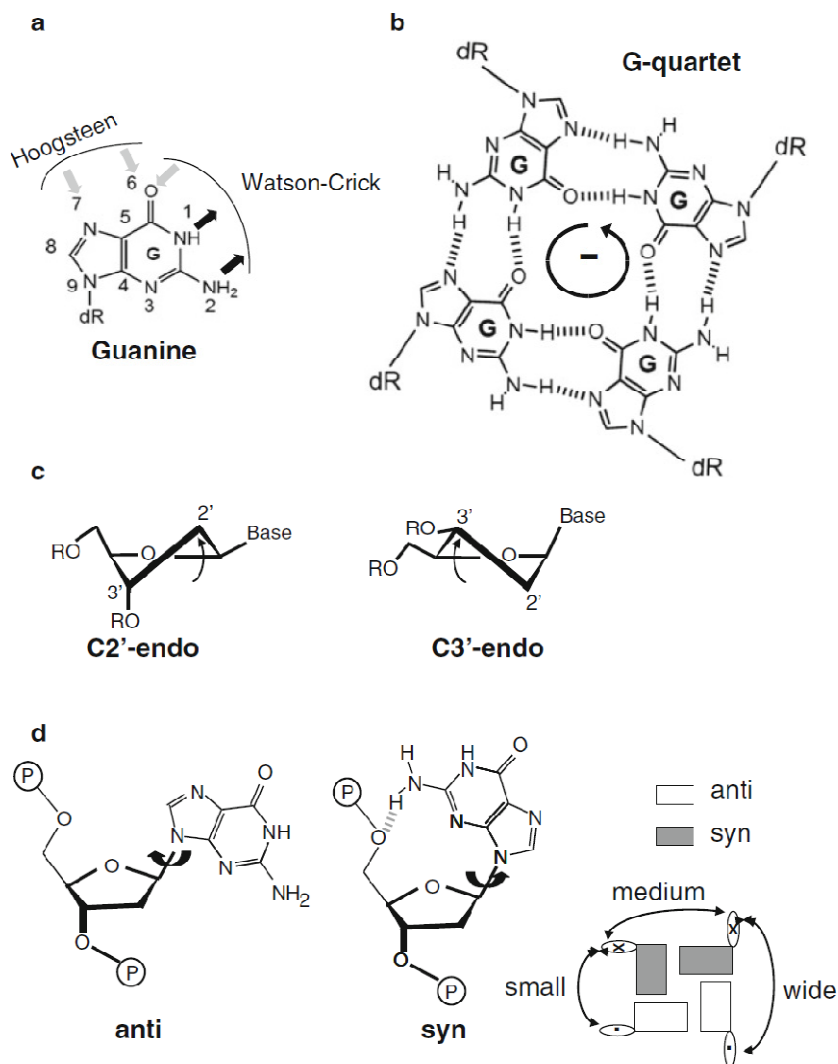


Figure 5. Guanine and G-quartet. (a) Chemical formula of canonical guanine and two hydrogen bonding faces (Watson–Crick and Hoogsteen) which are implicated in G-quartet formation. Arrows indicate H-bond donors (in black) and acceptors (in gray). (b) Classical G-quartet structure with anticlockwise rotation (-) of the donor NH to the acceptor C=O hydrogen bonds. (c) Two most favorable sugar conformations of guanine of quartet: C2'- or C3'-endo. (d) Two torsion angles of guanine glycosidic bond (*syn* and *anti*) that determine groove dimension of G-quartet: wide, medium and small.

In the case of K^+ , the stacked G-tetrads in G-quadruplex DNA provide a bipyramidyl antiprismatic coordination geometry, with each of eight carbonyl oxygens interacting equally with the cation²⁷.

1.3 Quadruplexes in telomeres or quadruplexes everywhere?

Sixty years ago, we learned that the DNA can also adopt many conformation in addition to the well-known duplex structure, and mainly that these conformations are involved in the gene regulation. Today, the study of these conformations represents a major biological opportunity to understand the role of non-coding DNA sequences. Since the discovery that G-quadruplexes DNA can form in the G-rich regions of telomeric oligonucleotides in the late 1980s²⁸, there has been a growing number of studies focusing on the structures and possible biological functions of these fascinating DNA motifs²⁹.

Many years ago it was reported that the phenomenon of cellular senescence is regulated by telomere shortening³⁰. Telomeres are overhang non-coding DNA present at the ends of human chromosomes and they are essential for the preservation of genetic material following successive DNA replications. Telomeric DNA is normally single-stranded, so in principle it could readily fold into intramolecular DNA quadruplex structures. In normal somatic cells, telomere length decreases with each cell division event by DNA polymerase on the contrary telomere shortening is absent in cancer cells due to telomere maintenance mechanism. The telomere maintenance mechanism is provided by a telomerase enzyme, a reverse transcriptase that is over-expressed in cancer cells³¹. Many antitumor strategies have been developed aiming at the telomere maintenance mechanism.

The classic model consists in the inhibition of telomerase in cancer cells in order to decrease the length of telomeric DNA³².

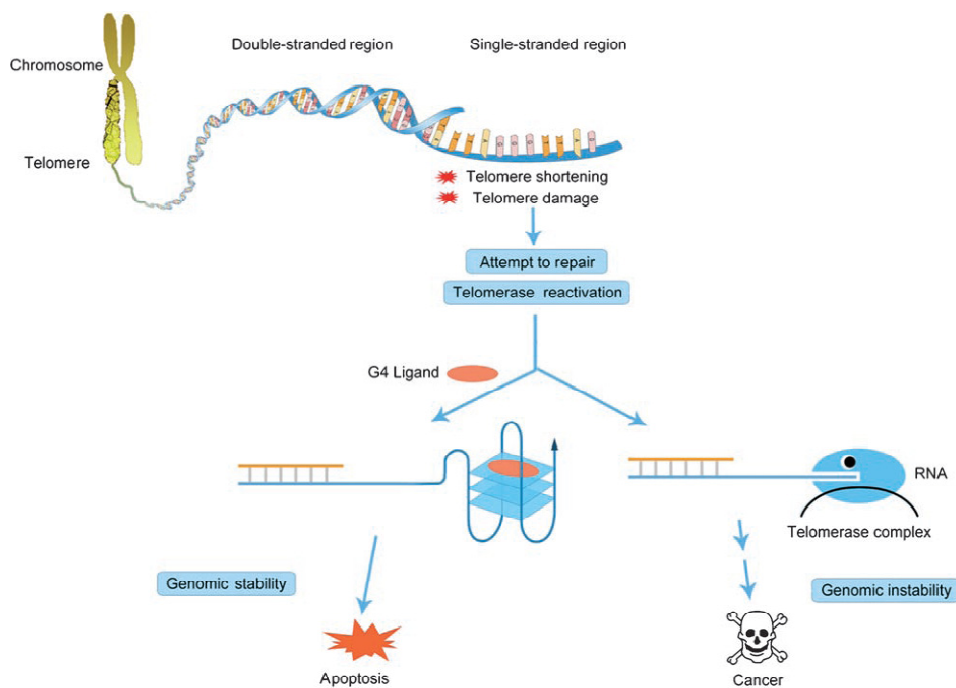


Figure 6. Mechanism of telomere shortening and telomere damage by telomerase activity.

The mechanism of telomerase inhibition, is based on the ability of a ligand molecule to induce or stabilize the fold into a G-quadruplex structure from a single-stranded telomeric DNA, that is not recognized by telomerase enzyme (**Figure 6**).

The formation of a quadruplex–ligand complex at telomere ends appears to be equivalent to the exposure of damaged DNA, since it elicits a rapid DNA damage response that is lethal to the affected cells³³. Since recent proved existence of G-quadruplex structures in repeat d(TTAGGG) sequences of human telomeric DNA⁷, the studies of G-quadruplexes as potential anti-telomerase have grown

exponentially. All these facts make G-quadruplexes an attractive target for drug design. Recently, structural studies on telomeric G-quadruplex have revealed a diversity of topologies, which are particular sensitive to the nature of the cations present and to the flanking sequences³⁴. In this context, it is reported the polymorphic nature of truncated human telomeric sequence, Tel22 (d[AG₃(T₂AG₃)₃]), whose NMR structure in Na⁺ solution³⁵ revealed an antiparallel topology, contrary to its crystal structure, obtained from a K⁺ solution which shows a parallel topology³⁶ (**Figure 7**).

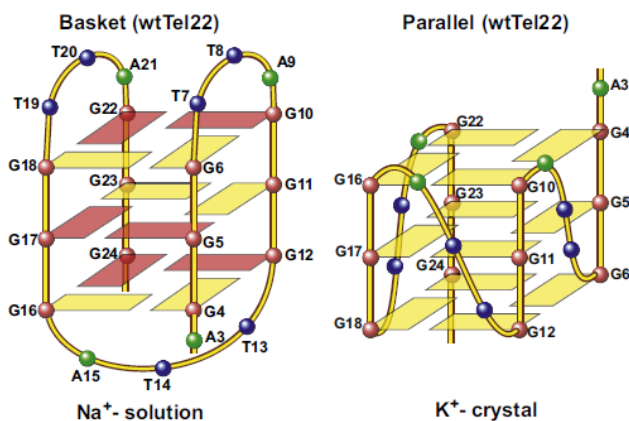


Figure 7. Folding topology of the basket-type intramolecular G-quadruplex formed by wtTel22 in Na⁺ solution as determined by NMR. Folding topology of the propeller-type parallel-stranded intramolecular G-quadruplex formed by wtTel22 in the presence of K⁺ in crystalline state.

The elevated polymorphism of telomeric G-quadruplex DNA structures could have important implications in the drug design of ligands as anti-telomerase drugs.

1.3.1 G-Quadruplex-binding ligands as anticancer drug

Natural and synthetic molecules (protein, ligands, and polymers) may act as molecular chaperones for G-quadruplex assembly. In these years, many molecules have been identified as ligands for G4 structures, and for their development as potential anticancer agents^{37,38}. So far, the rational design of G-quadruplex-interacting compounds has been guided by two criteria (π -stacking and electrostatics) but also by empirical approaches.

The majority of G-quadruplex ligands in literature contains a polycyclic hetero-aromatic core, because it is clear that the main G-quadruplex stabilization occurs via π - π stacking and electrostatic interactions resulting in the binding of the ligand (usually a flat aromatic molecule) on the G-quartet constitutive of the external-face of the G-quadruplex.

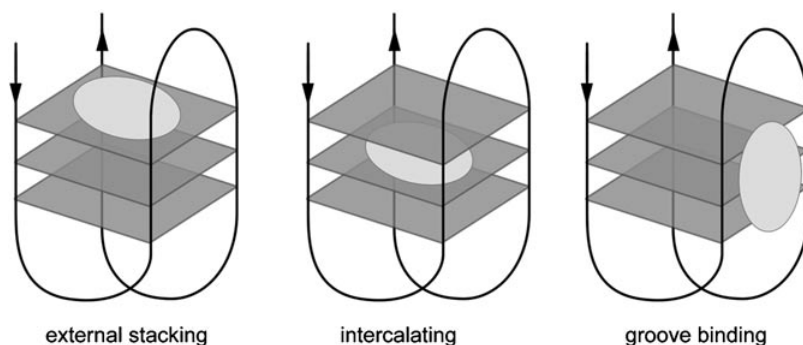


Figure 8. Different binding modes of G-quadruplex-ligand.

This binding mode (external stacking) has been thoroughly discussed since it represents a unique feature of quadruplex recognition as compared to other DNA forms³⁹. In order to design drug ligands able to bind selectively G-quadruplex structures, the

understanding of target G-quadruplex structures and their topologies is a key point⁴⁰. Actually few molecules distinguish between the various classes of G quadruplexes (intra- or inter-molecular, parallel or antiparallel). The particular geometry of the G-quadruplex structure is thought to allow specific recognition by small ligands through various binding modes (**Figure 8**): by an external stacking with the terminal quartet, by an intercalation between the G-tetrads, and finally through groove binding mode. In many studies, investigating the G-quadruplex-ligand complexes, it has been reported that the stacking of the drug on the outer planes of G-tetrads appears to be more energetically favorable and probable according with the rationale design supposed many years before.

The only ligand discovered so far, binding the groove of G-quadruplex is Distamycin A⁴¹. Martino et al. investigated the interaction of Distamycin A with d[TGGGGT]₄ and found that the ligand binds with a 4/1 ratio to the quadruplex (**Figure 9**).

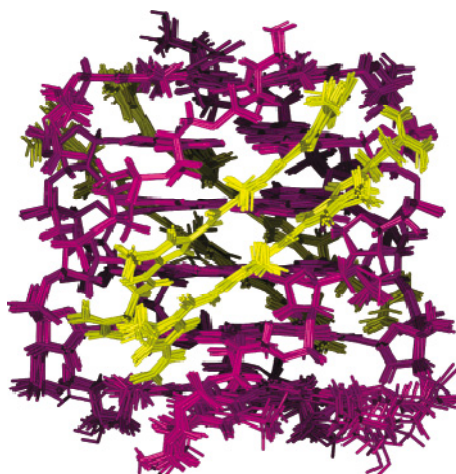


Figure 9. Side view of the superimposition of the 10 best structures of the 4:1 complex Dist-A/[d(TGGGGT)]₄. Dist-A is reported in yellow, and DNA is colored in magenta.

So far, knowing that the binding mode of ligand-G-quadruplex is mainly controlled by hydrophobic and Van der Waals interaction, the design of ligands is based on the same general features. Generally, G4 ligands, are characterized by a planar aromatic core able to stack with the G-tetrads, and by basic side chains which interact with the grooves/loops and the negatively charged phosphate backbone of G-quadruplexes^{42,43}. The aim of the basic side chains is the stabilization of G-quadruplex structures by electrostatic interactions, and also the increase of water solubility of ligands.

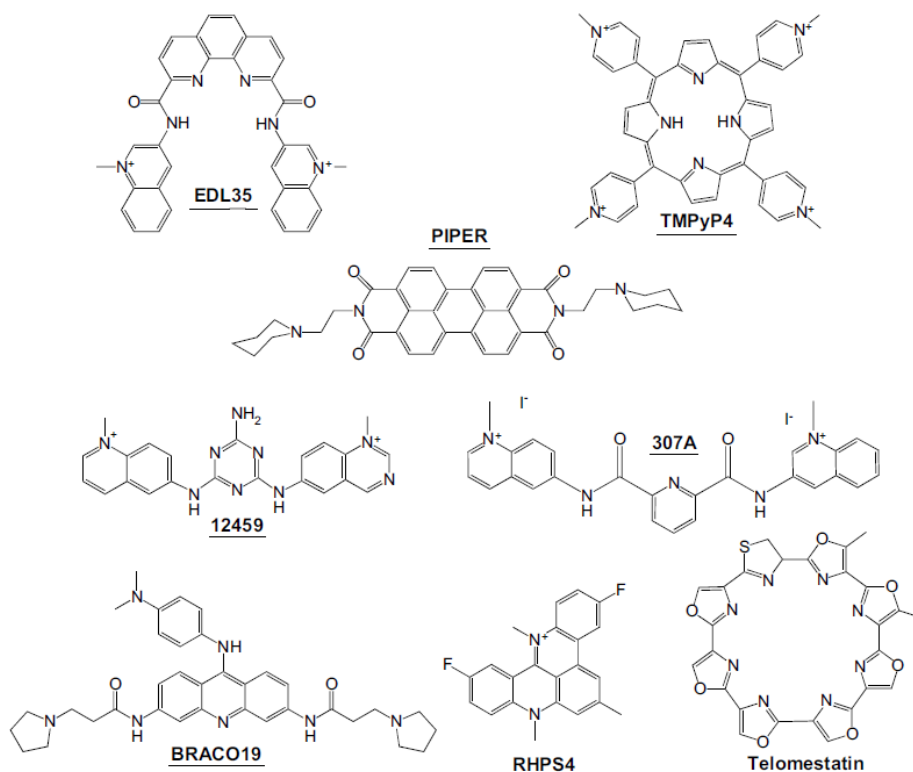


Figure 10. Some structures of G-quadruplex ligands.

In order to increase the selectivity of ligands for G4 compared with duplex, the size of the aromatic core is crucial, as much large core

improves the aromatic–aromatic overlap and provides selectivity for G-quadruplexes. Following these general structural features, in these years, many G-quadruplex-ligands have been identified. Some examples of the first generation of telomerase inhibitors are anthraquinones⁴⁴, 3,6-disubstituted acridines⁴⁵; these have a planar aromatic electron-deficient core, and thus it was originally hypothesized that these are able to stack efficiently onto the planar surface of a G-tetrad. Subsequently, the second generation of ligands, has continued to exhibit this feature with some enhancements and it included the trisubstituted acridines⁴⁶, the most important is **BRACO-19**⁴⁷, the porphyrins, among which **TMPyP4**⁴⁸ (**Figure 10**), and a non-polycyclic aromatic ligands, such as bis-triazole derivative⁴⁹. Ongoing research has revealed a large number of telomerase inhibitors from natural products displaying remarkable diversity in molecular structure. More recently, Kim et al. reported the high anti-telomerase activity of **Telomestatin**⁵⁰, a natural metabolite extracted from *Streptomyces annulatus* (**Figure 10**). Also some semi-synthetic derivatives of berberine, another natural product, was reported as anticancer drugs associated with down-regulation of telomerase activity. In this frame, the **Quarflorin**, a specific G4 ligand for myc G-quadruplex, is in Phase II clinical trials, as anticancer drug^{51,52}.

1.4 G-quadruplexes: new class of aptamers

Aptamers are short single strand oligonucleotides (< 100 bases) able to bind different targets, ranging from small molecules (amino acids, antibiotics) to proteins, with high affinity and specificity. These peculiar features are related to a tertiary structure, which presents a good shape complementarity with target molecules⁵³. In this frame, these oligonucleotides, ‘aptamers’, are an emergent class of molecules

that rival antibodies in both therapeutic and diagnostic application⁵⁴. Thank to their oligonucleotide structure, the aptamers offer a number of advantages in comparison with antibodies, including an inexpensive, rapid, and reproducible synthesis pathway, easily implemented chemical modifications, long-term stability and very low immunology. Usually, they are selected from a huge combinatorial library using the “systematic evolution of ligands by exponential enrichment” (SELEX), reported for the first time in the 1990⁵⁵. The SELEX method makes use of the powerful amplification capability of PCR in which a random mixture of DNA sequences with fixed 5’ and 3’-end sequences are screened for binding with a specific target. The few selected DNA sequences that exhibit strong binding with the target are then PCR amplified and screened for the strong target binding again. This process is repeated many times to obtain a few final sequences that usually contain well-conserved consensus sequences. Recently, two oligonucleotides have been validated as therapeutics: a phosphorothioate antisense oligonucleotide **ISIS 2922** (Formivirsen), approved to treat retinitis caused by Cytomegalovirus⁵⁶ and **Pegaptanib sodium**, 2’-fluoropyrimidine RNA-based, for the treatment of neovascular age-related macular degeneration⁵⁷. On the way of the search for ever more specific aptamers, particular interest has been growing for G-quadruplex structures, in particular for their very specific three-dimensional shapes. In this frame, the G-quadruplex aptamers, recently involved in clinical trials are the thrombin-binding aptamer (**TBA**)^{12,13} and **AS1411**⁵⁸. The TBA is a DNA 15-mer sequence, discovered in 1992 through the SELEX methodology in order to search new therapeutic agents to prevent thrombosis.

The solution structure of TBA was determined by NMR, by Wang and coworker in 1993. It consists in an unimolecular antiparallel G-quadruplex, with a chair-like conformation¹³ (**Figure 11**).

Thrombin Binding Aptamer (PDB Id 148D)
Sequence: d(GGTTGGTGTGGTTGG)

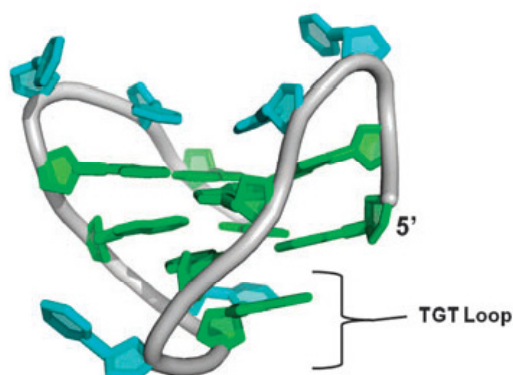


Figure 11. G-quadruplex structure of thrombin binding aptamer, solved by NMR in 1993.

The second one is AS1411, 26-mer oligonucleotide, implicated in the proliferation of cancer cells with nucleolin as its specific target. The nucleolin is a protein marker expressed at high levels in human cancer cells⁵⁹. Very recently AS1411 completed phase II clinical trials as anti-cancer drug with low toxicity and high therapeutic potential⁶⁰.

1.5 G-quadruplexes against HIV infection

Recently, G-quadruplexes have been exploited as therapeutic strategies in cancer chemotherapy and as anti-HIV agents due to their in vivo activity, playing important roles in controlling gene expression via protein recognition of their structures⁶¹. G-quadruplex based aptamers have been successfully designed to target the HIV virus at different stages of its life cycle. The potential targets of HIV infection are HIV-1 reverse transcriptase⁶², HIV RNase H⁶³, HIV-1

integrase⁶⁴ (IN) and viral surface glycoprotein known as gp120⁶⁵. Among the first G-quadruplex aptamer against HIV-1 integrase, is a parallel stranded G-quadruplex: **T30177** (**Figure 12a**). This aptamer was the first IN inhibitor tested in clinical trials (ZintevirTM developed by Aronex Pharmaceuticals in 1996) showing a high inhibition against the HIV-1 integrase at nanomolar levels⁶⁶.

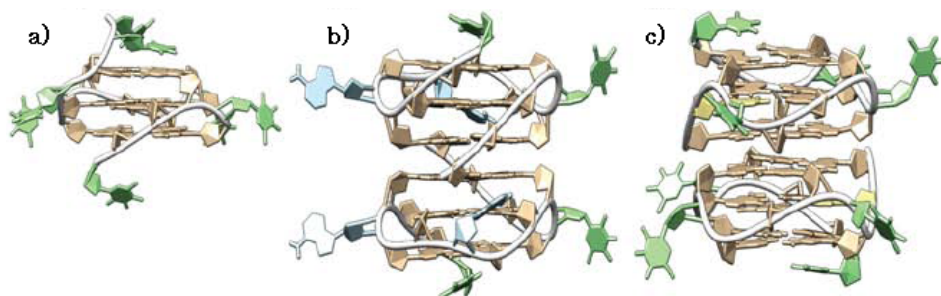


Figure 12. a) Intramolecular parallel G4 structure with three tetrads for the **T30177** anti-HIV aptamer (PDB ID: 2M4P); b) Interlocked bimolecular parallel G4 structure with six tetrads for the **93del** anti-HIV aptamer (PDB ID: 1Y8D); c) Two stacked parallel G4 structures with three tetrads each observed for the **T30923** anti-HIV aptamer (PDB ID: 2LE6).

Subsequently, similar to T30177, other G-quadruplex aptamers, a 16-mer oligonucleotides (**93del** and **T30923**) have been proved effective for inhibiting HIV-1 integrase^{67,68} (**Figure 12b, 12c**). In particular, the aptamer 93del shows a remarkably unique quadruplex arrangement with two quadruplex subunits strongly interlocked in dimer parallel structure⁶⁹, which is stable even at temperatures over 90 °C. Infection of human immunodeficiency virus type-I (HIV-1) to susceptible cell is initiated by the binding of the positively charged V3 loop of the viral envelope glycoprotein (gp120), to the cellular receptor, CD4, which is then followed by fusion of the virus particle with the cell membrane (**Figure 13**). Although the precise mechanism of virus entry is unclear, it is believed that specific regions of gp120 and the

transmembrane glycoprotein gp41 are involved in this process. Therefore, sequences able to recognize target proteins, such as gp120 and gp41, are potential antiviral drugs⁷⁰.

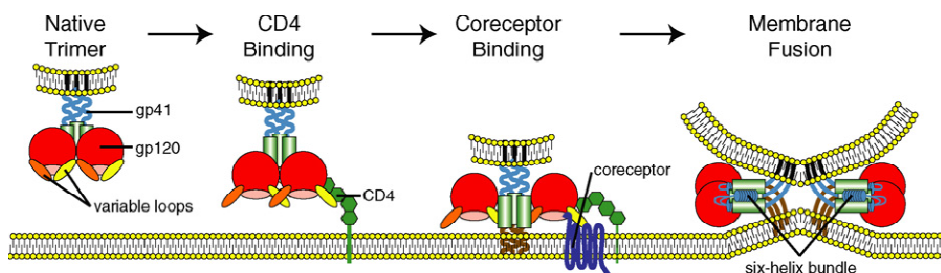


Figure 13. Model of the multi-step process of HIV entry. The CD4 and coreceptor molecules are located in the host membrane (bottom), while the gp120 and gp41 proteins are associated with the viral membrane (curved, top). HIV entry is initiated by attachment of gp120 to CD4, which results in conformational changes in gp120 that result in the formation of the bridging sheet mini-domain and extension of the V3 loop.

Among these, the aptamer phosphorothioate **ISIS-5320** formed by tetramolecular G-quadruplex structure⁷¹, has been reported to target glycoprotein gp120 of HIV virus. Based on these evidences, tetramolecular parallel G-quadruplexes, thank to their shorter sequences and simpler strand arrangements, could be a potential building block for the modifications requirement for its enhancement of pharmacokinetic and pharmacodynamic properties.

In this frame, in the '90s, Hotoda et al. identified a tetramolecular G-quadruplex based on the sequence d(TGGGAG), and able to target the gp120 of HIV-1^{72,73}. This sequence showed a high anti- HIV-1 activity only if conjugated with an aromatic group at the 5'-end. d(TGGGAG) sequence came to the precursor sequence d(TGGGAGGTGGGTCTG), both 5'-end modified sequences showed the same anti-HIV-1 activity by unique mechanism of action. The first modified active against HIV-1 infection, reported by Hotoda, was with

4,4'-dimethoxytrityl (DMT) group at the 5'-end of 6-mer, subsequently from the screening of the various modified 6-mer, was discovered the most potent inhibitor, **R-95288**, with high anti- HIV-1 activity and low toxicity (**Figure 14**).

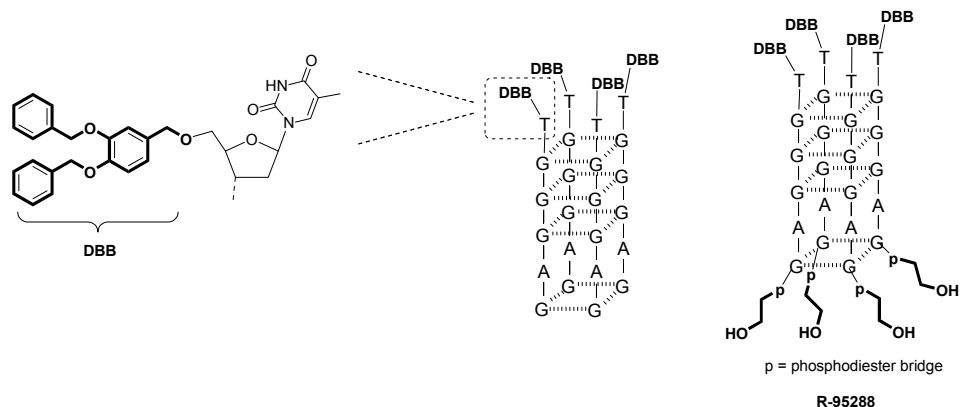


Figure 14. Structures of **DBB-d(TGGGAG)** and **R-95288**, potent aptamers against HIV infection discovered by Hotoda in 1997.

The sequence R-95288 is modified to bear a 3,4-dibenzyloxybenzyl (DBB) group at 5'-end and a 2-hydroxy-ethylphosphate at the 3'-end^{74,75} (**Figure 14**). Analysis on these Hotoda modified 6-mer, have indicated that G-quadruplex formation, as well as the presence of large aromatic groups at the 5'-end, were both essential for the antiviral activity. In this context, since the structural stability of G-quadruplex forming aptamers is closely related to their biological activities, a biophysical and structural investigation of Hotoda's modified sequences, was provided by D'onofrio and co-workers in 2007⁷⁶. They reported CD, DSC and molecular modeling studies on some representative anti-HIV 5'-modified Hotoda's 6-mers, in comparison with unmodified sequence d(TGGGAG). They concluded that the insertion of large aromatic groups, as DMT and DBB (**Figure**

14) at the 5'-end of the d(TGGGAG) sequence has dramatic effects on the thermodynamic of G-quadruplex formation. Indeed both 5'-modified G-quadruplexes, showed higher thermal stability than unmodified sequence. Moreover, they reported the thermodynamic origins of this stabilization, defining that the G-quadruplex with 5'-DBB is entropically stabilized for its hydrophobic interactions in comparison with G4 by d(TGGGAG).

In 2008 D'onofrio et al., aiming at ODNs endowed with potential anti-HIV activity, investigated the end-conjugation with sugars on d(TGGGAG) sequence, as a strategy to improve the pharmacological profile of these oligonucleotides⁷⁷. They reported from CD-monitored thermal denaturation studies on the resulting quadruplexes that the insertion of a single monosaccharide at the 3'-end improves the stability of G-quadruplex complex and also confers an anti-HIV activity to unmodified sequence. On the contrary, the 5'-tethering with same monosaccharides, in all cases decreases the G-quadruplex stability and did not improve the biological activity. Overall reported studies underline the crucial role of aromatic groups at the 5'-end in the stability of G-quadruplexes.

1.6 Aim of research work

In this context, my research activity is focused on the design, synthesis and structural characterization of several biomolecules, such as DNA modified sequences based on G-quadruplex structures as anti-HIV aptamers and G-quadruplex-ligands of natural origin with potential anti-telomerase activity. Notably, I mainly focused my attention on:

- **G-quadruplex aptamers based on d(TGGGAG) endowed with anti-HIV activity**

The first goal of this research was to achieve more potential anti-HIV aptamers based on Hotoda's sequences in order to get a more complete picture of their structure-activity relationships depending on the modifications at 5'-end of d(TGGGAG).

In this frame, in 2011 Di Fabio et al reported the synthesis and characterization of a new mini-library of d(TGGGAG) ODNs carrying aryl groups at the 5'-end connected by phosphodiester bond⁷⁸. The main goal of this work was to expand the repertoire of accessible end-modified G-rich ODNs, using a simpler and more general synthetic strategy to link the aryl groups at the 5'-end of ODNs. The results obtained showed that all 5'-end modified sequences formed G-quadruplexes with strongly increased thermal stability and that these sequences are endowed with high anti-HIV activity and high binding affinity for the HIV-1 envelope proteins gp120 and gp41. Furthermore, we can summarize that the biological activity of modified d(TGGGAG) is related to two main factors: **1.** the extent of interaction with the positively charged V3 loop of gp120 and **2.** the amount of G4 able to interact with the target, that in turn it is dependent on the G-quadruplex thermal stability, the kinetics of formation and the resistance to nucleases.

Starting from these considerations, we focused our attention on the synthesis and biophysically and biologically characterization of a mini-library of new d(TGGGAG) oligomers as potential anti-HIV aptamers. In this frame, aiming at extending the number of more effective oligonucleotide-based antivirals, we developed an efficient procedure to synthesize a new mini-library of d(TGGGAG) oligomers

carrying hydrophobic and aromatic groups at the 5'-end by a phosphodiester bond⁷⁹. The choice of conjugated groups aim to improve cellular uptake, extend the half-life of these molecules in plasma and most of all to stabilize DNA structures by hydrophobic interactions. In addition, in attempt to enhance the kinetic of G-quadruplex formation, we synthesized bimolecular G-quadruplex aptamers based on Hotoda's sequence, essentially different from the quadruplexes reported before for the number of strands, the number of aromatic moieties at 5'-end and for the presence of hexaethylenglycol (HEG) as a linker between two strands⁸⁰.

In order to achieve a more complete picture of structure-activity relationship, we started kinetic studies on the most active 5'-end modified d(TGGGAG) oligomers in collaboration with *Valérie Gabelica*, Research Director Inserm/Univ. Bordeaux (France). Notably, during the period that I spent to IECB in Bordeaux in the Gabelica's group, I performed kinetic experiments using ESI-Mass Spectrometry and Ion Mobility Spectrometry (IMS) technologies.

- **G-Quadruplex-ligands as telomerase inhibitor: potentialities of the silibinin**

While remaining within the G-quadruplex-forming oligonucleotides, it is already known that the formation of this structures has important consequences at the cellular level and that such structures have been evoked in the control of expression of genes involved in the perturbation of telomeric organization⁴. The structural investigation of G-quadruplexes is essential to find the factors stabilizing these structures and for the design of G-quadruplex-binding ligands. So far, the rational design of G-quadruplex-

interacting compounds has been guided by π -stacking and electrostatic interactions.

In this frame, there is a huge interest in a variety of small organic molecules able to induce the formation of G-quadruplex in G-rich sequences found in telomeres. Based on the wide number of natural products as ligands already reported in literature⁸¹, we aim to investigate the potential activity of **silibinin**, a flavonolignan isolated from the fruits of the milk thistle *Silybum marianum*⁸² (**Figure 15**). Silibinin is a prominent component (approximately 30%) of the silymarin complex. Structurally it is a diastereoisomeric mixture of two flavonolignans, namely **silybin A** and **silybin B** in a ratio of approximately 1:1, hardly separable (**Figure 15**).

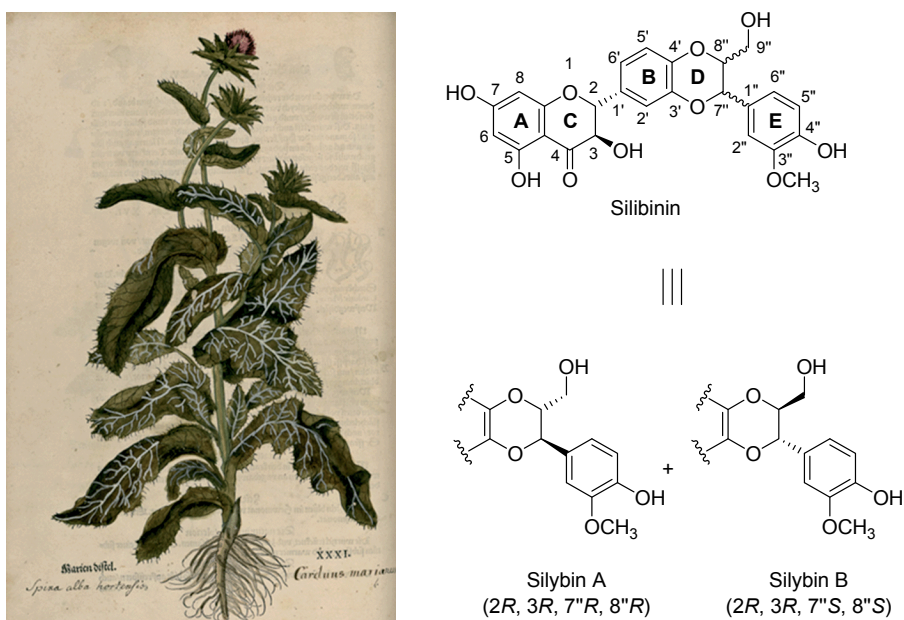


Figure 15. *Silybum marianum* (*Carduus marianus* L., Asteraceae; milk thistle) depiction in the Leonhart Fuchs herbal (1542); structure of **silibinin** and its diastereoisomers: **silybin A** and **B**.

Silibinin is one of the flavonoid antioxidants with multiple biological activities mostly related to its radical-scavenging activity. Recently, this metabolite has received attention due to its anticancer and chemopreventive actions⁸³, as well as hypocholesterolemic, cardioprotective, and neuroprotective activities⁸⁴. In addition to the activity of silibinin, other constituents of sylimarin such as isosilybin, silychristin and 2,3-dehydrosilybin, have been shown many attractive pharmacological properties. In particular, the oxidized form of silibinin, the 2,3- dehydrosilybin (**DHS**), displays major antioxidant and anticancer properties than silibinin suggesting that DHS may be a useful therapeutic agent⁸⁵. The pharmacological use of both silibinin and DHS *in vivo* experiments is dramatically limited by factors concerning their low solubility and bioavailability⁸⁶. In order to overcome these drawbacks, we developed different synthetic strategies for the insertion of suitable chemical modifications in attempt to improve their applications in biomedicine and biochemistry^{87–90}.

Based on biological activities of silibinin and DHS and aiming to evaluate their ability to induce inter- or intramolecular G-quadruplex structures, it is clear that their stereochemistry may play an important role with interesting structural implications. In this context, we are focused our attention on two key points: **a)** the separation of silybin A and silybin B from the commercial by HPLC⁹¹ and **b)** the development of an efficient preparative base-catalysed oxidation of silibinin to obtain good yields of DHS⁹².

References

- (1) Rich, A. (1993) DNA comes in many forms. *Gene* 135, 99–109.
- (2) Sundquist, W. I., and Klug, A. (1989) Telomeric DNA dimerizes by formation of guanine tetrads between hairpin loops. *Nature* 342, 825–9.
- (3) Williamson, J. R. (1993) Guanine quartets. *Current Opinion in Structural Biology* 3, 357–362.
- (4) Lea Spindler, W. F. (2012) Guanine Quartets (Spindler, L., and Fritzsche, W., Eds.). Royal Society of Chemistry, Cambridge.
- (5) Huppert, J. L., and Balasubramanian, S. (2005) Prevalence of quadruplexes in the human genome. *Nucleic acids research* 33, 2908–16.
- (6) Lipps, H. J., and Rhodes, D. (2009) G-quadruplex structures: in vivo evidence and function. *Trends in Cell Biology* 19, 414–422.
- (7) Biffi, G., Tannahill, D., McCafferty, J., and Balasubramanian, S. (2013) Quantitative visualization of DNA G-quadruplex structures in human cells. *Nature chemistry* 5, 182–6.
- (8) Neidle, S. (2010) Human telomeric G-quadruplex: the current status of telomeric G-quadruplexes as therapeutic targets in human cancer. *The FEBS journal* 277, 1118–25.
- (9) Shankar, Hurley, L. H., and Neidle, S. (2011) Targeting G-quadruplexes in gene promoters: a novel anticancer strategy? *Nature reviews. Drug discovery* 10, 261–275.
- (10) Gatto, B., Palumbo, M., and Sissi, C. (2009) Nucleic Acid Aptamers Based on the G-Quadruplex Structure: Therapeutic and Diagnostic Potential. *current medicinal chemistry* 16, 1248–1265.
- (11) Keefe, A. D., Pai, S., and Ellington, A. (2010) Aptamers as therapeutics. *Nature reviews. Drug discovery* 9, 537–50.
- (12) Bock, L. C., Griffin, L. C., Latham, J. A., Vermaas, E. H., and Toole, J. J. (1992) Selection of single-stranded DNA molecules that bind and inhibit human thrombin. *Nature* 355, 564–566.
- (13) Wang, K. Y., McCurdy, S., Shea, R. G., Swaminathan, S., and Bolton, P. H. (1993) A DNA aptamer which binds to and inhibits thrombin exhibits a new structural motif for DNA. *Biochemistry* 32, 1899–1904.
- (14) Rothemund, P. W. K. (2006) Folding DNA to create nanoscale shapes and patterns. *Nature* 440, 297–302.

- (15) Liu, S. P., Weisbrod, S. H., Tang, Z., Marx, A., Scheer, E., and Erbe, A. (2010) Direct measurement of electrical transport through G-quadruplex DNA with mechanically controllable break junction electrodes. *Angewandte Chemie - International Edition* 49, 3313–3316.
- (16) Marsh, T. C., and Henderson, E. (1994) G-Wires: Self-Assembly of a Telomeric Oligonucleotide, d(GGGTTGGG), into Large Superstructures. *Biochemistry* 33, 10718–10724.
- (17) Borovok, N., Molotsky, T., Ghabboun, J., Porath, D., and Kotlyar, A. (2008) Efficient procedure of preparation and properties of long uniform G4-DNA nanowires. *Analytical biochemistry* 374, 71–8.
- (18) Protozanova, E., and Macgregor, R. B. (1996) Frayed wires: a thermally stable form of DNA with two distinct structural domains. *Biochemistry* 35, 16638–45.
- (19) Venczel, E. A., and Sen, D. (1996) Synapsable DNA. *Journal of molecular biology* 257, 219–24.
- (20) Dai, J., Carver, M., and Yang, D. (2008) Polymorphism of human telomeric quadruplex structures. *Biochimie* 90, 1172–83.
- (21) Burge, S., Parkinson, G. N., Hazel, P., Todd, A. K., and Neidle, S. (2006) Quadruplex DNA: sequence, topology and structure. *Nucleic acids research* 34, 5402–15.
- (22) Largy, E., and Mergny, J.-L. (2014) Shape matters: size-exclusion HPLC for the study of nucleic acid structural polymorphism. *Nucleic Acids Research* 1–15.
- (23) Phillips, K., Dauter, Z., Murchie, A. I., Lilley, D. M., and Luisi, B. (1997) The crystal structure of a parallel-stranded guanine tetraplex at 0.95 Å resolution. *Journal of molecular biology*.
- (24) Tran, P. L. T., De Cian, A., Gros, J., Moriyama, R., and Mergny, J.-L. (2013) Tetramolecular quadruplex stability and assembly. *Topics in current chemistry* 330, 243–73.
- (25) Wong, A., and Wu, G. (2003) Selective binding of monovalent cations to the stacking G-quartet structure formed by guanosine 5'-monophosphate: a solid-state NMR study. *Journal of the American Chemical Society* 125, 13895–905.
- (26) Venczel, E. A., and Sen, D. (1993) Parallel and antiparallel G-DNA structures from a complex telomeric sequence. *Biochemistry* 32, 6220–6228.
- (27) Lane, A. N., Chaires, J. B., Gray, R. D., and Trent, J. O. (2008) Stability and kinetics of G-quadruplex structures. *Nucleic acids research* 36, 5482–515.

- (28) Henderson, E., Hardin, C. C., Walk, S. K., Tinoco, I., and Blackburn, E. H. (1987) Telomeric DNA oligonucleotides form novel intramolecular structures containing guanine-guanine base pairs. *Cell* *51*, 899–908.
- (29) Bochman, M. L., Paeschke, K., and Zakian, V. A. (2012) DNA secondary structures: stability and function of G-quadruplex structures. *Nature reviews. Genetics* *13*, 770–80.
- (30) Blackburn, E. H. (1991) Structure and function of telomeres. *Nature* *350*, 569–573.
- (31) Mergny, J.-L., Riou, J.-F., Mailliet, P., Teulade-Fichou, M.-P., and Gilson, E. (2002) Natural and pharmacological regulation of telomerase. *Nucleic acids research* *30*, 839–865.
- (32) De Cian, A., Lacroix, L., Douarre, C., Temime-Smaali, N., Trentesaux, C., Riou, J.-F., and Mergny, J.-L. (2008) Targeting telomeres and telomerase. *Biochimie* *90*, 131–55.
- (33) Salvati, E., Leonetti, C., Rizzo, A., Scarsella, M., Mottolose, M., Galati, R., Sperduti, I., Stevens, M. F. G., D’Incalci, M., Blasco, M., Chiorino, G., Bauwens, S., Horard, B., Gilson, E., Stoppacciaro, A., Zupi, G., and Biroccio, A. (2007) Telomere damage induced by the G-quadruplex ligand RHPS4 has an antitumor effect. *Journal of Clinical Investigation* *117*, 3236–3247.
- (34) Phan, A. T., and Patel, D. J. (2003) Two-Repeat Human Telomeric d(TAGGGTTAGGGT) Sequence Forms Interconverting Parallel and Antiparallel G-Quadruplexes in Solution: Distinct Topologies, Thermodynamic Properties, and Folding/Unfolding Kinetics. *Journal of the American Chemical Society* *125*, 15021–15027.
- (35) Wang, Y., and Patel, D. J. (1993) Solution structure of the human telomeric repeat d[AG₃(T₂AG₃)₃] G-tetraplex. *Structure (London, England : 1993)* *1*, 263–282.
- (36) Parkinson, G. N., Lee, M. P. H., and Neidle, S. (2002) Crystal structure of parallel quadruplexes from human telomeric DNA. *Nature* *417*, 876–80.
- (37) Guittat, L., Alberti, P., Gomez, D., De Cian, A., Pennarun, G., Lemarteleur, T., Belmokhtar, C., Paterski, R., Morjani, H., Trentesaux, C., Mandine, E., Boussin, F., Mailliet, P., Lacroix, L., Riou, J.-F., and Mergny, J.-L. (2004) Targeting human telomerase for cancer therapeutics. *Cytotechnology* *45*, 75–90.
- (38) Chen, C. Y., Wang, Q., Liu, J. Q., Hao, Y. H., and Tan, Z. (2011) Contribution of telomere G-quadruplex stabilization to the inhibition of telomerase-mediated telomere extension by chemical ligands. *Journal of the American Chemical Society* *133*, 15036–15044.
- (39) Monchaud, D., and Teulade-Fichou, M.-P. (2008) A hitchhiker’s guide to G-quadruplex ligands. *Organic & biomolecular chemistry* *6*, 627–36.

- (40) Neidle, S., and Parkinson, G. (2002) Telomere maintenance as a target for anticancer drug discovery. *Nature reviews. Drug discovery* 1, 383–393.
- (41) Martino, L., Virno, A., Pagano, B., Virgilio, A., Di Micco, S., Galeone, A., Giancola, C., Bifulco, G., Mayol, L., and Randazzo, A. (2007) Structural and thermodynamic studies of the interaction of distamycin A with the parallel quadruplex structure [d(TGGGGT)]₄. *Journal of the American Chemical Society* 129, 16048–16056.
- (42) Casagrande, V., Alvino, A., Bianco, A., Ortaggi, G., and Franceschin, M. (2009) Study of binding affinity and selectivity of perylene and coronene derivatives towards duplex and quadruplex dna by ESI-MS. *Journal of Mass Spectrometry* 44, 530–540.
- (43) Murat, P., Singh, Y., and Defrancq, E. (2011) Methods for investigating G-quadruplex DNA/ligand interactions. *Chemical Society reviews* 40, 5293–307.
- (44) Sun, D., Thompson, B., Cathers, B. E., Salazar, M., Kerwin, S. M., Trent, J. O., Jenkins, T. C., Neidle, S., and Hurley, L. H. (1997) Inhibition of Human Telomerase by a G-Quadruplex-Interactive Compound. *Journal of Medicinal Chemistry* 40, 2113–2116.
- (45) Read, M., Harrison, R. J., Romagnoli, B., Tanious, F. A., Gowan, S. H., Reszka, A. P., Wilson, W. D., Kelland, L. R., and Neidle, S. (2001) Structure-based design of selective and potent G quadruplex-mediated telomerase inhibitors. *Proceedings of the National Academy of Sciences of the United States of America* 98, 4844–9.
- (46) Harrison, R. J., Cuesta, J., Chessari, G., Read, M. a, Sanji, K., Reszka, A. P., Morrell, J., Gowan, S. M., Christopher, M., Tanious, F. a, Wilson, W. D., Kelland, L. R., and Neidle, S. (2003) Trisubstituted Acridine Derivatives as Potent and Selective Telomerase Inhibitors Trisubstituted Acridine Derivatives as Potent and Selective Telomerase. *Journal of Medicinal Chemistry* 4463–4476.
- (47) Gowan, S. M., Harrison, J. R., Patterson, L., Valenti, M., Read, M. A., Neidle, S., and Kelland, L. R. (2002) A G-Quadruplex-Interactive Potent Small-Molecule Inhibitor of Telomerase Exhibiting in Vitro and in Vivo Antitumor Activity. *molecular pharmacology* 61, 1154–1162.
- (48) Grand, C. L., Han, H., Muñoz, R. M., Weitman, S., Von Hoff, D. D., Hurley, L. H., and Bearss, D. J. (2002) The cationic porphyrin TMPyP4 down-regulates c-MYC and human telomerase reverse transcriptase expression and inhibits tumor growth in vivo. *Molecular cancer therapeutics* 1, 565–73.
- (49) Lombardo, C. M., Martínez, I. S., Haider, S., Gabelica, V., De Pauw, E., Moses, J. E., and Neidle, S. (2010) Structure-based design of selective high-affinity telomeric quadruplex-binding ligands. *Chemical communications (Cambridge, England)* 46, 9116–8.
- (50) Kim, M. Y., Vankayalapati, H., Shin-Ya, K., Wierzba, K., and Hurley, L. H. (2002) Telomestatin, a potent telomerase inhibitor that interacts quite specifically

with the human telomeric intramolecular G-quadruplex. *Journal of the American Chemical Society* 124, 2098–2099.

(51) Drygin, D., Siddiqui-Jain, A., O'Brien, S., Schwaebe, M., Lin, A., Bliesath, J., Ho, C. B., Proffitt, C., Trent, K., Whitten, J. P., Lim, J. K. C., Von Hoff, D., Anderes, K., and Rice, W. G. (2009) Anticancer activity of CX-3543: a direct inhibitor of rRNA biogenesis. *Cancer research* 69, 7653–61.

(52) Brooks, T. a, and Hurley, L. H. (2010) Targeting MYC Expression through G-Quadruplexes. *Genes & cancer* 1, 641–649.

(53) Patel, D. J. (1997) Structural analysis of nucleic acid aptamers. *Current opinion in chemical biology* 1, 32–46.

(54) Nimjee, S. M., Rusconi, C. P., and Sullenger, B. a. (2005) Aptamers: an emerging class of therapeutics. *Annual review of medicine* 56, 555–83.

(55) Tuerk, C., and Gold, L. (1990) Systematic evolution of ligands by exponential enrichment: RNA ligands to bacteriophage T4 DNA polymerase. *Science (New York, N.Y.)* 249, 505–10.

(56) Perry, C. M., and Balfour, J. A. (1999) Fomivirsen. *Drugs* 57, 375–380.

(57) Ng, E. W. M., Shima, D. T., Calias, P., Cunningham, E. T., Guyer, D. R., and Adamis, A. P. (2006) Pegaptanib, a targeted anti-VEGF aptamer for ocular vascular disease. *Nature reviews. Drug discovery* 5, 123–32.

(58) Bates, P. J., Laber, D. A., Miller, D. M., Thomas, S. D., and Trent, J. O. (2009) Discovery and development of the G-rich oligonucleotide AS1411 as a novel treatment for cancer. *Experimental and Molecular Pathology* 86, 151–164.

(59) Teng, Y., Girvan, A. C., Casson, L. K., Pierce, W. M., Qian, M., Thomas, S. D., and Bates, P. J. (2007) AS1411 alters the localization of a complex containing protein arginine methyltransferase 5 and nucleolin. *Cancer research* 67, 10491–500.

(60) Rosenberg, J. E., Bambury, R. M., Van Allen, E. M., Drabkin, H. a., Lara, P. N., Harzstark, A. L., Wagle, N., Figlin, R. a., Smith, G. W., Garraway, L. a., Choueiri, T., Erlandsson, F., and Laber, D. a. (2014) A phase II trial of AS1411 (a novel nucleolin-targeted DNA aptamer) in metastatic renal cell carcinoma. *Investigational New Drugs* 32, 178–187.

(61) Metifiot, M., Amrane, S., Litvak, S., and Andreola, M.-L. (2014) G-quadruplexes in viruses: function and potential therapeutic applications. *Nucleic Acids Research* 42, 12352–12366.

(62) Michalowski, D., Chitima-Matsiga, R., Held, D. M., and Burke, D. H. (2008) Novel bimodular DNA aptamers with guanosine quadruplexes inhibit phylogenetically diverse HIV-1 reverse transcriptases. *Nucleic acids research* 36, 7124–35.

- (63) Hannoush, R. N., Carriero, S., Min, K. L., and Damha, M. J. (2004) Selective inhibition of HIV-1 reverse transcriptase (HIV-1 RT) RNase H by small RNA hairpins and dumbbells. *ChemBioChem* 5, 527–533.
- (64) Greene, W. C., Debyser, Z., Ikeda, Y., Freed, E. O., Stephens, E., Yonemoto, W., Buckheit, R. W., Esté, J. A., and Cihlar, T. (2008) Novel targets for HIV therapy. *Antiviral Research* 80, 251–265.
- (65) Tilton, J. C., and Doms, R. W. (2010) Entry inhibitors in the treatment of HIV-1 infection. *Antiviral Research* 85, 91–100.
- (66) Esté, J. A., Cabrera, C., Schols, D., Cherepanov, P., Gutierrez, A., Witvrouw, M., Pannecouque, C., Debyser, Z., Rando, R. F., Clotet, B., Desmyter, J., and De Clercq, E. (1998) Human immunodeficiency virus glycoprotein gp120 as the primary target for the antiviral action of AR177 (Zintevir). *Molecular pharmacology* 53, 340–345.
- (67) Jing, N., and Hogan, M. E. (1998) Structure-Activity of Tetrad-forming Oligonucleotides as a Potent Anti-HIV Therapeutic Drug *. *Journal of Biological Chemistry* 273, 34992–34999.
- (68) De Soultrait, V. ., Lozach, P.-Y., Altmeyer, R., Tarrago-Litvak, L., Litvak, S., and Andréola, M. . (2002) DNA Aptamers Derived from HIV-1 RNase H Inhibitors are Strong Anti-integrase Agents. *Journal of Molecular Biology* 324, 195–203.
- (69) Phan, A. T., Kuryavyi, V., Ma, J.-B., Faure, A., Andréola, M.-L., and Patel, D. J. (2005) An interlocked dimeric parallel-stranded DNA quadruplex: a potent inhibitor of HIV-1 integrase. *Proceedings of the National Academy of Sciences of the United States of America* 102, 634–639.
- (70) Levy, J. A. (1993) Pathogenesis of human immunodeficiency virus infection. *Microbiological reviews* 57, 183–289.
- (71) Buckheit, R. W., Roberson, J. L., Lackman-Smith, C., Wyatt, J. R., Vickers, T. A., and Ecker, D. J. (1994) Potent and specific inhibition of HIV envelope-mediated cell fusion and virus binding by G quartet-forming oligonucleotide (ISIS 5320). *AIDS research and human retroviruses* 10, 1497–506.
- (72) Hotoda, H., Koizumi, M., Koga, R., Kaneko, M., Momota, K., and Ohmine, T. (1998) d (TGGGAG) Possesses Anti-Human Immunodeficiency Virus Type 1 Activity by Forming a G-Quadruplex Structure. *journal medicinal chemistry* 41, 3655–3663.
- (73) FURUKAWA, H., MOMOTA, K., AGATSUMA, T., YAMAMOTO, I., KIMURA, S., and SHIMADA, K. (1997) Identification of a Phosphodiester Hexanucleotide That Inhibits HIV-1 Infection In Vitro on Covalent Linkage of Its 5'-End with a Dimethoxytrityl Residue. *Antisense and Nucleic Acid Drug Development* 7, 167–175.
- (74) Koizumi, M., Koga, R., Hotoda, H., Momota, K., Ohmine, T., Furukawa, H., Agatsuma, T., Nishigaki, T., Abe, K., Kosaka, T., Tsutsumi, S., Sone, J., Kaneko, M., Kimura, S., and Shimada, K. (1997) Biologically active oligodeoxyribonucleotides-IX.

Synthesis and anti-HIV-1 activity of hexadeoxyribonucleotides, TGGGAG, bearing 3'- and 5'-end-modification. *Bioorganic and Medicinal Chemistry* 5, 2235–2243.

(75) Koizumi, M., Koga, R., Hotoda, H., Ohmine, T., Furukawa, H., Agatsuma, T., Nishigaki, T., Abe, K., Kosaka, T., Tsutsumi, S., Sone, J., Kaneko, M., Kimura, S., and Shimada, K. (1998) Biologically active oligodeoxyribonucleotides. Part 11: The least phosphate-modification of quadruplex-forming hexadeoxyribonucleotide TGGGAG, bearing 3'- and 5'-end-modification, with anti-HIV-1 activity. *Bioorganic and Medicinal Chemistry* 6, 2469–2475.

(76) D'Onofrio, J., Petraccone, L., Erra, E., Martino, L., Di Fabio, G., De Napoli, L., Giancola, C., and Montesarchio, D. (2007) 5'-Modified G-quadruplex forming oligonucleotides endowed with anti-HIV activity: Synthesis and biophysical properties. *Bioconjugate Chemistry* 18, 1194–1204.

(77) D'Onofrio, J., Petraccone, L., Martino, L., Di Fabio, G., Iadonisi, A., Baizarini, J., Giancola, C., and Montesarchio, D. (2008) Synthesis, biophysical characterization, and anti-HIV activity of glyco-conjugated G-quadruplex-forming oligonucleotides. *Bioconjugate Chemistry* 19, 607–616.

(78) Di Fabio, G., D'Onofrio, J., Chiapparelli, M., Hoorelbeke, B., Montesarchio, D., Balzarini, J., and De Napoli, L. (2011) Discovery of novel anti-HIV active G-quadruplex-forming oligonucleotides. *Chemical communications (Cambridge, England)* 47, 2363–2365.

(79) Romanucci, V., Milardi, D., Campagna, T., Gaglione, M., Messere, A., D'Urso, A., Crisafi, E., La Rosa, C., Zarrelli, A., Balzarini, J., and Di Fabio, G. (2014) Synthesis, biophysical characterization and anti-HIV activity of d(TG3AG) Quadruplexes bearing hydrophobic tails at the 5'-end. *Bioorganic & medicinal chemistry* 22, 960–6.

(80) Romanucci, V., Gaglione, M., Messere, A., Potenza, N., Zarrelli, A., Noppen, S., Liekens, S., Balzarini, J., and Di Fabio, G. (2015) Hairpin oligonucleotides forming G-quadruplexes: New aptamers with anti-HIV activity. *European Journal of Medicinal Chemistry* 89, 51–58.

(81) Chen, J. L.-Y., Sperry, J., Ip, N. Y., and Brimble, M. a. (2011) Natural products targeting telomere maintenance. *Medicinal Chemistry Communications* 2, 229.

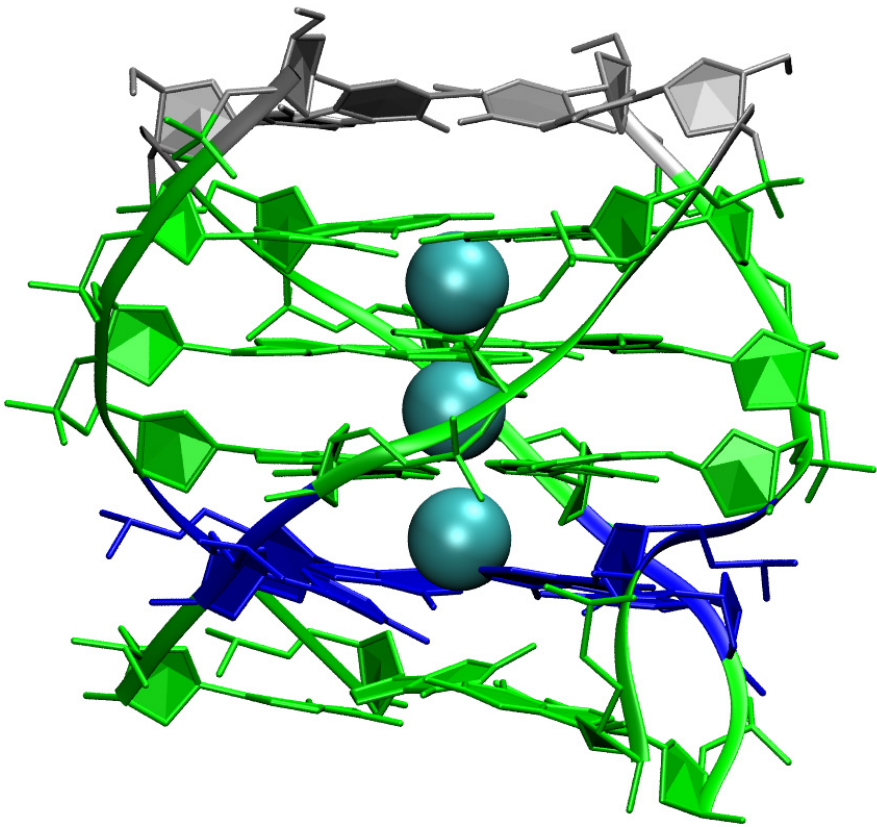
(82) Gazak, R., Walterova, D., and Kren, V. (2007, January) Silybin and Silymarin - New and Emerging Applications in Medicine. *Current Medicinal Chemistry*.

(83) Gallo, D., Giacomelli, S., Ferlini, C., Raspaglio, G., Apollonio, P., Prislei, S., Riva, A., Morazzoni, P., Bombardelli, E., and Scambia, G. (2003) Antitumour activity of the silybin-phosphatidylcholine complex, IdB 1016, against human ovarian cancer. *European Journal of Cancer* 39, 2403–2410.

(84) Zhao, H., Brandt, G. E., Galam, L., Matts, R. L., and Blagg, B. S. J. (2011) Identification and initial SAR of silybin: an Hsp90 inhibitor. *Bioorganic & medicinal chemistry letters* 21, 2659–64.

- (85) Huber, A., Thongphasuk, P., Erben, G., Lehmann, W. D., Tuma, S., Stremmel, W., and Chamulitrat, W. (2008) Significantly greater antioxidant anticancer activities of 2,3-dehydrosilybin than silybin. *Biochimica et Biophysica Acta* 1780, 837–847.
- (86) Morazzoni, P., Montalbetti, A., Malandrino, S., and Pifferi, G. (1993) Comparative pharmacokinetics of silipide and silymarin in rats. *European journal of drug metabolism and pharmacokinetics* 18, 289–297.
- (87) Zarrelli, A., Sgambato, A., Petito, V., De Napoli, L., Previtiera, L., and Di Fabio, G. (2011) New C-23 modified of silybin and 2,3-dehydrosilybin: Synthesis and preliminary evaluation of antioxidant properties. *Bioorganic and Medicinal Chemistry Letters* 21, 4389–4392.
- (88) Zarrelli, A., Romanucci, V., Greca, M. Della, De Napoli, L., Previtiera, L., and Di Fabio, G. (2013) New silybin scaffold for chemical diversification: Synthesis of novel 23-phosphodiester silybin conjugates. *Synlett* 24, 45–48.
- (89) Zarrelli, A., Romanucci, V., Tuccillo, C., Federico, A., Loguercio, C., Gravante, R., and Di Fabio, G. (2014) New silibinin glyco-conjugates: Synthesis and evaluation of antioxidant properties. *Bioorganic & Medicinal Chemistry Letters* 24, 5147–5149.
- (90) Zarrelli, A., Romanucci, V., De Napoli, L., Previtiera, L., and Di Fabio, G. (2015) Synthesis of New Silybin Derivatives and Evaluation of Their Antioxidant Properties. *Helvetica Chimica Acta* 98, 399–409.
- (91) Di Fabio, G., Romanucci, V., Di Marino, C., De Napoli, L., and Zarrelli, A. (2013) A rapid and simple chromatographic separation of diastereomers of silibinin and their oxidation to produce 2,3-dehydrosilybin enantiomers in an optically pure form. *Planta medica* 79, 1077–80.
- (92) Di Fabio, G., Romanucci, V., De Nisco, M., Pedatella, S., Di Marino, C., and Zarrelli, A. (2013) Microwave-assisted oxidation of silibinin: A simple and preparative method for the synthesis of improved radical scavengers. *Tetrahedron Letters* 54, 6279–6282.

G-Quadruplex



CHAPTER 2

Discovery of novel anti-HIV active G-quadruplex-forming oligonucleotides

The first stage of the HIV infection is the entry of human immunodeficiency virus (HIV) into host cells. This stage involves the attachment to host cells and CD4 binding, co-receptor binding, and membrane fusion (**Figure 1**). All of these stages are mediated by viral envelope proteins, gp120 and gp41, which are the only viral proteins that project from the membrane of the virion¹. This interaction is the initial event in the viral replicative cycle and consequently is an important target for therapeutic intervention.

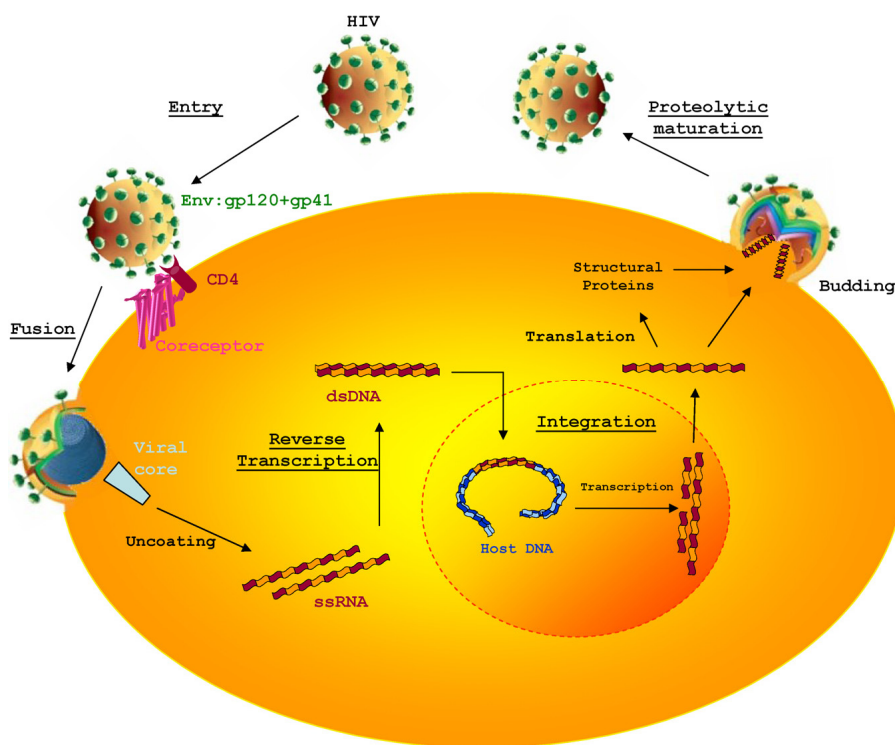


Figure 1. HIV replication cycle. The targets of approved antiretroviral agents are underlined, namely: virus entry, fusion, reverse transcription, integration and proteolytic maturation.

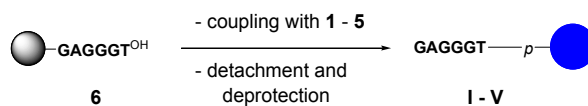
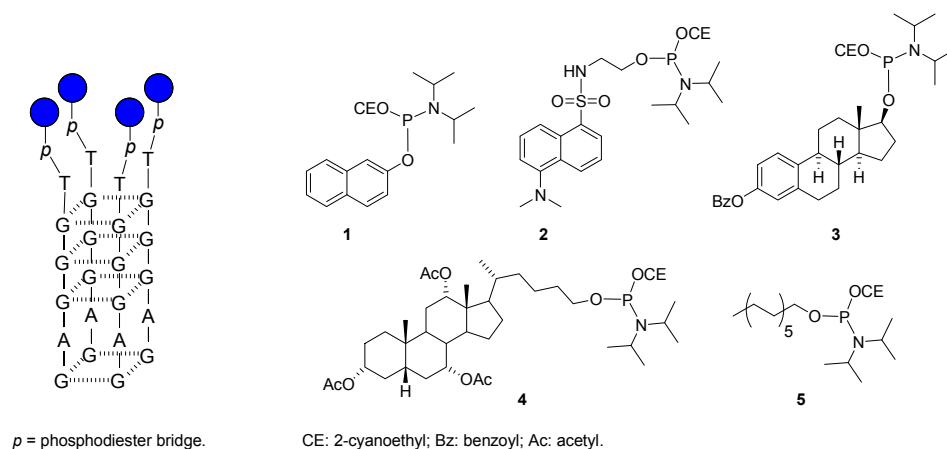
In this frame, G-quadruplex based aptamers have been successfully designed to target the HIV virus at different stages of its life cycle. Some examples targeting glycoprotein gp120 of HIV virus, have been reported as anti-HIV aptamers among which the ODN phosphorothioate **ISIS-5320**^{2,3} and Hotoda modified sequence **R-95288**, both forming tetramolecular G-quadruplex structure^{4,5}.

Recently, in order to improve aptamers' bioavailability and pharmacokinetic profiles, some chemical modifications have been described that affect the nucleobases⁶, the backbone^{7,8} and 3' and 5'-ends, in addition to the introduction of inversion of polarity sites and natural or non-nucleosidic linkers⁹⁻¹¹. The structural variability of G-quadruplexes is further increased by these modifications. Moreover, in 2011, Di Fabio et. al synthesized a mini-library of 5'-end modified d(TGGGAG) oligomers, bearing different aromatic groups at 5'-end with potent inhibition of HIV-1 infection¹². Surface Plasmon Resonance (SPR) assays revealed specific binding to HIV-1 gp120 and gp41. Circular dichroism (CD) and Differential scanning calorimetry (DSC) studies conducted on these modified oligonucleotides, revealed once again, the importance of the aromatic groups at 5'-end for the thermal stability of G-quadruplex complexes and therefore for their anti-HIV activity. Given the importance of G-quadruplexes forming ODNs as potent anti-HIV inhibitors, in order to extend the number of modified ODNs and to perform a detailed study of the structure-activity relationship on modified d(TGGGAG), we synthesized and biophysically and biologically characterized a mini-library of new d(TGGGAG) oligomers with different type of modification at 5'-end, potential inhibitors of HIV infection. In addition in order to improve the slow kinetics of tetramolecular G-quadruplex formation, we

designed and synthesized new modified bimolecular G-quadruplexes (Hairpin ODNs) using the same lead sequence d(TGGGAG).

2.1. Synthesis, biophysical characterization and anti-HIV activity of d(TGGGAG) Quadruplexes bearing hydrophobic tails at the 5'-end

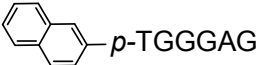
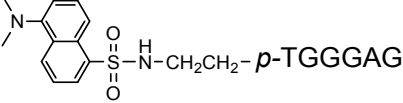
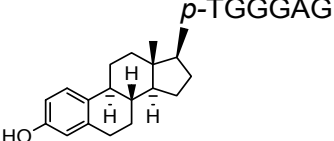
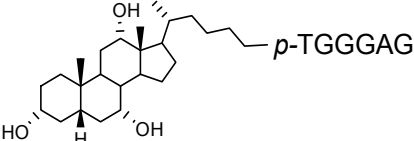
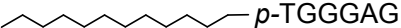
Aiming at extending the number of more efficient oligonucleotide-based antivirals, we developed an efficient procedure to synthesize a new mini-library of d(TGGGAG) oligomers carrying hydrophobic and aromatic groups at the 5'-end by a phosphodiester bond. The choice of conjugated groups aim to improve cellular uptake, the half-life of these molecules in plasma and especially to stabilize DNA structures by hydrophobic interactions.



Scheme 1. Phosphoramidite building blocks 1–5 and synthetic scheme for the preparation of conjugated oligonucleotides I–V.

The synthesis of 5'-modified oligomers initially started by the conversion of commercially available selected alcohols into the corresponding phosphoramidite derivatives (**Scheme 1**) by reaction

with 2-cyanoethyl-N,N-diisopropylaminochloro-phosphoramidite and N,N-diisopropylethylamine (DIEA) in dichloromethane anhydrous (DCM). The identity of compounds **1–5**, all obtained in good yields (85%), was confirmed by NMR (^1H and ^{31}P) and MS data. Simultaneously the scaffold **6** (**Scheme 1**) was synthesized using standard solid phase β -cyanoethylphosphoramidite chemistry protocols starting from a commercially available DMT-protected guanosine functionalized CPG support^{13,14}. Phosphoramidite derivatives **1–5** (**Figure 1**) were exploited in the last coupling step of the ODN chain assembly.

Table 1. Oligonucleotide Characterization		
	Sequence (5'-3')	MS <i>calcd for [M]</i> data (found)
I	 <i>p</i> -TGGGAG	<i>2077.37</i> 2078.64 [MH] ⁺ 2101.23 [MNa] ⁺
II	 <i>p</i> -TGGGAG	<i>2227.42</i> 2228.25 [MH] ⁺ 2250.84 [MNa] ⁺
III	 <i>p</i> -TGGGAG	<i>2205.49</i> 2206.54 [MH] ⁺ 2228.28 [MNa] ⁺
IV	 <i>p</i> -TGGGAG	<i>2341.64</i> 2342.59 [MH] ⁺ 2365.87 [MNa] ⁺ 2380.46 [MK] ⁺
V	 <i>p</i> -TGGGAG	<i>2119.51</i> 2120.46 [MH] ⁺ 2145.21 [MNa] ⁺

^a: for HPLC conditions see Experimental Session

The resulting supports were reacted with triethylamine (Et₃N)/pyridine (1:1, v/v), at 50°C for 1 h, followed by treatment with conc. aq. ammonia at 50°C for 5 h, allowing full deprotection and detachment from the solid support of target oligomers I–V. The combined filtrates and washings were concentrated in vacuo, dissolved in H₂O, analyzed and purified by HPLC. The modified oligonucleotides were characterized by MALDI-TOF mass spectrometry, in all cases giving masses in accordance with the expected values (Table 1).

- **CD studies and characterization**

In order to study the influence of the aromatic groups at the 5'-end of the oligonucleotide chains on their ability to form G-quadruplex structures, a CD analysis was undertaken on oligomers I–V in comparison with the corresponding unmodified d(TGGGAG). CD spectroscopy can be used to obtain details about the G-quadruplex structures by comparing their spectra with those of G-quadruplex DNAs with known conformations. **Figure 2** shows the CD spectra of all oligonucleotides at temperatures ranging from 15 to 90°C in the same buffer conditions. Overall CD spectra recorded at 15°C show a positive peak at 260 nm and a small negative band around 240 nm. These spectral shapes are consistent with the reported spectra of other d(TGGGAG) sequences¹⁵ and clearly indicate that all of the strands fold into a parallel strand structures¹⁶. The melting temperature values (Table 2) were determined from the CD melting profiles for conjugates I–V monitored at 263 nm with an heating rate of 1°C/min (Figure 4, bottom). All denaturation curves did not reflect an equilibrium process, and the apparent melting temperatures 'T_m' or 'T_{1/2}' determined by CD, strongly depend on the rate of heating¹⁷.

A direct comparison of the CD and DSC data obtained for identical samples can be used to rule out the possibility of incompletely formed G-quadruplexes before heating and provide a more detailed description of the thermal transitions. All heating runs were fully irreversible.

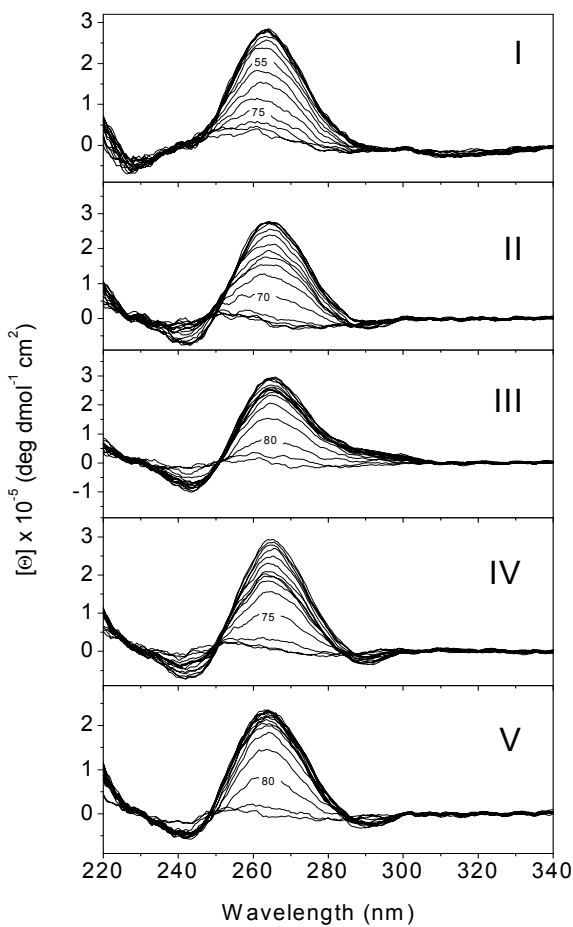


Figure 2. CD spectra of I–V. The spectra were collected at 15°C and at steps of 5°C up to 90°C in a 10mM potassium phosphate buffer (pH 7.0), supplemented with 200mM KCl, at 10 μ M of single strand. To guide the eye throughout the figures, some representative curves are marked with the temperature at which the CD signal was recorded.

Therefore, neither an extrapolation of the thermodynamic parameters ΔG and ΔS from the melting curves nor a deconvolution of the C_p curves by statistical mechanic methods were possible.

Table 2. Thermodynamic parameters for the thermally-induced Quadruplex dissociation

Sequences	CD		DSC			
	T_m ($^{\circ}\text{C}$) ± 1		T_m ($^{\circ}\text{C}$) ± 1		$\Delta H^{\circ}_{\text{cal}}$ (KJmol^{-1})	
	1 st	2 nd	1 st	2 nd	1 st	2 nd
I	Nd	56	nd	61	nd	314 \pm 15
II	46	71	46	74	nd	305 \pm 10
III	33	79	33	90	15 \pm 5	124 \pm 11
IV	45	79	45	81	24 \pm 15	252 \pm 15
V	Nd	76	nd	84	nd	182 \pm 10

[†]The same sample was splitted in two parts used in parallel for CD and DSC analysis.

Consequently, in these non-equilibrium conditions only the enthalpy change relative to the G-quadruplex dissociation process may be directly obtained¹⁸. For compound **I**, DSC runs exhibited a broad monophasic peak centred at $T_m = 60^{\circ}\text{C}$ and $\Delta H_{\text{cal}} = 314 \text{ kJ mol}^{-1}$ (**Figure 3**), which indicates the formation of four G-tetrads, as reported elsewhere. The melting temperature of compound **I** derived from the DSC curves was 4°C higher than that obtained from the CD results. This difference in the melting temperatures may be ascribed to the asymmetry of the calorimetric trace. The CD melting curve of compound **II** shows biphasic behaviour with a first melting point centred at 46°C and a second one observed at 71°C (**Figure 3**, bottom).

The corresponding DSC curve shows a large asymmetric peak with a maximum at 73°C and a small shoulder at 46°C (**Figure 3**, top). The overall calorimetric enthalpy of this peak is 305 kJ mol^{-1} .

Biphasic behaviour is observed in the CD melting curve of compound **III**; the first transition is observed at 33°C, and the second transition is observed at 79°C.

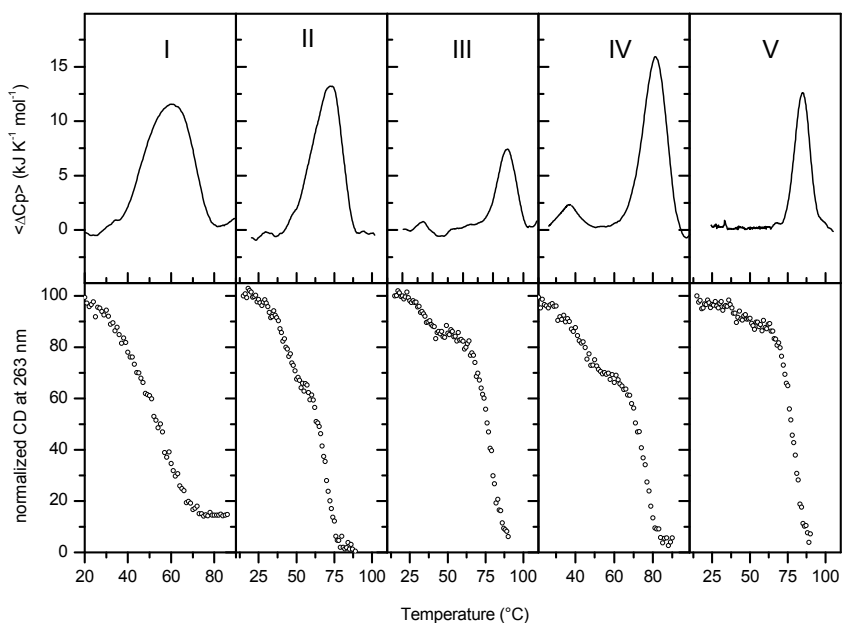


Figure 3. DSC (top) and CD (bottom) melting profiles of **I–V**.

The DSC curve of compound **III** shows an endothermic peak at 33°C corresponding to the CD transition and a second, distinct peak at 89°C. The calorimetric enthalpies for these two transitions are 15 and 124 kJ mol⁻¹, respectively. The CD melting profile of compound **IV** exhibits biphasic behaviour, with the first transition at 45°C and a second transition at 79°C. The corresponding DSC curve shows an initial, smaller peak at 45°C and a second peak at 81°C. The calorimetric enthalpies for the two transitions are 24 and 252 kJ mol⁻¹, respectively. Finally, the CD melting profile of compound **V** shows a single transition at 76°C. The DSC curve of compound **V** shows

monophasic behaviour, with an endothermic peak centred at 84°C with a calorimetric enthalpy of 188 kJ mol⁻¹. Several research groups have reported that modified G-quadruplex d(TGGGAG) sequences are stabilized at increasing melting temperatures relative to the parent unmodified sequence^{12,15}.

Our results (**Table 2**) are consistent with these reports; however, we found that the melting of many of these structures is not a simple two-state process, as assumed in previous studies. Although the irreversible nature of the melting processes of the studied assemblies made a thorough analysis of the $\langle \Delta C_p \rangle$ curves in thermodynamic terms difficult, our integrated CD and DSC dissociation studies provide a better understanding of the complexities in the melting mechanism. The CD melting data for compounds **II**, **III** and **IV** clearly show that these G-quadruplex structures deviate from a simple two-state melting and support the hypothesis that intermediate states along the dissociation pathway may exist. Such complex behaviour is consistent with the analysis of the DSC thermograms. However, the existence of intermediates along the broad melting curve of compound **I** cannot be excluded. It should be noted that the folding/unfolding reactions of G-quadruplexes are almost always assumed for convenience to be two-state processes, with negligible concentrations of any intermediate species along the melting pathway¹⁹⁻²¹. A thermally dependent equilibrium between two G-quadruplex isoforms with different stabilities would explain the biphasic melting curves observed. Lower thermal stability is generally attributed to flanking inter-strand contacts at the edges of the G-quadruplex structures. Another interpretation of this biphasic transition observed by CD melting curve and DSC profile it has been reported by Balasubramaniann and coworkers²², they ascribed a biphasic

transition of d(GGGT) to the formation of an high order DNA structure^{23,24}, more exactly to interlocked quadruplex dimer by d(GGGT).

- **Anti-HIV activity and Surface Plasmon Resonance (SPR): directed affinity binding analyses for the HIV envelope.**

Compounds **I–V** were evaluated for their anti-HIV-1 and -HIV-2 activities in CEM cell cultures (**Table 3**). All compounds showed pronounced anti-HIV activities, with some preference for HIV-1. This inhibitory activity (except compound **I**) was invariably in the low micromolar range [50% effective concentration (EC₅₀): 4.9–10 μM for HIV-1 and 6.7–32 μM for HIV-2]. Compound **I** was clearly less inhibitory (EC₅₀ >8 μM for HIV-1 and 69 μM for HIV-2).

Table 3. Antiviral (HIV) and RT activities of test compounds in CEM cell cultures.

Sequences	EC ₅₀ ^a (μM)		IC ₅₀ ^b (μM)
	HIV-1(III _B)	HIV-2(ROD)	RT (Pol.rC.dG)
I	>8	69 ± 18	n. d.
II	10 ± 4.5	32 ± 0.0	>30
III	4.9 ± 0.3	6.7 ± 1.9	2.5 ± 0.63
IV	6.9 ± 1.8	12 ± 9.8	>30
V	5.4 ± 0.2	≥ 8	6.72 ± 0.48

^a50% Effective concentration or compound concentration required to inhibit HIV-induced cytopathicity by 50% in CEM cell cultures. ^b50% inhibitory concentration required to inhibit the RT reaction by 50%

A concentration higher than 8 μM could not be microscopically scored due to unexplained toxicity in the HIV-1-infected (but not HIV-2-infected) CEM cell cultures. In light of the thermodynamic data and biological activity, it is reasonable to conclude that the nature of the 5'-end modification on the d(TGGGAG) quadruplexes played only a

minor role in the anti-HIV activity. Because the conjugated G-quadruplexes may inhibit HIV entry into its target cells due to their negative charge, conjugates **II–V** were also evaluated for their affinity to HIV envelope gp120 and gp41, as well as human serum albumin (HSA) as a control, by SPR technology (**Table 4**) and for their inhibitory effect against HIV-1 reverse transcriptase (RT).

The biosensor chips for the SPR analyses were loaded with 3531 RU gp120, 3091 RU gp41, or 3333 RU HSA and exposed to 1 OD/ml of the compounds. A binding signal was recorded for each of the compounds against the three proteins. However, the binding amplitudes measured after compound exposure to the protein for 120 s differed significantly depending on the nature of the compound and the glycoprotein evaluated.

Table 4. Interaction of the quadruplex derivatives with viral and human glycoproteins

Sequences	Amplitude of the SPR signal (RU) ^a		
	HIV-1 gp120	HIV-1 gp41	HSA ^b
II	0.4	4.0	13
III	8.7	28	45
IV	4.7	35	6.0
V	0.1	21	21

^aAmplitude of the SPR signal was measured after 120 sec exposure of the compounds to the glycoproteins. ^bHuman Serum Albumin.

The compounds **III** and **IV** showed a clear binding capacity (amplitude range: 4.7–8.7 RU) to gp120 whereas **II** and **V** showed poor, if any binding. Compounds **III**, **IV** and **V** were by far superior for binding to gp41, and compound **III** showed the strongest binding to HSA (**Table 4**).

Compounds **III** and **V** bound to HSA better than to gp41. In the HIV-1 RT experiments, **II**, **III**, **IV** and **V** showed varying inhibitory activities (**I** was not evaluated). Their IC₅₀ values were in the range 2.5–69 μM, respectively, when using poly rC.dG as the template/primer and radio-labeled [³H] dGTP as the substrate (**Table 3**). Considering all of the SPR data, there does not appear to be any selectivity for gp120 or gp41 binding compared with HSA binding. Also, no correlation between anti-HIV-1 and anti-RT activity was found. Therefore, it remains unclear whether selective binding to the HIV envelope or RT inhibition represents a mechanism for the selective antiviral action of these conjugates. The affinity of the synthetic oligonucleotides (**II–V**) for HSA is an interesting finding because the use of albumin as a versatile drug carrier in anti-HIV strategy is increasing. In fact, many albumin-based formulations have received market approval or are being evaluated in clinical trials²⁵.

2.1.2 Experimental Session

General procedures. Starting compounds for the synthesis of phosphoramidites **1–5** were all purchased from Sigma-Aldrich. TLC analyses were carried out on silica gel plates from Merck (Kieselgel 60, *F254*). Reaction products were visualized on TLC plates by UV light and then by treatment with a H₂SO₄/AcOH aqueous solution. For column chromatography, silica gel from Merck (Kieselgel 40, 0.063–0.200 mm) was used. NMR spectra were recorded in CDCl₃ with a Bruker WM 400 spectrometer. The chemical shifts (δ) are given in ppm with respect to the residual solvent signal (7.26 ppm), and the coupling constants (J) are in Hz. ³¹P NMR spectra were recorded at 161.98 MHz on a Bruker WM-400 spectrometer using 85% H₃PO₄ as an external standard. MALDI TOF mass spectrometric analyses were performed on a PerSeptive Biosystems Voyager–De Pro MALDI mass spectrometer in the linear mode using a picolinic/3-hydroxypicolinic/sinapinic acid mixture as the matrix. For the ESI MS analyses, a Waters Micromass ZQ instrument equipped with an Electrospray source was used in the positive mode. HPLC analyses were performed on an Agilent Technologies 1200 series instrument equipped with a UV detector. The crude material was analysed and purified by HPLC on a Nucleogel SAX column (Macherey–Nagel, 1000–8/46) or Phenomenex RP18 column [LUNA, 5 μ m C18(2), 10.0 \times 250 mm]. Desalting was carried out by gel filtration chromatography on a Sephadex G25 column eluted with H₂O/EtOH 4:1 (v/v).

General procedure for the Preparation of Phosphoramidite 1–5. 1.26 mmol of alcohol was dissolved in 10 mL of anhydrous dichloromethane, and 880 μ L DIEA (5.05 mmol) and 565 μ L 2-cyanoethyl-N,N-diisopropylamino-chlorophosphoramidite (2.52 mmol)

were added under argon. After 30 minutes, the solution was diluted with ethyl acetate, and the organic phase was washed twice with brine and then concentrated. Silica gel chromatography of the residue (eluent hexane/ethyl acetate) afforded the desired compounds (1-5).

2-naphthol-[O-(2-cyanoethyl)-N,N'-diisopropylphosphoramidite] (1):

Starting from 2-naphthol (181 mg, 1.26 mmol) and following the general procedure, the compound **1** was obtained (368 mg, 85 % yield); *Compound 1* ¹H NMR (CDCl₃, 400 MHz): δ 7.58 (3H, overlapped signals, H-4, H-8 and H-5), 7.15 (2H, overlapped signals, H-7 and H-9), 7.17 (1H, m, H-1), 7.04 (1H, d, *J* = 8.5 Hz, H-3), 3.73 (2H, m, OCH₂CH₂CN), 3.56 (2H, m, N[CH(CH₃)₂]₂), 2.46 (2H, t, *J* = 8.0 Hz, OCH₂CH₂CN), 1.04 (6H, d, *J* = 8.0 Hz, N[CH(CH₃)₂]₂), 0.98 (6H, d, *J* = 8.0 Hz, N[CH(CH₃)₂]₂); ¹³C NMR (CDCl₃, 75 MHz): δ. 151.8, 134.0, 129.5, 129.1, 127.4, 126.8, 126.0, 124.0, 121.1, 117.4, 114.7, 58.7, 43.4, 24.2, 24.0, 20.3, 19.9. ³¹P NMR (CDCl₃, 161.98 MHz): δ 149.2. ESI-MS: calculated for C₂₀H₂₆NO₂P 343.17. Found (positive ions): 344.26 (M-H)⁺.

5-(dimethylamino)-N-(2-hydroxyethyl)-[O-(2-cyanoethyl)-N,N'-

diisopropylphosphoramidite]naphthalene-1-sulfonamide (2): Starting

from 5-(dimethylamino)-N-(2-hydroxyethyl)naphthalene-1-sulfonamide (370 mg, 1.26 mmol) and following the general procedure, the compound **2** was obtained (620 mg, 81 % yield); *Compound 2* ¹H NMR (CDCl₃, 400 MHz, 20 °C, mixture of enantiomers): δ 8.53 (1H, d, *J* = 8.4 Hz), 8.30 (1H, d, *J* = 8.4 Hz), 8.24 (1H, d, *J* = 7.2 Hz), 7.53 (2H, m), 7.18 (1H, d, *J* = 7.6 Hz), 3.75–3.44 (6H, overlapped signals, OCH₂CH₂CN, NHCH₂CH₂O and N[CH(CH₃)₂]₂), 3.08 (2H, m, NHCH₂CH₂O), 2.86 (6H, s, NCH₃), 2.55 (2H, m, OCH₂CH₂CN), 1.25 (6H, d, *J* = 6.6 Hz, N[CH(CH₃)₂]₂), 1.04

(6H, d, $J = 6.7$ Hz, $\text{N}[\text{CH}(\text{CH}_3)_2]_2$). ^{13}C NMR (CDCl_3 , 75 MHz): δ 151.9, 130.3, 129.7, 129.4, 128.3, 123.1, 119.6, 118.6, 117.6, 115.1, 62.2, 58.3, 45.3, 44.1, 42.9, 24.4, 20.1. ^{31}P NMR (CDCl_3 , 161.98 MHz): δ 151.7. ESI-MS: calculated for $\text{C}_{34}\text{H}_{61}\text{N}_2\text{O}_5\text{P}$ 608.43. Found (positive ions): 609.51 (M-H)⁺.

β -Estradiol-3-benzoate-17-hydroxy-[O-(2-cyanoethyl)-N,N'-

diisopropylphosphoramidite] (**3**): Starting from β -Estradiol-3-benzoate (475 mg, 1.26 mmol) and following the general procedure, the compound **3** was obtained (459 mg, 77 % yield); *Compound 3* ^1H NMR (CDCl_3 , 400 MHz, 20 °C, mixture of diastereoisomers): δ 8.23 (2H, d, $J = 7.6$ Hz), 7.63 (1H, t, $J = 7.6$ Hz), 7.51 (2H, t, $J = 7.6$ Hz), 7.33 (1H, dd, $J = 8.4, 3.2$ Hz), 6.97 (1H, d, $J = 8.4$ Hz), 6.93 (1H, s), 3.80–3.76 (3H, complex signal, $\text{OCH}_2\text{CH}_2\text{CN}$, H-17 of β -estradiol residue), 3.64–3.58 (2H, complex signal, $\text{N}[\text{CH}(\text{CH}_3)_2]_2$). ^{13}C NMR (75 MHz, CDCl_3): δ 165.4, 148.6, 138.3, 138.1, 133.4, 130.1, 129.6, 128.5, 126.4, 121.6, 118.6, 117.8, 83.7, 82.5, 58.4, 57.8, 49.7, 44.1, 43.5, 42.9, 38.4, 37.2, 36.9, 29.6, 26.9, 26.1, 24.6, 23.2, 20.4, 11.9, 11.7. ^{31}P NMR (161.98 MHz, CDCl_3): δ 150.5, 149.5. ^{31}P NMR (CDCl_3 , 161.98 MHz): δ 150.5, 149.5. ESI-MS: calculated for $\text{C}_{27}\text{H}_{41}\text{N}_2\text{O}_3\text{P}$ 473.29. Found (positive ions): 474.69 (M-H)⁺.

3- α ,7- α ,12- α -tri-O-acetyl-24-hydroxy-[O-(2-cyanoethyl)-N,N'-diisopropylphosphoramidite]-cholane (**4**): 3- α ,7- α ,12- α -24-tetrahydroxycholane (1.0 g, 2.54 mmol) was dissolved in anhydrous pyridine (15 mL), was reacted with DMTCl (1.30 g, 3.05 mmol). The reaction mixture, left at room temperature overnight under stirring, was then diluted with CH_3OH and concentrated under reduced pressure. The crude was next purified on a silica gel column, eluted with DCM containing growing amounts of CH_3OH (from 1 to

5%) in the presence of a few drops of triethylamine, affording pure 3- α ,7- α ,12- α -24-O-DMT-tetrahydrocholane (1.53 g, 85%). The compound thus obtained, dissolved in anhydrous pyridine (15 mL), was reacted with Ac₂O (5 mL). The mixture was left under stirring at room temperature 5 h and then quenched by addition of a few drops of CH₃OH. The mixture, concentrated under reduced pressure, was diluted with CHCl₃, transferred into a separatory funnel, and washed three times with a saturated NaHCO₃ aqueous solution and then twice with water. The organic phase, dried over anhydrous Na₂SO₄ and filtered, was then concentrated under reduced pressure, furnishing the desired product 3- α ,7- α ,12- α -tri-O-acetyl-24-O-DMT-cholane, in an almost quantitative yield. A solution of iodine (150 mg, 0.55 mmol) in 10 mL of anhydrous CH₃OH was added to the above product (1.5g, 1.81 mmol). The mixture was stirred vigorously at room temperature for 2h, then, sodium thiosulfate solution was added to remove excess iodine. The reaction mixture was extracted with DCM. The organic phase was combined, washed with water, dried over anhydrous Na₂SO₄, and the solvent was removed under reduced pressure. The crude product was purified by chromatography on silica gel column (eluent CHCl₃/n-hexane, 9:1, v/v) to give a desired 3- α ,7- α ,12- α -tri-O-acetyl-24-hydroxycholane (1.26 mmol, 69% yield).

Starting from 3- α ,7- α ,12- α -tri-O-acetyl-24-hydroxycholane (660 mg, 1.26 mmol) and following the general procedure, the compound **4** was obtained (600 mg, 80 % yield); *Compound 4* ¹H NMR (CDCl₃, 400 MHz, 20 °C, mixture of diastereoisomers): δ 5.02 (1H, br s), 4.90 (1H, br s), 4.58 (1H, m), 4.09 (2H, t, $J = 5.0$ Hz), 3.80 (2H, complex signals), 3.58 (4H, complex signals), 2.63 (2H, t, $J = 6.3$ Hz), 2.13 (3H, s), 2.08 (3H, s), 2.05 (3H, s),

1.95-0.65 (45H, complex signals). ^{13}C NMR (CDCl_3 , 75 MHz): δ 169.0, 169.1, 168.7, 74.2, 73.0, 69.2, 63.8, 60.2, 48.5, 47.6, 43.3, 43.1, 42.3, 41.2, 40.6, 37.2, 36.6, 36.0, 33.4, 31.3, 30.8, 30.5, 29.7, 28.9, 28.0, 25.4, 24.4, 23.3, 23.0, 20.02, 18.2, 13.1. ^{31}P NMR (CDCl_3 , 161.98 MHz): δ 151.7, 150.7. ESI-MS: calculated for $\text{C}_{33}\text{H}_{59}\text{N}_2\text{O}_5\text{P}$ 594.42 Found (positive ions): 595.32 ($\text{M}\cdot\text{H}$) $^+$.

1-dodecanol-[O-(2-cyanoethyl)-N,N'-diisopropylphosphoramidite] (**5**): Starting from 1-dodecanol (235 mg, 1.26 mmol) and following the general procedure, the compound **5** was obtained (380 mg, 78 % yield); *Compound 5* ^1H NMR (CDCl_3 , 400 MHz, 20 °C, mixture of enantiomers): δ 3.80 (2H, m, $\text{OCH}_2\text{CH}_2\text{CN}$), 3.58 (4H, complex signals, $\text{N}[\text{CH}(\text{CH}_3)_2]_2$, $\text{OCH}_2\text{CH}_2(\text{CH}_2)_9\text{CH}_3$), 2.63 (2H, t, $J = 6.3$ Hz, $\text{OCH}_2\text{CH}_2\text{CN}$), 1.56 (2H, m, $\text{OCH}_2\text{CH}_2(\text{CH}_2)_9\text{CH}_3$), 1.34-1.12 (30H, m, $\text{N}[\text{CH}(\text{CH}_3)_2]_2$, $\text{OCH}_2\text{CH}_2(\text{CH}_2)_9\text{CH}_3$), 0.87 (3H, t, $J = 6.0$ Hz). ^{13}C NMR (CDCl_3 , 75 MHz): δ 119.4, 63.7, 58.3, 42.9, 31.9, 31.2, 29.8, 29.6, 29.5, 26.1, 24.5, 22.6, 20.3, 14.0. ^{31}P NMR (CDCl_3 , 161.98 MHz): δ 152.9. ESI-MS: calculated for $\text{C}_{21}\text{H}_{43}\text{N}_2\text{O}_2\text{P}$ 386.31. Found (positive ions): 387.55 ($\text{M}\cdot\text{H}$) $^+$.

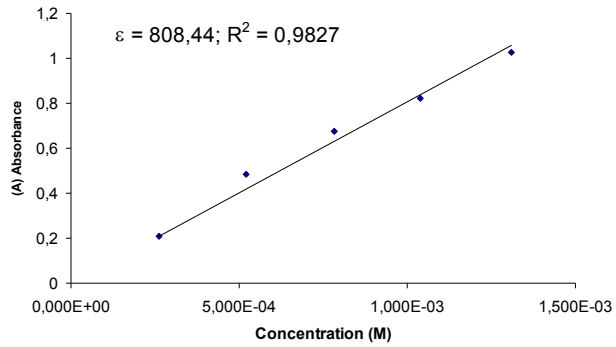
Synthesis and Characterisation of ODNs (I-V). As depicted in **Scheme 1**, oligomers **I-V** were synthesised, starting from functionalised CPG support **6** with 0.07-0.08 meq/g initial loading, on which the sequence d(TGGGAG) was assembled in a standard manner. Starting with 100 mg of commercially available CPG-dG support with 0.10 meq/g initial loading, and after the assembly of the sequence d(TGGGA), an additional coupling with phosphoramidite building blocks **1-5** was then performed. Target oligomers **I-V** were detached from the solid support and deprotected by treatment with Et_3N /pyridine (1:1, v/v) at 50 °C for 1 h, followed by treatment with conc. aq. ammonia at 50 °C

for 5 h. The combined filtrates and washings were concentrated under reduced pressure, re-dissolved in H₂O, and analysed and purified by HPLC. Purification of the crude conjugated oligonucleotides **I-V** was carried out on Phenomenex RP18 column or RP18 column (LUNA, 5µm C18(2), 10.0 × 250 mm) using a linear gradient of CH₃CN in 0.1 M AcNH₄ in H₂O, pH 7.0 from 5% to 100% over 30 min at a flow rate of 1.5 mL/min with detection at 260 nm. In all cases 50-80 OD units of pure **I-V** could be on average recovered starting from 100 mg of functionalized solid support (average yields 10-25%).

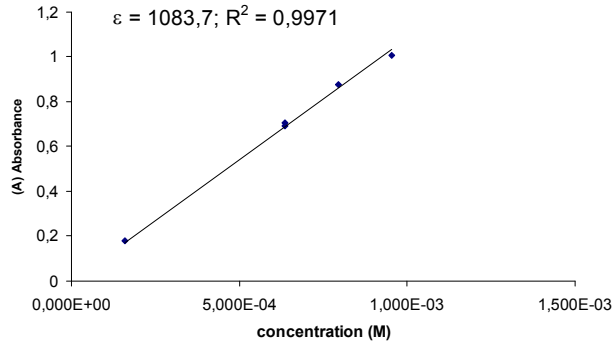
Quadruplexes Preparation. The quadruplex complexes were obtained by dissolving the lyophilized oligonucleotide at a single strand concentration of 1×10⁻⁴ M in the appropriate buffer. The solution was then annealed by heating at 90°C for 5 min and slow cooling to room temperature. The buffer used was 10mM potassium phosphate, 200mM KCl, 0.1mM EDTA at pH 7.0. The concentration of the dissolved oligonucleotides **I-V** was determined by UV measurements at 260 nm and at 95°C, using, as the molar extinction coefficients, the values calculated by the nearest neighbour model for the sequence d(TGGGAG), and the values experimentally calculated for labels **1-3** (808, 1083, and 703 cm⁻¹ M⁻¹, respectively).

General procedure for determination of the corresponding ε values for 1-3 labels. Determination of the ε values at 25°C for labels **1-3** was carried out by averaging at least five independent A²⁶⁰ measurements of the water soluble samples at different known concentrations (see graphics), allowing to determine the following ε data: 808, 1083 and 703 cm⁻¹ M⁻¹, respectively for 1-naphthyl phosphate disodium salt, 5-(dimethylamino)-1-naphthalenesulfonic acid and β-estradiol 17-(β-D-glucuronide) sodium salt which purchased from Sigma-Aldrich.

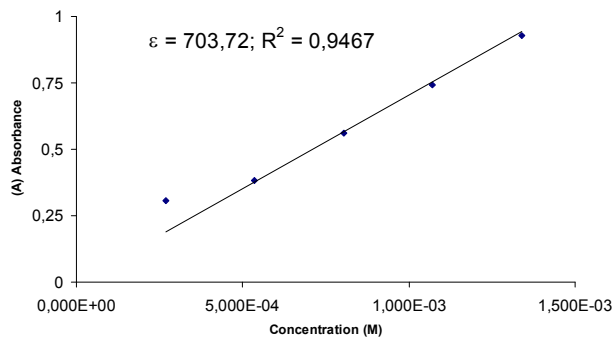
Molar extinction coefficient (ϵ_{260}) in H₂O of
1-Naphthyl phosphate disodium salt.



Molar extinction coefficient (ϵ_{260}) in H₂O of
5-(Dimethylamino)-1-naphthalenesulfonic acid.



Molar extinction coefficient (ϵ_{260}) in H₂O of
 β -Estradiol 17-(β -D-glucuronide) sodium salt.



CD Experiments. CD spectra were recorded by a JASCO J-810 spectropolarimeter equipped with a thermostatically controlled accessory (JASCO PTC-348), using a quartz cuvette with a 0.5 cm optical path. CD spectra were collected from 220 to 340 nm, at 20 nm/min, with a response time of 4 s and at 1 nm bandwidth. The CD signal of the buffer was subtracted from all CD spectra, corresponding to an average of 5 scans. The molar ellipticity was calculated by the equation $[\theta] = 100 \theta / cl$ where θ is the ellipticity value, c is the concentration of the single strand (1.0×10^{-5} M), and l is the path length of the cell in cm. The thermally-induced dissociation of the quadruplexes was studied by monitoring the CD signal at 263 nm upon increasing the temperature from 15 to 90°C (heating rate = 1°C/min). The melting temperatures were calculated from the peaks of the first derivative of the CD signal *vs* T.

DSC experiments. DSC runs were all performed by a VP-DSC calorimeter (MicroCal). All samples, after a degassing process, were scanned at a heating rate of 1°C min⁻¹ in the temperature range 20–120°C in the same experimental conditions adopted for the CD experiments. An extra external pressure of about 29 psi was applied to the solution to prevent the formation of air bubbles during heating. To ensure a complete equilibration of the calorimeter, several buffer–buffer heating scans were routinely performed prior to the measurement. Only after obtaining invariant buffer–buffer baselines samples were scanned. Additional buffer–buffer baselines were obtained immediately after the protein scans to double-check for uncontrolled drifts in instrumental baseline. For each sample, three independent DSC experiments were carried out under the same buffer conditions. To obtain the heat capacity C_p curves, buffer–buffer base lines were recorded at the same scanning rate and then

subtracted from sample curves, as previously described²⁶. In all experiments, one or several heating–cooling cycles were carried out to determine the reversibility of the denaturation process. To obtain the excess heat capacity profiles $\langle\Delta C_p\rangle$, the DSC curves, after instrumental baseline correction, were subtracted from a baseline obtained by a third-order polynomial fit of the pre- and post-transition C_p trends as reported elsewhere^{27–29}. Melting temperatures were calculated from the maximum C_p value of the DSC curve.

Anti-HIV experiments. Inhibition of HIV-1(III_B)- and HIV-2(ROD)-induced cytopathicity in CEM cell cultures was measured in microliter 96-well plates containing $\sim 3 \times 10^5$ CEM cells/mL infected with 100 CCID₅₀ of HIV for milliliter and containing appropriate dilutions of the test compounds. After 4–5 days of incubation at 37°C in a CO₂-controlled humidified atmosphere, CEM giant (syncytium) cell formation was examined microscopically. The EC₅₀ (50% effective concentration) was defined as the compound concentration required to inhibit HIV-induced giant cell formation by 50%.

Surface Plasmon Resonance (SPR) analysis. Interaction studies were performed on a Biacore T200 instrument (GE Healthcare, Uppsala, Sweden) at 25°C in HBS-P (10 mM HEPES, 150 mM NaCl and 0.05% surfactant P20; pH 7.4) supplemented with 10mM CaCl₂. Recombinant HIV-1(III_B) gp120 (ImmunoDiagnostics Inc., Woburn, MA), recombinant HIV-1(HxB2) gp41 (Acris Antibodies GmbH, Herford, Germany) and human serum albumin (HSA) (Sigma) were covalently immobilized on a CM5 sensor chip in 10mM sodium acetate, pH 4, using standard amine coupling chemistry, resulting in chip densities of respectively 3531, 3091 and 3333 RU. A reference flow cell was used as a control for non-specific binding and refractive

index changes. Samples were injected for 2 minutes at a flow rate of 45 $\mu\text{l}/\text{min}$ and followed by a dissociation phase of 2 minutes. The CM5 sensor chip surface was regenerated with a single injection of Glycine-HCl pH = 3.

HIV-1 reverse transcriptase assay. Enzyme reactions (50 μL in volume) were carried out in a 50mM Tris-HCl (pH 7.8) buffer that contained 5mM dithiothreitol, 300mM glutathione, 0.5mM EDTA, 150mM KCl, 5mM MgCl_2 , 1.25 μg of bovine serum albumin, 0.06% Triton X-100, an appropriate concentration of 2.8 μM $[\text{3H}]\text{dGTP}$ (2 $\mu\text{Ci}/\text{assay}$), varying concentrations of the test compounds, and a fixed concentration of poly(rC)/oligo(dG) (0.1 mM). Reactions were initiated by the addition of 1 μL of wild-type or mutant RT and were incubated for 30 min at 37°C. Reactions were terminated by the addition of 200 μL of 2 mg/mL yeast RNA, 2 mL of 0.1 M $\text{Na}_4\text{P}_2\text{O}_7$ (in 1M HCl), and 2 mL of 10% (v/v) trichloroacetic acid. The solutions were kept on ice for 30 min, after which the acid-insoluble material was washed and analyzed for radioactivity.

2.2 Hairpin oligonucleotides forming G-quadruplexes: New aptamers with anti-HIV activity

Even if tetramolecular complexes have recently displayed interesting biological properties, and have been proposed for many therapeutic applications, their use is limited by unfavourable kinetics³⁰. The in vitro formation of a tetramolecular G-quadruplex is very slow and may require high ODN and salt concentrations. In order to improve the kinetics of G-quadruplex formation, a variety of tetra-branched linked d(TGGGAG) ODNs (TEL-ODNs) were reported by Piccialli et al. and strong activity was found for some of these sequences^{31,32}.

With the aim to improve the kinetic of G-quadruplex formation using d(TGGGAG) as a lead sequence, and therefore to enhance the anti-HIV activity of these aptamers, we designed, for the first time, bimolecular G-quadruplexes on d(TGGGAG) sequence. Basically, these new bimolecular G-quadruplexes diverged from the G-quadruplexes so far reported, for the number of strands involved in the complex, the hexaethylenglycole (HEG) as linker and the number of aromatic residues at 5'-end. Here, it is reported the synthesis of new Hairpins ODNs with inversion of polarity 3'-3' and 5'-5' and some 5'-end conjugations (**I-V**, **Figure 4**) and their biophysical and biological characterization. The scaffold of new ODNs is formed by hairpin structures containing two d(TGGGAG) domains, whose 3' or 5'-ends are joint through a HEG loop (**I** and **V**, **Figure 4**). In addition, the synthesis of **II-IV**, which contain a HEG linker³³ in the 3'-3' inversion of polarity site and an aromatic residues at one 5'-end linked by phosphodiester linkage were developed.

Aromatic phosphoramidate compounds **2-4** were selected on the basis of our previously reported data for homologous tetramolecular G-quadruplexes, which were efficiently tethered to the d(TGGGAG) model sequence by exploiting classical phosphoramidite chemistry.

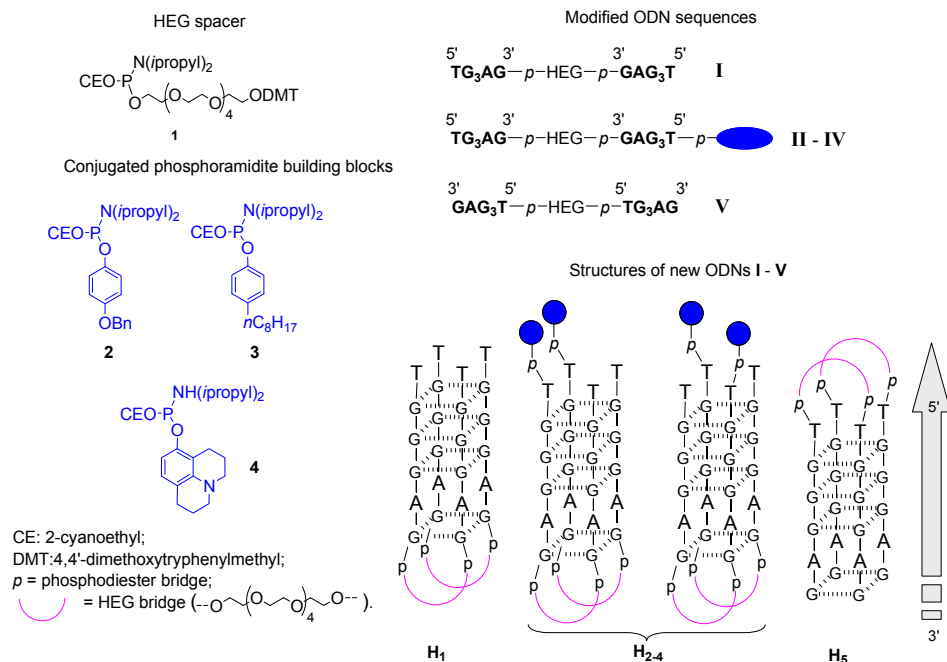
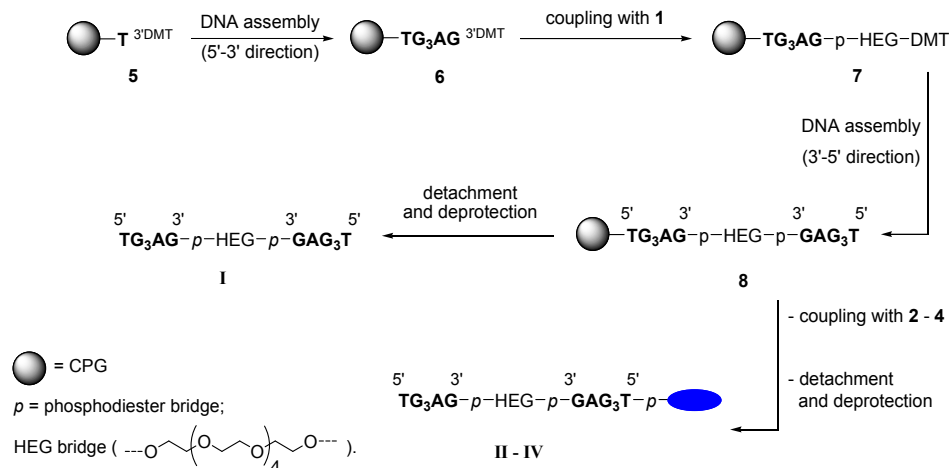


Figure 4. Phosphoramidite building blocks **1-4**, modified ODN sequences **I-V** and potential hairpin structure **H₁-H₅**.

ODN tracts were synthesized using standard solid-phase β -cyanoethylphosphoramidite chemistry protocols (in both 3'→5' and 5'→3' directions) on an automated DNA synthesizer, starting from commercially available, DMT-protected, nucleoside functionalized CPG supports. A CPG solid support that anchors 3'-O-(4,4'-dimethoxytrityl)-thymidine **5** (Scheme 2) was used to synthesize the first DNA tract (synthesis by 5'→3' direction), leading to **6**.

Phosphoramidite **1** (Figure 4), commercially available, was then exploited to insert a HEG linker unit using classical phosphoramidite protocols.



Scheme 2. Synthetic scheme of ODNs **I** and **III – V** by standard automated DNA synthesis.

After DMT removal (1% DCA in DCM), the second DNA tract was assembled (synthesis by 3'→5' direction), leading to **8**. Spectroscopic measurements monitored DMT cation formation, indicating chain assembly for each coupling cycle. Compound yields of at least 98% were obtained. After detachment and deprotection, the crude material was analyzed and then purified by HPLC and gel filtration chromatography. Two main peaks were observed in the SAX-HPLC profiles (Figure 5B). The fastest eluting peak, attributed to a 12-mer single strand, was always accompanied by a major peak that had a higher retention time due to its G-quadruplex structure generated under HPLC elution conditions. These two peaks, accounting for more than 90% of the total integrated area, corresponded to desired **I**, as ascertained by MALDI-TOF MS (Table 5). Subsequently, phosphoramidite derivatives **2-4** were exploited in the last coupling

step, starting from support **8**, to synthesize 5'-conjugated oligomers **II-IV**. Target oligomers **I-IV** were detached from the solid support, deprotected and the crude materials were then analyzed and purified using HPLC and gel filtration chromatography.

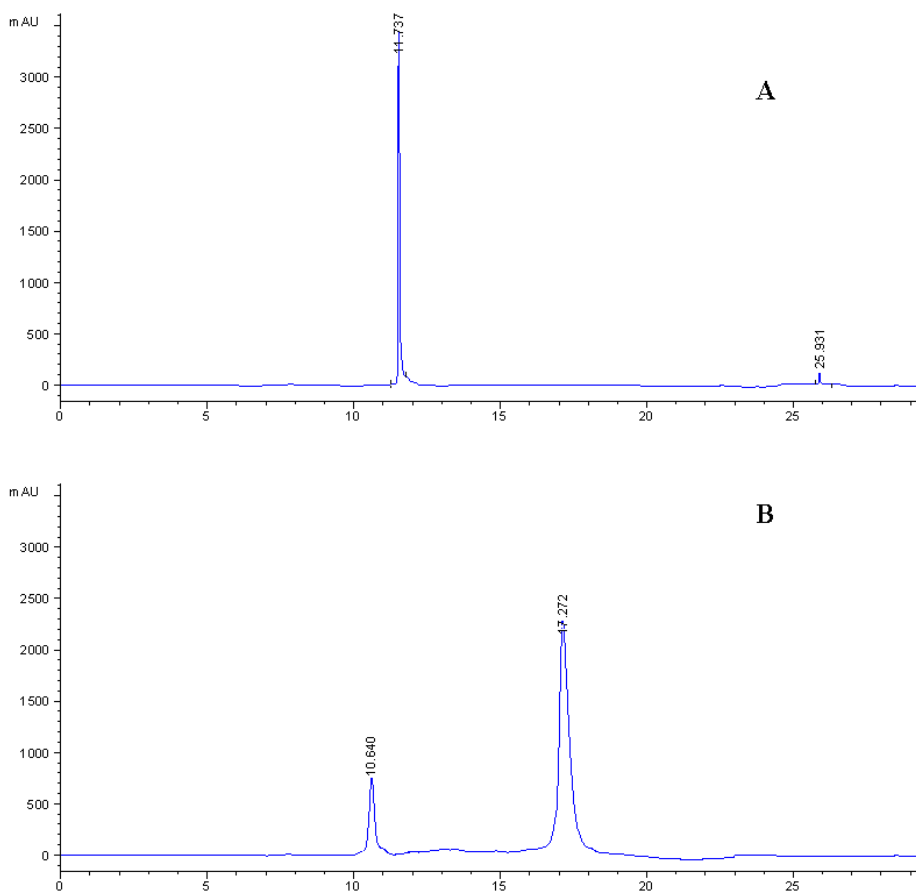


Figure 5. Typical RP-HPLC (**A**) and SAX (**B**) profiles of purified and desalted ODNs.

The modified oligonucleotides were characterized by MALDI-TOF MS, in all cases giving masses in accordance with their expected values (**Table 5**). ODN sequence **V** was obtained from the CPG solid support that anchored 5'-O-(4,4'-Dimethoxytrityl)-N-isobutyryl-20-deoxy-guanosine-3'-[(2-cyanoethyl)-N,N-diisopropyl]- phosphoramidite

and previously described procedures (for synthetic scheme see Experimental Session).

Table 5. Oligonucleotide mass characterization and melting temperatures (T_m) of the quadruplexes formed by ODNs **I–V**

ODN sequences	MS	Yield (%) ^b	T_m (°C)
	<i>calcd</i> for [M] ^a data (found)		
I	<i>4148.79 / 4150.78</i> 4150.65 [MH] ⁺ ; 4172.58 [MNa] ⁺	8.8	76.0 ± 0.5
II	<i>4410.83 / 4412.97</i> 4412.59 [MH] ⁺ ; 4434.32 [MNa] ⁺	7.0	84.0 ± 0.5
III	<i>4416.91 / 4419.07</i> 4418.54 [MH] ⁺ ; 4440.91 [MNa] ⁺	8.2	83.0 ± 0.5
IV	<i>4399.87 / 4401.99</i> 4401.52 [MH] ⁺ ; 4423.84 [MNa] ⁺ ;	7.8	83.5 ± 0.5
V	<i>4148.79 / 4150.78</i> 4150.88 [MH] ⁺ 4172.46 [MNa] ⁺	6.6	75.5 ± 0.5
d(TGGGAG)	—	—	41.0 ± 0.5

^aExact mass / Average mass values; ^bYields calculated on the pure oligonucleotide after gel filtration, with respect to the starting functionalization of the supports.

- **CD studies and characterization**

To study the influence of the loops and 5'-end aromatic groups on the ability of sequence to form G-quadruplex structures, CD analyses was undertaken on oligomers **I** and **V** in comparison with a corresponding unmodified d(TGGGAG) oligomer. For all sequences, the CD spectra at 20°C showed typical, positive bands at 264 nm and small negative bands at 243 nm, indicative of parallel-stranded, bimolecular G-quadruplex structures (**Figure 6**). T_m values were obtained from the CD melting profiles and are reported in **Table 5**. The melting curves recorded by heating a preformed G-quadruplexes did not correspond to equilibrium melting curves (hysteresis

phenomenon), and the ‘ T_m ’ or ‘ $T_{1/2}$ ’ deduced from these experiments depends on the heating rate¹⁷.

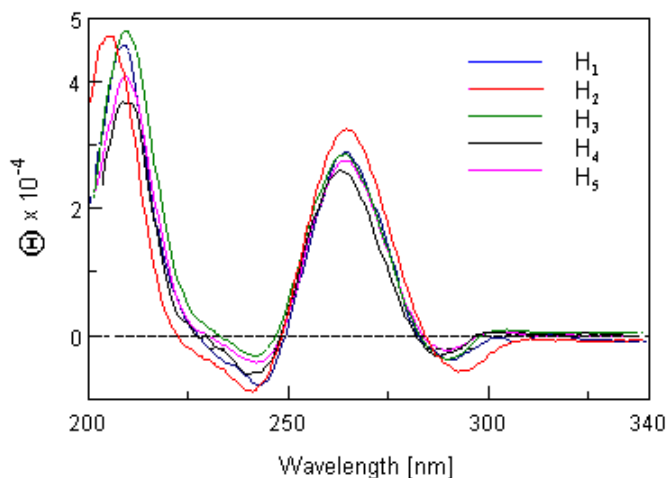


Figure 6. CD spectra of modified oligonucleotides **I–V**.

These data clearly showed that all modified ODNs formed G-quadruplexes with strongly increased thermal stabilities compared with unmodified d(TGGGAG) quadruplex (**Table 5**). From the data analysis, the HEG linker at the 5'-or 3'-end clearly makes the G-quadruplexes **H₁** and **H₅** much more stable than the corresponding tetramolecular complexes lacking of HEG bridges ($\Delta T > 35^\circ\text{C}$). The presence of two aromatic residues at the 5'-end further stabilized the resulting G-quadruplexes **H₂–H₄** ($\Delta T \approx 8^\circ\text{C}$) in comparison with unconjugated hairpin G-quadruplex **H₁** and **H₅** (**Figure 7**). Noteworthy, the different aromatic groups at the 5'-end of conjugates **H₂–H₄** contributed equally to thermal stabilization, possibly promoting a well-packed cluster at the end of the structures. We expected that the introduction of aromatic moieties at only one of the hairpin 5'-end could lead to the formation of two different populations of conjugated

G-quadruplexes, in which the aromatic residues were either in a lateral or diagonal position. In all CD profiles, any transition related to these two expected **H₂-H₄** populations was observed.

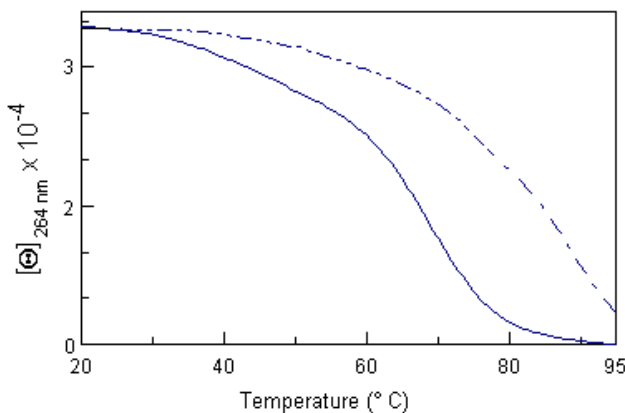


Figure 7. CD melting profiles of ODNs **H₁** ($T_m = 76.0$ °C; *bold line*) and **H₂** ($T_m = 84$ °C; *dotted line*).

- **Anti-HIV activity and Surface Plasmon Resonance (SPR): directed affinity binding analyses for the HIV envelope**

Considering anti-HIV activity (**Table 6**), low micromolar inhibition of HIV-1 infection in CEM cell cultures was found for **II-IV**, but not for unconjugated **I** and **V**. These favourable selectivity indices amounted to >1.0 . Anti-HIV-2 activity was markedly less pronounced than that for HIV-1. Compound **II** (containing the phenylbenzyl **2** moiety) proved to be the most effective derivative with EC_{50} values as low as 0.96 μM (HIV-1) and 3.2 μM (HIV-2). This compound lacked measurable toxicity at 8 μM in CEM cell cultures. Interestingly, the conjugated G-quadruplexes **II-IV** were less active than the corresponding tetramolecular complexes¹², reasonably, because each tetrameric G-quadruplex bears four terminal aromatic groups,

whereas the dimeric G-quadplexes (**II-IV**) contain only two aromatic moieties.

Table 6. Anti-HIV-1 and –HIV-2 activity and cytostatic properties of the test compounds **I** to **V** in human T-lymphocyte (CEM) cell cultures

ODN sequences	EC ₅₀ ^a (μM)		CC ₅₀ ^b (μM)	S.I. ^c
	HIV-1 (III _B)	HIV-2 (ROD)		
I	> 8	> 8	> 8	-
II	0.96 ± 0.24	3.2 ± 0.5	> 8	> 8.3
III	1.92 ± 1.1	> 8	> 8	> 4.1
IV	3.4 ± 0.06	6.9 ± 1.6	> 8	> 2.3
V	> 8	> 8	> 8	-

^aEC₅₀, 50% effective concentration or compound concentration required to protect CEM cells against the cytopathicity of HIV by 50%; ^bCC₅₀, 50% cytostatic concentration or compound concentration required to reduce CEM cell proliferation by 50%; ^cSelectivity index for HIV-1, calculated as the ratio of CC₅₀/EC₅₀.

Compounds **I-V** were then evaluated for their binding capacity to HIV-1 gp120, gp41 and the albumin (HSA) (**Figure 8**). Albumin is commonly employed as a versatile drug carrier in anti-HIV strategies^{25,34}. Un-conjugated compounds **I** and **V** did not show measurable binding to any of the HIV glycoproteins and HSA. In contrast, binding was observed against these three proteins for the compounds **II-IV**. In particular, compound **II** bound somewhat more efficiently than **III** and **IV**; however, no compounds showed exclusive selectivity for binding to HIV envelope glycoproteins. In fact, when the RU values of gp120, gp41 and HSA binding on the sensorchips and the molecular weight of the ligands were taken into account, binding efficiency of all three ligands were within the same order of magnitude. The k_{on} , k_{off} and K_D values could not be accurately determined since the data could not fit in a 1:1 binding model.

Thus, because binding to HIV-1 glycoproteins was only observed for the modified G-quadruplexes that also showed anti-HIV activity in cell culture, envelope binding might serve as the cause of eventual antiviral activity.

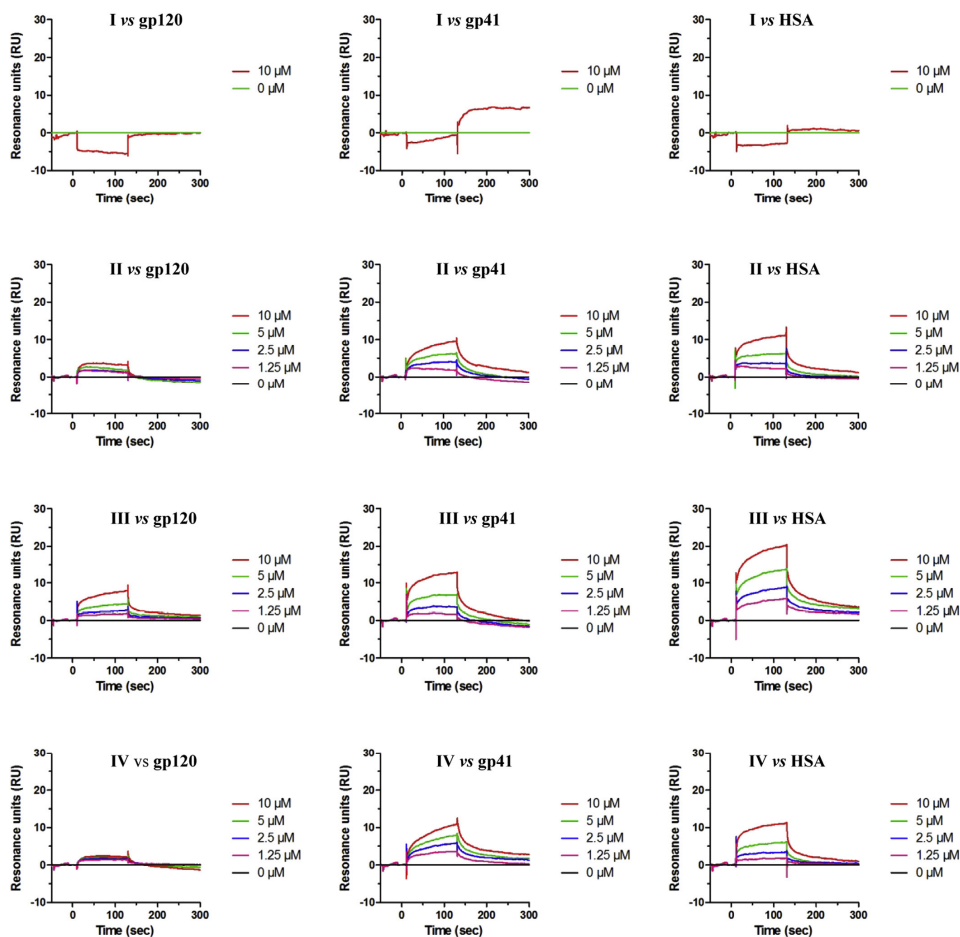


Figure 8. SPR plots of compound I and II–IV interactions with HIV-1(IIIB) gp120, HIV-1/HxB2 gp41 and HSA.

On the other hand, the antiviral activity of these G-quadruplexes may be due to the amphiphilic properties as well as the formation of multimeric complexes of these ODNs, as recently reported⁸.

However, to further ascertain whether entry (i.e., fusion) is the main antiviral target of the compounds, other assays should be performed.

- **Serum stability studies**

As efficient anti-HIV therapies require the retention of high drug concentrations for prolonged time periods *in vivo*, we investigated the stabilities of hairpin ODNs **II-IV** in human serum. The bio-stability of **II-IV** sequences were assessed *in vitro* and compared to unmodified d(TGGGAG). As shown in **Figure 9**, the enhancement in the bio-stability was observed for all sequences. In particular, **I** and **V** proved stable for 4 days, while the unmodified sequence was completely degraded after 4 h, suggesting the high stabilization effect produced by the HEG loop. This serum stability was dramatically enhanced in conjugated hairpin ODNs, in particular **II**, which was stable for at least 8 days.

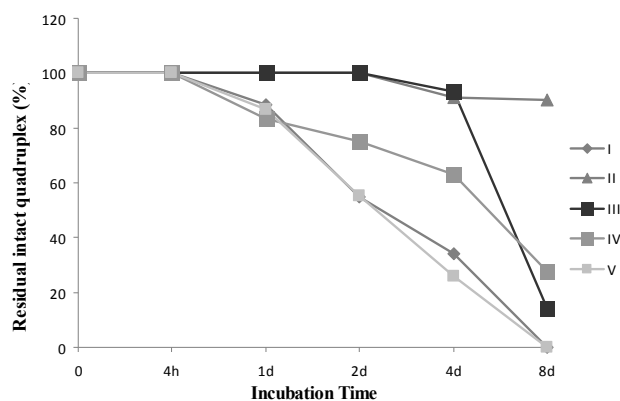


Figure 9. Stability of I–V in Human Serum.

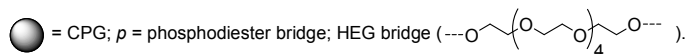
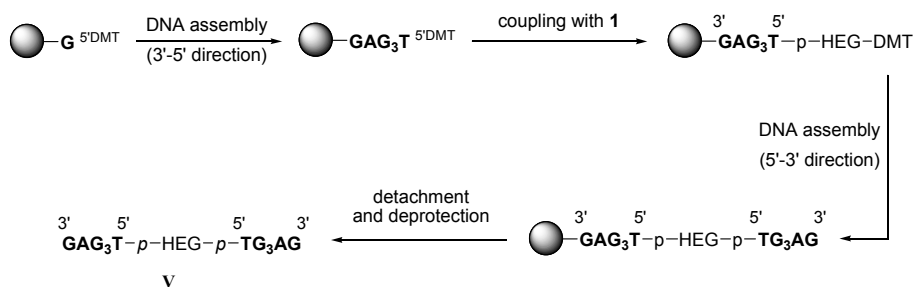
2.2.1 Experimental Session

General procedures. MALDI-TOF MS analyses were performed on a PerSeptiveBiosystems Voyager-De Pro MALDI mass spectrometer in the linear mode using a picolinic/3-hydroxypicolinic/sinapinic acid mixture matrix. HPLC analyses were performed on an Agilent Technologies 1200 series instrument equipped with a UV detector. The crude material was purified and analysed using HPLC on a Phenomenex RP18 column [LUNA, 5 μ m C18, 10.0 \times 250 mm] and Nucleogel SAX column (Macherey-Nagel, 1000-8/46), respectively. Desalting was conducted using gel filtration chromatography on a Sephadex G10 column, eluted with H₂O/EtOH 4:1 (v/v).

Synthesis and characterization of ODNs (I-V). As depicted in **Scheme 2**, oligomers **I-IV** were synthesised, starting with functionalised CPG support **5** with 0.1 meq/g (100 mg) initial loading, on which the sequence d(GAG₃T) was assembled in a standard manner. After coupling with phosphoramidite **1**, assembly of the second ODN tract was then performed. Target oligomers were detached from the solid support and deprotected via treatment with conc. aq. NH₄OH at 50°C for 5 h. The combined filtrates and washings were concentrated under reduced pressure, re-dissolved in H₂O, and analysed and purified with HPLC. Purification of the crude detachments were performed on a Phenomenex RP18 column or RP18 column (LUNA, 5 μ m C18, 10.0 \times 250 mm), using a linear gradient of CH₃CN in 0.1 M AcNH₄/H₂O (pH 7.0), from 5% to 100% in 30 min, at a flow rate of 1.5 mL/min and with detection at 260 nm. HPLC analyses of oligonucleotides **I-IV** was conducted on an analytical anion exchange Nucleogel SAX column (Macherey-Nagel, 1000-8/46, 4.6 \times 50 mm, 5 μ m), adopting the following eluents: buffer A, 20 mM KH₂PO₄/K₂HPO₄ aq. solution (pH = 7.0), containing 20% (v/v) CH₃CN; buffer B, 1.0 M KCl, 20 mM

$\text{KH}_2\text{PO}_4/\text{K}_2\text{HPO}_4$ aq. solution (pH = 7.0), containing 20% (v/v) CH_3CN , using a linear gradient from 0% to 100% B in 20 min, flow rate 0.8 mL/min and detection at $\lambda = 260$ nm. In a typical experiment, starting from 100 mg of CPG that anchored the first nucleoside, 60 – 110 OD units (8.8 – 6.6% yields) of purified **I–V** were obtained (**Table 5**).

Synthetic scheme of **V**



Quadruplex Preparation and CD experiments. CD spectra were registered on a JASCO J-715 spectrophotometer equipped with a thermoelectrically controlled cuvette holder (JASCO PTC-348) in a 0.2 cm path length cuvette. The quadruplex complexes (5×10^{-5} M) were obtained by dissolving the lyophilised oligonucleotide in an appropriate buffer, annealed by heating at 95 °C for 5 min and slowly cooled to room temperature. The buffer used was 10 mM potassium phosphate, 200mM KCl and 0.1 mM EDTA (pH 7.0). The concentrations of dissolved oligonucleotides **I – V** were determined with UV measurements at 260 nm and 90°C, using the calculated molar extinction coefficient of $d(\text{TGGGAG})_2$ ϵ ($125,000 \text{ cm}^{-1} \text{ M}^{-1}$). CD spectra were collected from 200 to 340 nm, at 20 nm/min, with a response time of 16 s and at 2 nm bandwidth. The thermal

denaturation curves were registered at the $\lambda = 264$ nm and a heating rate of 0.5°C/min.

Stability of G-quadruplexes in Human Serum. Unmodified and modified sequences were incubated with 93% Human Serum (Lonza) at 37°C. Aliquots of 100 pmol were withdrawn at different time points and immediately frozen. The solutions were then extracted with phenol and ODNs were precipitated with ethanol. Samples were analyzed on denaturing (7M urea) 20% polyacrylamide gel and visualized by SYBR® Green I (Invitrogen) staining. Equal amounts of ODNs before serum incubation were extracted with phenol in parallel and loaded as an input control. Gel images were captured using a ChemiDoc™ XRS (Bio-Rad), and the electrophoretic bands were quantified with Image Lab™ software (Bio-Rad). The signal intensity value of an intact quadruplex was set at 1.

Anti-HIV experiments. Inhibition of HIV-1(III_B) and HIV-2(ROD)-induced cytopathicity in CEM cell cultures was measured in microtitre 96-well plates containing $\sim 3 \times 10^5$ CEM cells/mL infected with 100 CCID₅₀ of HIV per millilitre and containing appropriate dilutions of test compounds. After 4–5 days of incubation at 37°C in a CO₂-controlled humidified atmosphere, giant CEM (syncytium) cell formations were examined microscopically. The EC₅₀ (50% effective concentration) was defined as the compound concentration required to inhibit HIV-induced, giant cell formation by 50%.

Surface Plasmon Resonance (SPR) analysis. Interaction studies were performed on a Biacore T200 instrument (GE Healthcare, Uppsala, Sweden) at 25°C in HBS-P (10mM HEPES, 150mM NaCl and 0.05% surfactant P20; pH 7.4) supplemented with 10mM CaCl₂. Recombinant HIV-1(III_B) gp120 (ImmunoDiagnostics Inc., Woburn,

MA), recombinant HIV-1(HxB2) gp41 (Acris Antibodies GmbH, Herford, Germany) and human serum albumin (HSA) (Sigma) were covalently immobilised on a CM5 sensor chip in 10 mM sodium acetate, pH 4, using standard amine coupling chemistry, resulting in chip densities of 3531, 3091 and 3333 RU, respectively. A reference flow cell was used as a control for non-specific binding and refractive index changes, several buffer blanks were used for double referencing, and the blank signals automatically subtracted from the test values. Samples were injected for 2 minutes at a flow rate of 45 μ l/min and followed by a dissociation phase of 2 minutes. Since several samples contained DMSO, a DMSO concentration series was also included to eliminate the contribution of DMSO to the response signal. The CM5 sensor chip surface was regenerated with a single injection of Glycine-HCl pH = 3.

2.3 General Conclusions and Perspective

In this chapter, it was described the synthesis of a variety of modified aptamers based on “Hotoda sequence” with high anti-HIV activity. Biophysical and biological characterization were performed on all modified sequences. Particularly, the first mini library of d(TGGGAG) ODNs carrying aromatic and hydrophobic tails at the 5'-end were synthesized via a fully automated, on-line phosphoramidite-based solid-phase method (**Scheme 1**). The new ODN 5'-conjugated showed anti-HIV activity with some preference for HIV-1, with inhibitory activity invariably in the low micromolar range. SPR data, did not suggested any selectivity for gp120 or gp41 binding compared with HSA binding, yet highlighted the interesting potentialities of HSA as a versatile drug carrier in anti-HIV²⁵.

The CD and DSC monitored thermal denaturation studies on the resulting G-quadruplexes, suggested that the insertion of lipophilic residue at the 5'-end, leads always to a stability enhancement of G-quadruplex complexes ($20 < \Delta T_m < 40^\circ\text{C}$). Moreover, a detailed CD and DSC analyses indicated a monophasic behaviour for sequences **I** and **V**, while for ODNs (**II–IV**) clearly shown that these G-quadruplex structures deviate from simple two-state melting, suggesting the formation of intermediate states (**Figure 3**). For all sequences, the CD spectra at 20°C showed diagnostic profiles of parallel-stranded quadruplex structures. (**Figure 2**).

In the second part of this chapter, we also reported the synthesis of bimolecular G-quadruplex oligonucleotides based on “Hotoda sequence” containing a HEG loop as a 3'-3' or 5'-5' inversion of polarity site. CD studies assessed that the introduction of a HEG loop, produces an improvement of the thermal stability of all hairpin ODNs compared to d(TGGGAG) tetramolecular G-quadruplexes and that this insertion has no effect on the original parallel folding of the G-quadruplex structure (**Figure 4**). This thermal stabilization was further increased, once more, by introduction of different aromatic residues at the 5'-end of hairpins **H1**. Moreover, only 5'-conjugated hairpins (**H2–H4**), have proven to exhibit significant anti-HIV activity in cell culture (**Table 6**). Besides the anti-HIV activity, the conjugated hairpin G-quadruplexes exhibited interesting properties in terms of slight cytotoxicity, favourable $\text{CC}_{50}/\text{EC}_{50}$ (selectivity index) ratio and increased stability in human serum. Finally, also the 5'-conjugated hairpins (**H2–H4**), shown a good affinity for HSA.

In light of all results, we can confirm that the presence of lipophilic residues at the 5'-end is essential for the stability and anti-HIV

activity of these G-quadruplexes. These results are in agreement with that reported by D'onofrio et al. on the 5'-sugar-conjugated d(TGGGAG)¹⁵. The conjugation of sugars (polar groups) at the 5'-end of d(TGGGAG) cause low thermal stability and no anti-HIV activity for these sequence. Most importantly, we clarified that the major stability of the investigated complexes is not directly correlated with their pronounced anti-HIV activity.

Considering the amount of G-quadruplexes formed and able to interact with targets (gp120 and gp41), a fundamental prerequisite for the biological activity of these sequences, it is evident that their thermal stabilities and kinetics of formation are essential. In order to achieve a more complete picture of the structure-activity relationships of the most active 5'-end modified d(TGGGAG), we have started to examine the kinetic aspects of G-quadruplex formation based on these sequences by ESI-MS technique, in collaboration with Dr. *Valérie Gabelica* in Inserm/Univ.Bordeaux (see Chapter 4).

References

- (1) Tilton, J. C., and Doms, R. W. (2010) Entry inhibitors in the treatment of HIV-1 infection. *Antiviral Research* 85, 91–100.
- (2) Wyatt, J. R., Vickers, T. A., Roberson, J. L., Buckheit, R. W., Klimkait, T., DeBaets, E., Davis, P. W., Rayner, B., Imbach, J. L., and Ecker, D. J. (1994) Combinatorially selected guanosine-quartet structure is a potent inhibitor of human immunodeficiency virus envelope-mediated cell fusion. *Proceedings of the National Academy of Sciences* 91, 1356–1360.
- (3) Buckheit, R. W., Roberson, J. L., Lackman-Smith, C., Wyatt, J. R., Vickers, T. A., and Ecker, D. J. (1994) Potent and specific inhibition of HIV envelope-mediated cell fusion and virus binding by G quartet-forming oligonucleotide (ISIS 5320). *AIDS research and human retroviruses* 10, 1497–506.
- (4) Koizumi, M., Koga, R., Hotoda, H., Momota, K., Ohmine, T., Furukawa, H., Agatsuma, T., Nishigaki, T., Abe, K., Kosaka, T., Tsutsumi, S., Sone, J., Kaneko, M., Kimura, S., and Shimada, K. (1997) Biologically active oligodeoxyribonucleotides-IX. Synthesis and anti-HIV-1 activity of hexadeoxyribonucleotides, TGGGAG, bearing 3'- and 5'-end-modification. *Bioorganic and Medicinal Chemistry* 5, 2235–2243.
- (5) Koizumi, M., Koga, R., Hotoda, H., Ohmine, T., Furukawa, H., Agatsuma, T., Nishigaki, T., Abe, K., Kosaka, T., Tsutsumi, S., Sone, J., Kaneko, M., Kimura, S., and Shimada, K. (1998) Biologically active oligodeoxyribonucleotides. Part 11: The least phosphate-modification of quadruplex-forming hexadeoxyribonucleotide TGGGAG, bearing 3'- and 5'-end-modification, with anti-HIV-1 activity. *Bioorganic and Medicinal Chemistry* 6, 2469–2475.
- (6) Gros, J., Rosu, F., Amrane, S., De Cian, A., Gabelica, V., Lacroix, L., and Mergny, J.-L. (2007) Guanines are a quartet's best friend: impact of base substitutions on the kinetics and stability of tetramolecular quadruplexes. *Nucleic acids research* 35, 3064–75.
- (7) Englund, E. A., Xu, Q., Witschi, M. A., and Appella, D. H. (2006) PNA-DNA duplexes, triplexes, and quadruplexes are stabilized with trans-cyclopentane units. *Journal of the American Chemical Society* 128, 16456–16457.
- (8) Pedersen, E. B., Nielsen, J. T., Nielsen, C., and Filichev, V. V. (2011) Enhanced anti-HIV-1 activity of G-quadruplexes comprising locked nucleic acids and intercalating nucleic acids. *Nucleic acids research* 39, 2470–81.
- (9) Esposito, V., Virgilio, A., Randazzo, A., Galeone, A., and Mayol, L. (2005) A new class of DNA quadruplexes formed by oligodeoxyribonucleotides containing a 3'-3' or 5'-5' inversion of polarity site. *Chemical communications (Cambridge, England)* 3953–5.
- (10) Galeone, A., Mayol, L., Virgilio, A., Virno, A., and Randazzo, A. (2008) A further contribution to the extreme variability of quadruplex structures from

oligodeoxyribonucleotides containing inversion of polarity sites in the G-tract. *Molecular bioSystems* 4, 426–30.

(11) Martino, L., Virno, A., Randazzo, A., Virgilio, A., Esposito, V., Giancola, C., Bucci, M., Cirino, G., and Mayol, L. (2006) A new modified thrombin binding aptamer containing a 5'-5' inversion of polarity site. *Nucleic acids research* 34, 6653–62.

(12) Di Fabio, G., D'Onofrio, J., Chiapparelli, M., Hoorelbeke, B., Montesarchio, D., Balzarini, J., and De Napoli, L. (2011) Discovery of novel anti-HIV active G-quadruplex-forming oligonucleotides. *Chemical communications (Cambridge, England)* 47, 2363–2365.

(13) Woodsley, J. (1992, April) Oligonucleotides and Analogues: A Practical Approach. *Biochemical Education* (oxford press, Ed.).

(14) Beaucage, S. L., and Iyer, R. P. (1993) The synthesis of modified oligonucleotides by the phosphoramidite approach and their applications. *Tetrahedron* 49, 6123–6194.

(15) D'Onofrio, J., Petraccone, L., Erra, E., Martino, L., Di Fabio, G., De Napoli, L., Giancola, C., and Montesarchio, D. (2007) 5'-Modified G-quadruplex forming oligonucleotides endowed with anti-HIV activity: Synthesis and biophysical properties. *Bioconjugate Chemistry* 18, 1194–1204.

(16) Paramasivan, S., Rujan, I., and Bolton, P. H. (2007) Circular dichroism of quadruplex DNAs: applications to structure, cation effects and ligand binding. *Methods (San Diego, Calif.)* 43, 324–31.

(17) Zhou, J., Rosu, F., Amrane, S., Korkut, D. N., Gabelica, V., and Mergny, J. L. (2014) Assembly of chemically modified G-rich sequences into tetramolecular DNA G-quadruplexes and higher order structures. *Methods (San Diego, Calif.)* 67, 159–68.

(18) Pagano, B., Randazzo, A., Fotticchia, I., Novellino, E., Petraccone, L., and Giancola, C. (2013) Differential scanning calorimetry to investigate G-quadruplexes structural stability. *Methods (San Diego, Calif.)* 64, 43–51.

(19) Petraccone, L., Erra, E., Esposito, V., Randazzo, A., Mayol, L., Nasti, L., Barone, G., and Giancola, C. (2004) Stability and Structure of Telomeric DNA Sequences Forming Quadruplexes Containing Four G-Tetrads with Different Topological Arrangements. *Biochemistry* 43, 4877–4884.

(20) Olsen, C. M., and Marky, L. A. (2010) G-Quadruplex DNA. *Spectroscopies, Circular Dichroism* (Baumann, P., Ed.) 608, 147–158.

(21) Yatsunyk, L. A., Piétrement, O., Albrecht, D., Tran, P. L. T., Renčičuk, D., Sugiyama, H., Arbona, J. M., Aimé, J. P., and Mergny, J. L. (2013) Guided assembly of tetramolecular G-quadruplexes. *ACS Nano* 7, 5701–5710.

(22) Krishnan-Ghosh, Y., Liu, D., and Balasubramanian, S. (2004) Formation of an interlocked quadruplex dimer by d(GGGT). *Journal of the American Chemical Society* 126, 11009–16.

- (23) Sotoya, H. (2004) Method for direct discrimination of intra- and intermolecular hydrogen bonds, and characterization of the G(:A):G(:A):G(:A):G heptad, with scalar couplings across hydrogen bonds. *Nucleic Acids Research* 32, 5113–5118.
- (24) Kato, Y., Ohyama, T., Mita, H., and Yamamoto, Y. (2005) Dynamics and thermodynamics of dimerization of parallel G-quadruplexed DNA formed from d(TTAGn) (n = 3-5). *Journal of the American Chemical Society* 127, 9980–9981.
- (25) Park, K. (2012) Albumin: a versatile carrier for drug delivery. *Journal of controlled release* □: official journal of the Controlled Release Society 157, 3.
- (26) Grasso, D., La Rosa, C., Milardi, D., and Fasone, S. (1995) The effects of scan rate and protein concentration on DSC thermograms of bovine superoxide dismutase. *Thermochimica Acta* 265, 163–175.
- (27) Milardi, D., Arnesano, F., Grasso, G., Magrì, A., Tabbì, G., Scintilla, S., Natile, G., and Rizzarelli, E. (2007) Ubiquitin stability and the Lys63-linked polyubiquitination site are compromised on copper binding. *Angewandte Chemie (International ed. in English)* 46, 7993–5.
- (28) Arena, G., Fattorusso, R., Grasso, G., Grasso, G. I., Isernia, C., Malgieri, G., Milardi, D., and Rizzarelli, E. (2011) Zinc(II) complexes of ubiquitin: speciation, affinity and binding features. *Chemistry (Weinheim an der Bergstrasse, Germany)* 17, 11596–603.
- (29) Palmieri, M., Malgieri, G., Russo, L., Baglivo, I., Esposito, S., Netti, F., Del Gatto, A., de Paola, I., Zaccaro, L., Pedone, P. V., Isernia, C., Milardi, D., and Fattorusso, R. (2013) Structural Zn(II) implies a switch from fully cooperative to partly downhill folding in highly homologous proteins. *Journal of the American Chemical Society* 135, 5220–8.
- (30) Mergny, J. L., De Cian, A., Ghelab, A., Saccà, B., and Lacroix, L. (2005) Kinetics of tetramolecular quadruplexes. *Nucleic Acids Research* 33, 81–94.
- (31) Oliviero, G., Amato, J., Borbone, N., Galeone, A., Petraccone, L., Varra, M., Piccialli, G., and Mayol, L. (2006) Synthesis and characterization of monomolecular DNA G-quadruplexes formed by tetra-end-linked oligonucleotides. *Bioconjugate Chemistry* 17, 889–898.
- (32) Oliviero, G., Amato, J., Borbone, N., D'Errico, S., Galeone, A., Mayol, L., Haider, S., Olubiyi, O., Hoorelbeke, B., Balzarini, J., and Piccialli, G. (2010) Tetra-end-linked oligonucleotides forming DNA G-quadruplexes: a new class of aptamers showing anti-HIV activity. *Chemical communications (Cambridge, England)* 46, 8971–3.
- (33) Ng, P. S., Laing, B. M., Balasundaram, G., Pingle, M., Friedman, A., and Bergstrom, D. E. (2010) Synthesis and evaluation of new spacers for use as dsDNA end-Caps. *Bioconjugate Chemistry* 21, 1545–1553.
- (34) Elsadek, B., and Kratz, F. (2012, January 10) Impact of albumin on drug delivery - New applications on the horizon. *Journal of Controlled Release*.

CHAPTER 3

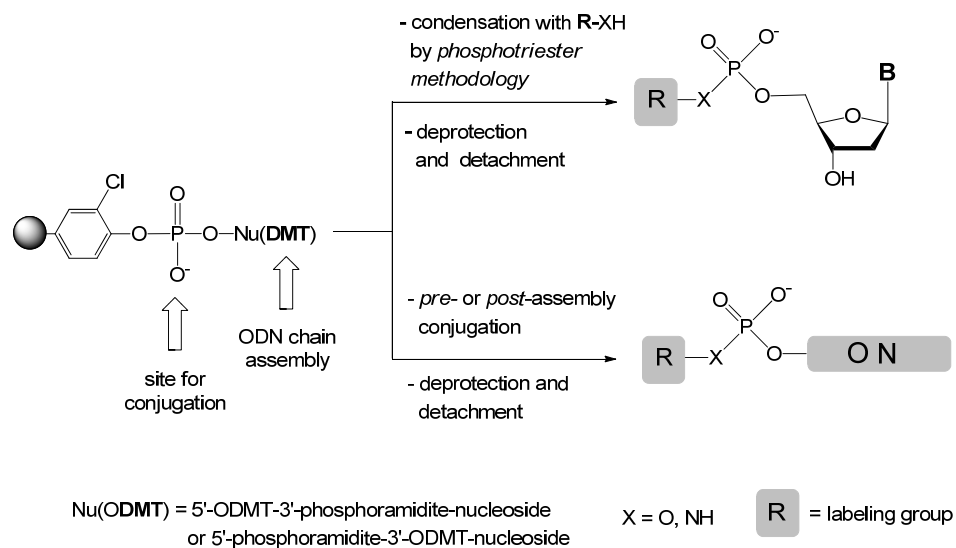
Improvement of Solid Phase Synthetic Approach

Oligonucleotides (ODNs) and nucleotides represent two classes of potential therapeutic agents with a broad spectrum of pharmacological activities. Desired improvements of certain properties, such as cell-specific delivery, cellular uptake efficiency, intracellular distribution, and target specificity, can be achieved by chemical modifications. Conjugation of ODNs to other molecules such as proteins and peptides, saccharides, fluorophores, inhibitors, and vitamins offers a feasible way to address these requirements¹⁻³. The methods used for the preparation of these molecules fall into two major categories: solution and solid phase approaches. The solid phase method, in association with combinatorial chemistry approaches, is a successful approach for the synthesis of a large number of nucleic acid analogues⁴. An advantage of the solid-supported method compared with conjugation or derivatization in solution is that it is less laborious, among other advantages. In fact, on a solid support, the unreacted compounds are usually used in considerable excess, and the possible by-products can be removed by simple washing. Within this framework, the low loading of the solid supports has proven to be a limitation to the different strategies proposed, as it strongly restricts the amount of targets that can be obtained.

3.1 Aim of research work

In these years, many efforts have been made, towards the synthesis of new solid supports useful to generate pharmacologically interesting libraries of molecules of high purity and in large

quantities⁵⁻¹⁰. The goal of my project was the improvement of the more recent solid phase strategy reported by my research group. The solid phase methodology at issue, it was reported by De Napoli et al. in 2005 (**Scheme 1**), and was devised to obtain phosphodiester and phosphoramidate monoester nucleoside analogues and 5' and 3'-ODN conjugates in extremely pure form using standard phosphotriester chemistry⁷.



Scheme 1. Solid phase methodology to obtain phosphodiester, phosphoramidate monoester nucleoside analogues and oligonucleotide conjugates.

The key step of this strategy was the derivatization of the solid support (TG, CPG) with a 3-chloro-4-hydroxyphenylacetic linker, onto which the nucleotide is attached through a phosphate triester linkage. Due to the structure of the linker, after cleavage from the support, the HPLC analyses of the released nucleotides and ODNs showed only the desired product. High purity can be obtained due the cleavage from the resin of phosphotriester or phosphoramidate diester bonds after ammonia treatment, in whereas the nucleoside or ODN

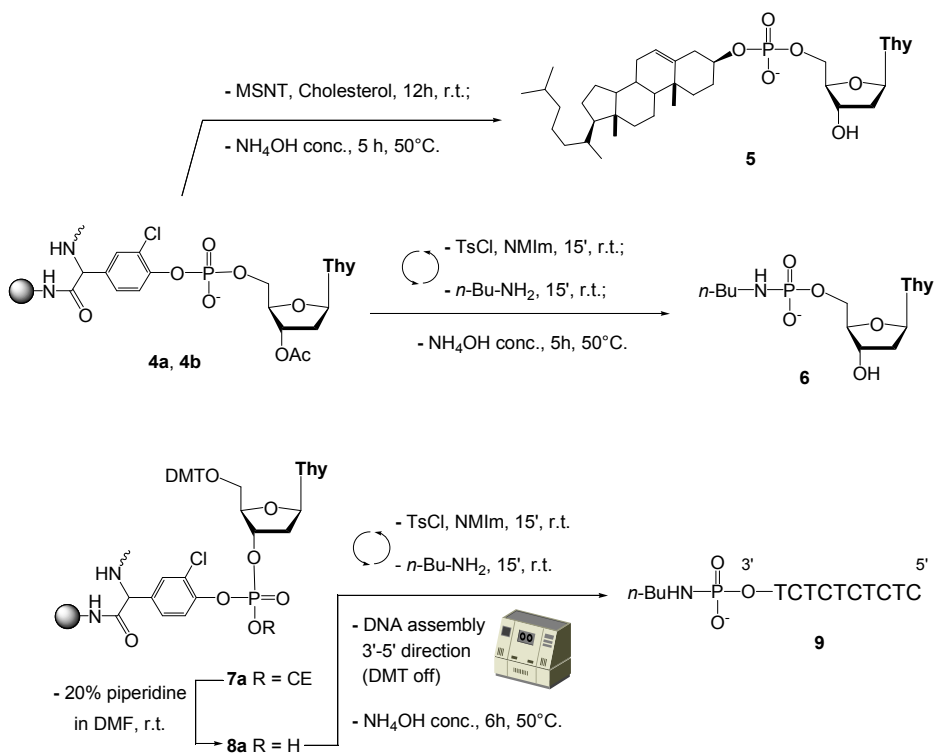
anchored by a phosphodiester bond (the unreacted ODN chain) is not affected.

3.2 Results and Discussion

Aiming to improve the load of the solid support currently available⁷ and that is also compatible with phosphoramidite and phosphotriester chemistry, we devised a straightforward and efficient synthetic protocol to prepare a new support in which the loading of the *o*-chloro-functional group is very high (0.20–0.50meq/g).

The key step was the derivatisation of commonly used long chain amino alkyl (LCAA-CPG and TG) solid supports with *N*- α -Fmoc-3-chloro-L-tyrosine (3-Cl-Tyr). Unlike the 3-chloro-4-hydroxyphenylacetic linker, used previously, the 3-chloro-L-tyrosine linker not only contains an *o*-chloro-phenol skeleton but also simultaneously has amino and acidic functional groups, which allow a versatile elongation of the peptide chain, with a resulting increase of the functionalization of the OH groups. In an initial series of experiments, we synthesized supports LCAA-CPG (load 0.10meq/g) or TG (load 0.29meq/g), with a homopeptide (3-Cl)-Tyr₃ following an Fmoc protocol, leading to **1a** and **1b**, respectively (**Scheme 2**). The peptide chain was prepared using DCCI/HOBt (N,N'-dicyclohexylcarbodiimide/*N*-hydroxybenzotriazole) as coupling agents, with each monomer addition monitored by the Kaiser test¹¹; the yields were always in the range of 65–85%, corresponding to 0.19–0.25meq/g for **1a** and 0.50–0.75 meq/g for **1b**.

nucleotide models. Initially, the 5'-phosphoramidite thymidine derivative **2** was anchored to matrices (CPG and TG) by exploiting classical phosphoramidite chemistry (**Scheme 3**). After conversion of the phosphite to phosphate triesters, affording supports **3a** and **3b**, the incorporation of the nucleotide, as determined by the DMT test, was always in the range of 0.18–0.22meq/g for LCAA- CPG (**3a**) and 0.25–0.50meq/g starting from a TG amino resin (**3b**). Compared with previous work, here we have doubled resin loading (0.08–0.10meq/g and 0.19–0.22meq/g, resp.).



Scheme 3. The feasibility tests of new supports for the solid phase synthesis of nucleotide analogues and oligonucleotide conjugates.

To obtain the phosphodiester thymidine derivative **5** (**Scheme 3**), support **4b** was reacted with MSNT [1-(mesitylene-2-sulfonyl)-3-nitro-

1,2,4-triazole] and cholesterol in pyridine at room temperature (r.t.) for 12 hours (h). To prepare the phosphoramidate thymidine derivative, support **4a** was treated three times with p-tosyl chloride in pyridine and then reacted with the n-butylamine dissolved in pyridine. As expected, the conjugation efficiency was always in the range of 70–80%, leading to supports with 0.13–0.18 meq/g and 0.18–0.40 meq/g loading for **4a** and **4b**, respectively. These yields could be indirectly evaluated by DMT tests on weighed samples of the support after ammonia treatment, determining the amount of un-conjugated material left on the solid support. Only nucleosides linked to the support through a phosphotriester or phosphoramidate diester linkage are easily removed upon basic treatment (28% NH₄OH, 50°C, 5 h), whereas nucleosides anchored through a phosphodiester bond are not cleaved from the resin under the same conditions. After DMT removal and detachment from the supports, the obtained crude material was analyzed by RP-HPLC, and the profiles showed a single major peak with an area (85%–91%) similar to values reported previously (**Figure 1**).

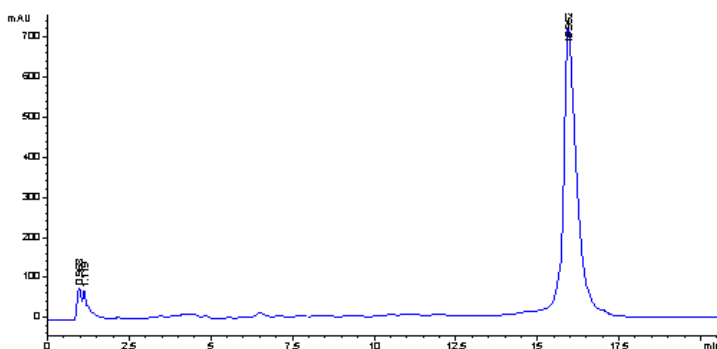


Figure 1. SAX-HPLC profile of crude detached **5** (Phenomenex LUNA, 5 μ m C18, 10.0 \times 250 mm) eluted with a linear gradient from 10 to 100 % B in 30 min, A = H₂O, B = CH₃CN; detection at λ = 260 nm; flow rate 0.8 mL/min.

The identity of **5** and **6** was determined by ^1H , ^{31}P NMR, and ESI-MS experiments that were conducted directly on the crude detached material. As expected, starting from 30 mg of support **4a** or **4b**, the target nucleotides were recovered as discrete compounds in 2–4 mg and 4–9 mg quantities, respectively, in a highly pure form.

To demonstrate the reliability of the CPG supports for the automatic synthesis of ODNs, automated assembly has been explored for the synthesis of the ODN chains, adopting the elongation directions (3'–5'). Starting from support **8a**, a 10-mer was synthesized (**Scheme 3**), and after ammonia cleavage and deprotection (6 h, 50°C), ion exchange HPLC analysis of the released ODN showed a single product corresponding to the desired compound **9**. The purity of the isolated compound was then checked by HPLC, and its identity was determined by MALDI-TOF MS analysis. In a typical experiment, starting from 35 mg of functionalized support **8a** with an average 0.15 meq/g incorporation of the conjugating residue, 150–200 OD units of pure ODNs were isolated after gel filtration.

3.3 Conclusions and Perspective

In conclusion, we have reported the synthesis of a new *o*-chlorophenol-functionalized solid support, characterized by a higher loading of hydroxyl phenol functions than previously achievable (0.18–0.22 meq/g to CPG and 0.25–0.50 meq/g to TG). This support allows the facile and high yield preparation of phosphodiester and phosphoramidate monoester nucleosides, as well as other yet unexplored classes of phosphodiester and phosphoramidate molecules. To test the efficiency of this support, we prepared model thymidine analogues conjugated at the 5'-position to cholesterol and *n*-butylamine through phosphodiester and phosphoramidate bridges,

respectively. In all cases, the coupling yields and purity of crude detached materials were comparable to our previous results, and twice as much target was obtained, due to the loading being doubled on average. Based on these preliminary studies, the method is efficient and very reliable. This synthetic approach can be a starting point for the development of a preparative method for obtaining new phosphodiester and phosphoramidate nucleotides and oligonucleotide conjugates. Further studies are currently in progress to extend this solid phase approach to synthesized 3'-conjugates and 5',3'-biconjugates of the well-known d(TGGGAG) sequence (see Chapter 2).

3.4 Experimental Session

Synthesis of supports 1a and 1b. Support **1a**: 250 mg of LCAA-CPG-NH₂ (0.10 meq/g, 0.02 mmol) was reacted, at r.t. overnight, with a mixture of 109.5 mg (0.25 mmol) of N- α -Fmoc-3-chloro-L-tyrosine, 51.5 mg (0.25 mmol) of DCCl, 45 μ L (0.25 mmol) of DIEA and 38.0 mg (0.25 mmol) of N-hydroxybenzotriazole (HOBt·H₂O) dissolved in 3 mL of anhydrous pyridine. After exhaustive washing with DCM and Et₂O, the support was dried under reduced pressure and then treated with 20% piperidine in DMF three times for 5 min. The coupling and Fmoc removal were repeated twice more in similar conditions. According to the Kaiser test¹¹, the incorporation of the linker was always in the range of 65–85%, corresponding to 0.19–0.25 meq/g. After capping the unreacted amino functional groups with Ac₂O/pyridine (1:1, v/v) for 1 h at r.t., the support was treated with conc. aq. ammonia (28%) at 50°C for 1 h. After exhaustive washing with CH₃OH, DCM and Et₂O, the resulting support **1a** was dried under reduced pressure.

Synthesis of support 1b. 250 mg of TG-NH₂ LL (0.29 meq/g, 0.07 mmol) was reacted, at r.t. overnight, with a mixture of 317.5 mg (0.72 mmol) of N-3-chloro-Tyrosine acid, 150.0 mg (0.72 mmol) of DCCI, 126.0 μ L of DIEA and 110.0 mg (1.5 mmol) of N-hydroxybenzotriazole (HOBT·H₂O) dissolved in 5 mL of anhydrous pyridine. After exhaustive washing with DCM and Et₂O, the support was dried under reduced pressure and then treated with 20% piperidine in DMF three times for 5 min. The coupling and Fmoc removal were repeated twice more in similar conditions. The incorporation of the linker was always in the range of 65–85%, corresponding to 0.50–0.75 meq/g, according to the Kaiser and Fmoc tests. After capping the unreacted amino functional groups with Ac₂O/pyridine (1:1, v/v) for 1 h at r.t., the support was treated with conc. aq. ammonia (28%) at 50°C for 1 h. After exhaustive washing with CH₃OH, DCM and Et₂O, the resulting support **1b** was dried under reduced pressure.

Synthesis of supports 4a, 4b and 8a. Support **4a**: 1.1 mL (0.5 mmol) of a commonly used ‘activator solution’ (0.45 M tetrazole in CH₃CN) was added to 0.08 mmol of 5'-O-(2-cyanoethyl)-N,N-diisopropylphosphoramidite-3'-O-(4,4'-dimethoxytriphenylmethyl)-thymidine and 250 mg (0.22 meq/g, 0.05 mmol) of support **1a**. After 1 h the support was exhaustively washed with CH₃CN and treated (3 times) with 5 mL of a commonly used “oxidiser” solution (I₂/pyridine/H₂O/THF) for 5 min. After exhaustive washing with CH₃CN, DCM and Et₂O, the resulting support **3a** was dried under reduced pressure. Incorporation yields of the nucleotides were always in the range of 82–99% (0.18–0.22 meq/g), as determined by a quantitative DMT test performed on dried and weighed samples of support **3a**. After the standard capping procedure with Ac₂O/pyridine (1:1, v/v), the 2-cyanoethyl group from the phosphate was then

removed by treatment with 20% piperidine in DMF for 5 min at r.t. (3 times), resulting in support **4a**.

Support 4b: 4.9 mL (2.2 mmol) of a commonly used ‘activator solution’ (0.45 M tetrazole in CH₃CN) was added to 0.35 mmol of the 5'-*O*-(2-cyanoethyl)-*N,N*-diisopropylphosphoramidite-3'-*O*-(4,4'-dimethoxytriphenylmethyl)-2'-deoxyribonucleoside and 250 mg (0.55 meq/g, 0.14 mmol) of support **1b**. After 1 h the support was exhaustively washed with CH₃CN and treated (5 times) with 5 mL of a commonly used ‘oxidiser’ solution (I₂/pyridine/H₂O/THF) for 5 min. After exhaustive washing with CH₃CN, DCM and Et₂O, the resulting support was dried under reduced pressure. The complete oxidation of the phosphate triester into a phosphate triester, leading to support **3b**, was monitored by ³¹P NMR of the resin suspended in CDCl₃. As is typical, a relevant upfield shift of the signal at 137 ppm to two signals centred at δ -6.5 ppm was observed. After a standard capping procedure with Ac₂O/pyridine (1:1, v/v), the 2-cyanoethyl group was removed from the phosphate by treatment with 20% piperidine in DMF for 5 min at r.t. (5 times), resulting in support **4b**. Incorporation yields of nucleotides, calculated after capping, were always in the range of 75–91% (0.40–0.50 meq/g), as determined by a quantitative DMT test performed on dried and weighed samples of support **4b**. The total deprotection of the phosphates was confirmed by a characteristic upfield shift in the signal of the ³¹P NMR spectrum of the solid support suspended in CDCl₃.

Support 8a: this support was obtained by following the procedure described for the synthesis of support **4a**, using 5'-*O*-(4,4'-dimethoxytriphenylmethyl)-3'-*O*-(2-cyanoethyl)-*N,N*-diisopropylphosphoramidite-thymidine starting from support **1a**.

Synthesis of thymidine analogue 5. 30 mg (0.40 meq/g, 0.012 mmol) of dried support **4b** was washed and swelled in anhydrous pyridine and then reacted with a mixture of 46 mg (0.12 mmol) of cholesterol and 36 mg (0.12 mmol) of MSNT in 500 μ L of anhydrous pyridine for 12 h at r.t. After exhaustive washing with pyridine, CH₃OH, DCM and Et₂O, the target analogues were detached from the support by conc. aq. ammonia treatment at 50°C for 5 h. The crude material of **5** was analysed by HPLC on a C18 Phenomenex LUNA column (5 μ m, 10.0 x 250 mm) eluted with a linear gradient (from 10 to 100% B over 30 min, A = H₂O, B = CH₃CN), flow rate = 0.8 mL/min, detection at λ = 260 nm, t_R = 16.5 min, HPLC purity 88% (see **Figure 1**). ¹H NMR (CD₃OD, 400 MHz) δ 7.79 (1H, s, H-6 T), 6.35 (1H, dd, J = 6.4, 6.4 Hz, H-1' T), 5.32 (1H, m, H-6 cholesterol residue), 4.50 (1H, m, H-3' T), 4.04-3.90 (3H, overlapped signals, H-4' and H₂-5' T), 3.65 (1H, s, H-3 cholesterol residue), 2.30 (2H, m, H₂-2' T), 2.20-0.65 (complex signals of cholesterol residue), 1.94 (3H, s, CH₃ T) ppm. ³¹P NMR (CD₃OD, 161.98 MHz) δ 2.6 ppm. ESI-MS m/z : 688.51 [(M-H)⁻].

Synthesis of thymidine analogue 6. Synthesis of **6** starting from **4a**: 50 mg (0.22 meq/g, 0.011 mmol) of dried support **4a** was washed and swelled in anhydrous pyridine. The support was then treated with 1 mL of a freshly prepared tosyl chloride solution (0.2M TsCl, 0.4M NMI in pyridine) for 15 min at r.t. to generate the active ester, followed by addition of 1 mL of the amine solution (0.45M in pyridine), with appropriate washing steps in between¹². This procedure was repeated six times. After exhaustive washing with pyridine, CH₃OH, DCM and Et₂O, the resulting support was dried under reduced pressure. The conjugation yields were evaluated by the DMT cation test on a weighed sample of the support after ammonia treatment (28% NH₄OH, 50°C, 5 h). The conjugation yields were

always in the range of 65–75%. The target analogue **6** was detached from the support by conc. aq. ammonia treatment at 50°C for 5 h. The crude material was analysed by HPLC on a C18 Phenomenex LUNA column (5µm, 10.0 x 250 mm) eluted with a linear gradient (from 0 to 100% B over 30 min, A = H₂O, B = CH₃CN), flow rate = 0.8 mL/min, detection at λ = 260 nm, t_R = 13.6 min, HPLC purity 91%.

Synthesis of 6 starting from 4b. 30 mg (0.40 meq/g, 0.012 mmol) of dried support **4b** was washed and swelled in anhydrous pyridine. The support was then treated with 2 mL of a freshly prepared tosyl chloride solution (0.2M TsCl, 0.4M NMI in pyridine) for 15 min at r.t. to generate the active ester, followed by addition of 1 mL of the n-butylamine solution (0.45M in pyridine), with appropriate washing steps in between. This procedure was repeated ten times. After exhaustive washings with pyridine, CH₃OH, DCM and Et₂O, the resulting support was dried under reduced pressure. The conjugation yields were evaluated by the DMT cation test on a weighed sample of the support after ammonia treatment (28% NH₄OH, 50°C, 5 h). The conjugation yields were always in the range of 85–90%. The target analogue **6** was detached from the support by conc. aq. ammonia treatment at 50°C for 5 h. The crude material was analysed by HPLC on a C18 Phenomenex LUNA column (5µm, 10.0 x 250 mm) eluted with a linear gradient (from 0 to 100% B over 30 min, A = H₂O, B = CH₃CN), flow rate = 0.8 mL/min, detection at λ = 260 nm, t_R = 13.6 min, HPLC purity 86%. ¹H NMR (CD₃OD, 400 MHz) δ 7.89 (1H, s, H-6 T), 6.35 (1H, dd, J = 6.4, 6.4 Hz, H-1' T), 4.52 (1H, m, H-3' T), 4.03 (1H, bs, H-4' T), 3.96 (2H, bs, H₂-5' T), 2.86 (2H, m, CH₂-NH), 2.33-2.18 (2H, m, H₂-2' T), 1.95 (3H, s, CH₃ T), 1.46 (2H, m, CH₃-CH₂-CH₂-CH₂-NH), 1.32 (2H, m, CH₃-CH₂-CH₂-CH₂-NH), 0.89 (3H, t, J = 7.2

Hz, CH₃ butyl residue) ppm. ³¹P NMR (CD₃OD, 161.98 MHz) δ 11.0 ppm. ESI-MS m/z: 376.24 [(M-H)].

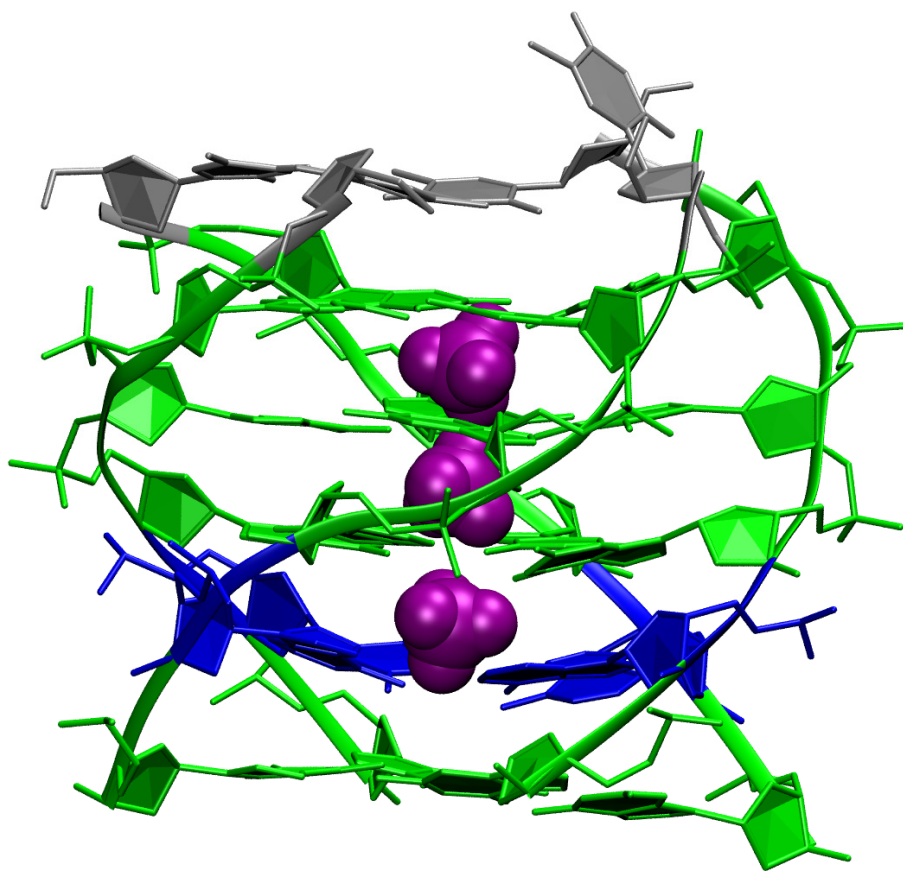
Synthesis of oligonucleotide conjugated 9. 50 mg (0.22 meq/g, 0.011 mmol) of dried support **8a** was washed and swelled in anhydrous pyridine. The support was then treated with 1 mL of a freshly prepared tosyl chloride solution (0.2M TsCl, 0.4M NMI in pyridine) for 15 min at r.t. to generate the active ester, followed by the addition of 1 mL of the n-butylamine solution (0.45M in pyridine), with appropriate washing steps in between. This procedure was repeated six times. After exhaustive washings with pyridine, CH₃OH, DCM and Et₂O, the resulting support was dried under reduced pressure. Starting from 25 mg of support, a 10 mer oligodeoxyribonucleotide was assembled by the automated standard phosphoramidite procedure (DMT off), using commercially available phosphoramidite nucleosides. Detachment from the support and deprotection was achieved by treatment with conc. aq. ammonia solution (28%, 6 h, 55°C), and the crude material thus released was then purified by a simple gel filtration chromatography on a Sephadex G25 column eluted with H₂O/EtOH (4:1, v/v). The purity of the isolated compounds was then checked by ion exchange HPLC analysis and their identities determined by MALDI-TOF mass spectrometry. t_R = 31.2 min. MALDI-TOF m/z: 3040.63 [(M-H)⁺] (obsv.), 3038.55 (calcd.).

References

- (1) Dean, N. M., and Bennett, C. F. (2003) Antisense oligonucleotide-based therapeutics for cancer. *Oncogene* 22, 9087–9096.
- (2) Aboul-Fadl, T. (2005) Antisense Oligonucleotides: The State of the Art. *Current Medicinal Chemistry* 12, 2193–2214.
- (3) Richter, Y., and Fischer, B. (2006) Nucleotides and inorganic phosphates as potential antioxidants. *Journal of biological inorganic chemistry* 11, 1063–74.
- (4) Zhou, W., Roland, A., Jin, Y., and Iyer, R. P. (2000) Combinatorial synthesis using nucleic acid-based (NAB(TM)) scaffold: Parallel solid-phase synthesis of nucleotide libraries. *Tetrahedron Letters* 41, 441–445.
- (5) De Napoli, L., Di Fabio, G., D’Onofrio, J., and Montesarchio, D. (2004) New nucleoside-based polymeric supports for the solid phase synthesis of ribose-modified nucleoside analogues. *Synlett* 1975–1979.
- (6) D’Onofrio, J., Montesarchio, D., De Napoli, L., and Di Fabio, G. (2005) An efficient and versatile solid-phase synthesis of 5'- and 3'-conjugated oligonucleotides. *Organic Letters* 7, 4927–4930.
- (7) De Napoli, L., Di Fabio, G., D’Onofrio, J., and Montesarchio, D. (2005) An efficient solid phase synthesis of 5'-phosphodiester and phosphoramidate monoester nucleoside analogues. *Chemical communications (Cambridge, England)* 2586–2588.
- (8) Moggio, L., De Napoli, L., Di Blasio, B., Di Fabio, G., D’Onofrio, J., Montesarchio, D., and Messere, A. (2006) Solid-phase synthesis of cyclic PNA and PNA-DNA chimeras. *Organic Letters* 8, 2015–2018.
- (9) Fabio, G. Di, Malgieri, G., Isernia, C., D’Onofrio, J., Gaglione, M., Messere, A., Zarrelli, A., and De Napoli, L. (2012) A novel synthetic strategy for monosubstituted cyclodextrin derivatives. *Chemical Communications*.
- (10) Gaglione, M., Potenza, N., Di Fabio, G., Romanucci, V., Mosca, N., Russo, A., Novellino, E., Cosconati, S., and Messere, A. (2013) Tuning RNA interference by enhancing siRNA/PAZ recognition. *ACS Medicinal Chemistry Letters* 4, 75–78.
- (11) Kaiser, E., Colescott, R. L., Bossinger, C. D., and Cook, P. I. (1970) Color test for detection of free terminal amino groups in the solid-phase synthesis of peptides. *Analytical Biochemistry* 34, 595–598.

(12) Davis, P. W., and Osgood, S. A. (1999) A new method for introducing amidate linkages in oligonucleotides using phosphoramidite chemistry. *Bioorganic & medicinal chemistry letters* 9, 2691–2.

G-Quadruplex



CHAPTER 4

Kinetic study of G-quadruplex formation by ESI-MS

Over the years, it was assessed that the knowledge of the energetic parameters inherent in G-quadruplex formation is crucial in view of their applications as therapeutic agents. It is evident, in fact, that both kinetic and thermodynamic factors may be important in physiological conditions¹. Tetramolecular G-quadruplexes constituted from four identical strands arranged in parallel orientation have been extensively studied, because they offer a good model system to determine the potential folding pathways. In contrast to bi- and unimolecular G-quadruplexes, tetramolecular G4 formed by short nucleic acid sequences show limited polymorphism and very slow kinetic of formation that facilitate experimental studies². Many studies have been conducted to follow the stability and kinetic of G-quadruplexes formation, using a wide range of methodologies, such as UV, circular dichroism (CD), fluorescence, chromatography, native PolyAcrylamide Gel Electrophoresis (PAGE), NMR and more recently electrospray mass spectrometry (ESI-MS)^{3,4}. Some years ago, potential pathways of tetramolecular G-quadruplex formation have been reported, overall involve in multiple steps and with the formation of some intermediates^{5,6}. In 2010, Gabelica and coworkers⁷ reported a kinetic study by ESI-MS that confirmed the formation of some intermediates previously proposed by Stefl. Following the assembly of G4 complexes by ESI-MS, they proved unambiguously the formation of dimers and trimers and reported a pre-equilibrium between monomer, dimers, and trimers as potential association pathway (**Figure 1**).

Recently many research efforts have been devoted to the design and synthesis of modified ODNs, the alteration of chemical composition of G-rich strands for example at 3'- or 5'-ends or in the backbone, is a successful strategy to improve their therapeutic applications.

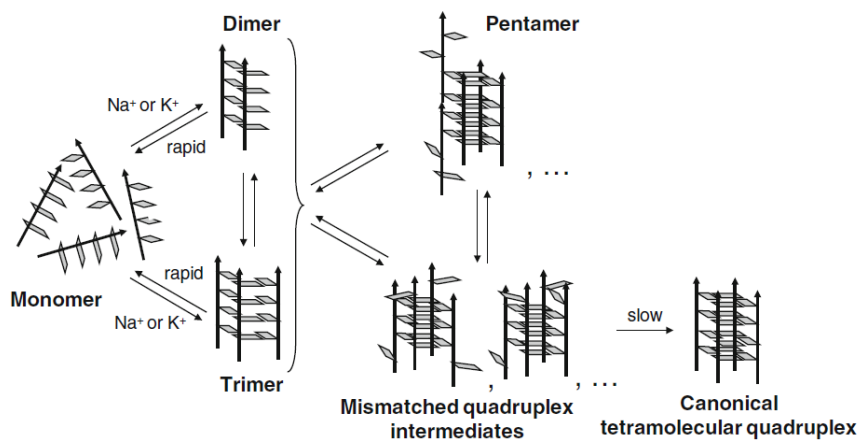


Figure 1. Potential pathway of G-quadruplex assembly proposed (6), (7) and (28).

In order to understand the impact of these modifications on the kinetic of G4 formation, many studies have been conducted using NMR and ESI-MS methodologies. These two techniques, allow to follow the association process of these structure, in a more precise manner than absorbance by UV or CD. Particular emphasis has been directed on the ESI-MS and its application to study the kinetic of G4 formation and the drug-nucleic acid complexes. By ESI-MS experiments it is possible to have much information about the number of strands⁸ and the cations within each structure^{9,10}. Moreover the use of this technique is exploit to detect all possible intermediate complexes⁷, to determine the relative equilibrium binding constants¹¹ and finally to conduct ligand screening assays¹². Basically the study of nucleic acids in the gas phase allows to isolate

molecules from their environment and to study their intrinsic properties, defining the gas phase method as an indirect way to understand the solvent effect on folding or binding¹³.

4.1 ESI-MS to detect nucleic acids

Particular interest regarding the study of nucleic acid complexes in gas phase, is growing due to the use of electrospray ionization (ESI) source, capable to minimize covalent fragmentation and even to preserve non-covalent complexes.

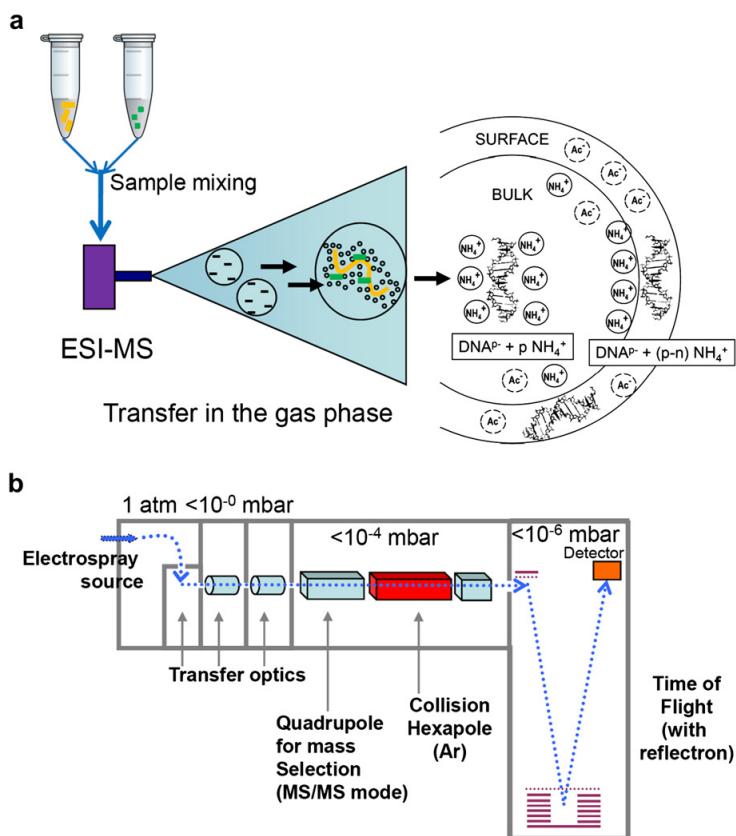


Figure 2. Generic electrospray mass spectrometry experiment on nucleic acid complexes reported in (11). (a) Sample is prepared by mixing DNA and NH_4OAc buffer and it is injected in the mass spectrometer via the electrospray source. (b) Schematic representation of a hybrid quadrupole-time of flight mass spectrometer. The ion trajectory is in blue.

ESI is a soft ionization method in which the analyte can be given little internal energy during the transfer to the gas phase¹⁴. Thanks to the soft ionization it is possible to detect non-covalent complexes as DNA structures and also to observe interactions between small drug molecules and DNA complexes. Double helical duplex^{15,16} and quadruplex¹⁷ DNA has been first detected in 1993 by B. Ganem and co-workers.

ESI typically generates protonated and/or deprotonated molecular ions of the type $(M+nH)n^+$ and $(M-nH)n^-$, respectively. High charge states are often formed, and the charge state distribution depends on the molecular mass of the analyte, the solvent conditions in the sprayed solution, and ion-source conditions, skimmer voltage (collisional-induced desolvation and dissociation). Critical parameters in the study of non-covalent complexes are the source or capillary temperatures (kept as low as possible), and all acceleration voltages in the transfer optics (all cone, skimmer, and lens voltages).

Usually to high acceleration voltages, the dissociation of non-covalent complexes can occur. The typical solvent conditions used to achieve maximum sensitivity are not always optimal to maintain an intact biomolecular complex. A major limitation of ESI-MS, is its low salt tolerance, in fact even minute amounts of sodium or potassium result in the detection of a wide distribution of non specific adducts on the DNA¹¹. Therefore, a majority of non-covalent complexes studied by ESI-MS is done in volatile salts like ammonium acetate (NH_4OAc). Organic solvents such as methanol or acetonitrile may be added to the solution to obtain maximum sensitivity and signal stability, but only with low percentage in order to preserve the native structure⁷.

Recently, quantitative mass spectrometry determination of absolute concentration of complexes from relative peak intensities has been described by Gabelica¹⁸. This method requires the determination of the factor relating the peak intensity of each species, known as electrospray response factor (R)^{19,20} and defined in *Eq. 1* for compound M:

$$\text{Eq. 1} \quad I_M = R_M[M]$$

To this aim is used an internal standard (**T6**) and the mass balance equation applied to each complex detected in the electrospray mass spectra. Briefly, for each stoichiometry adopted by the sequence, the ratio between the area of a peak attributable unambiguously to that stoichiometry and the area of a peak of the internal standard, is calculated at each time-point. The method for the determination of response factors can also be used to study the kinetics involving non-covalent complexes, following the signals relative to each complex, in respect of the internal standard.

4.2 Aim of research work

In this frame is focused my research work, the goal of my project was to complete the biophysical characterization of the most active 5'-modified ODNs (**Figure 3**), synthesized in our laboratories. As described in the previous chapter, the thermal stability of these 5'-end modified ODNs carried out by CD is not directly correlated with their high anti-HIV activity. In order to achieve a more complete picture of the relationship between G-quadruplexes formed by 5'-end modified ODNs and their pronounced anti-HIV activities, it is necessary to explore not only the structural and thermodynamic, but also the kinetic aspects of G-quadruplex folding. In this context, we chose to

study the kinetics of 5'-end modified G-quadruplex formation by ESI-MS (**Figure 3**), taking in advantage of the precious collaboration of Valérie Gabelica, Research Director of ARNA Inserm/Univ. Bordeaux (France). Valérie Gabelica is a pioneer in the study of non-covalent DNA complexes by ESI-MS⁷.

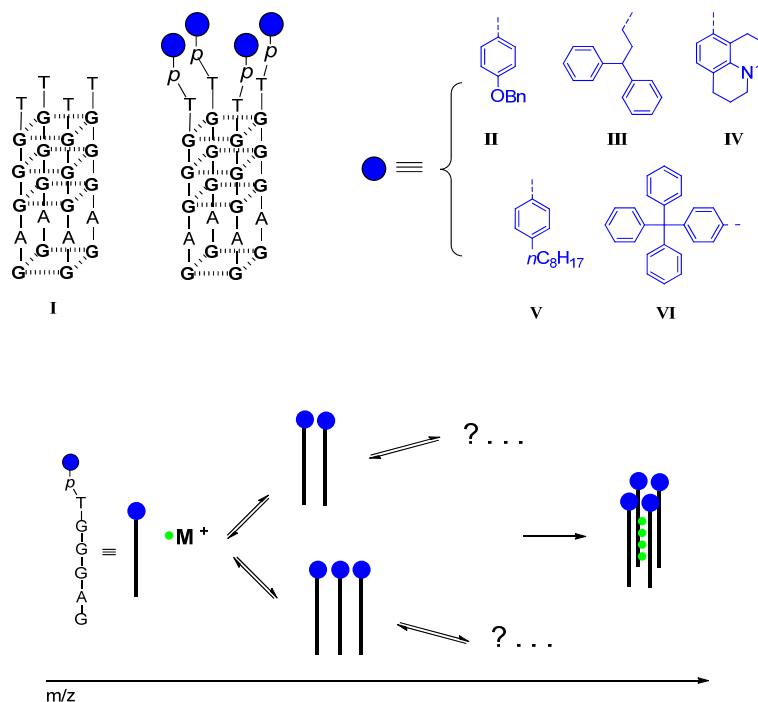


Figure 3. d(TGGGAG) G-quadruplex and its 5'-end modified with pronounced anti-HIV activities (on the top). Schematic representation of potential pathway of G-quadruplexes folding (on the bottom).

Aiming at investigating the influence of the 5'-end conjugated moiety on the kinetics of G4 formation, we have studied the kinetics of G-quadruplex formed by 5'-end modified ODNs in comparison with that formed by unmodified sequence (**Figure 3**). From ESI-MS experiments we have followed the formation of all possible complexes, determining the number of strands and the cations inside each complex. In addition to ESI-MS studies, we assessed the molecularity

of non-covalent complexes, in particular that of high order DNA structures using non-denaturing polyacrylamide gel electrophoresis.

4.3 Results and Discussion

All 5'-conjugates d(TGGGAG) endowed with high anti-HIV activity (**Figure 3**, top) are dissolved in water (nuclease-free), and the 1 mM stock solutions are stored at -20°C. The modified sequences are obtained from synthesis, purification (RP-HPLC) and desalting (Sephadex G25) carried out in our laboratory (synthetic strategy reported in Chapter 2). The stock concentrations are determined by UV absorbance at 260 nm, and measured on an Agilent Cary 100 UV spectrophotometer. Before G-quadruplex formation, aqueous stock solutions of each sequence, including the unmodified sequence, are heated at 80°C for 5 min. Heating, commonly called annealing, is required to remove all pre-formed G-quadruplex complexes.

To study the kinetic of G-quadruplex formation, we recorded ESI-MS spectra as a function of the time after addition of cation in the ODN solutions. These experiments are carried out in NH₄OAc (150 mM) and also using a new buffer developed very recently by Gabelica and co-workers¹⁰. In order to observe DNA G-quadruplexes with K⁺ ions specifically bound between G-quartets, as occur in physiological conditions, they replaced the NH₄OAc with trimethylammonium acetate (TMAA), doping the solution with potassium chloride (KCl) at concentration up to 1 mM. The TMA ion is too large to fit between G-quartets, hence, only K⁺ ions can coordinate. Before the ESI-MS experiments, aiming to follow G4 association pathway, we looked for a proper concentration of stock solution and time-scale in which the kinetics are representative. The concentration chosen is 600 μM, fixing as a T₀ the time of addition of cation, we monitored the kinetics

of formation for each sample over 14 days. At each time point, an aliquot of the sample is diluted to 20 μM , final single-strand concentration, and injected in the ESI-MS. For the preparation of a stock solution in NH_4OAc , the solution 1 mM in single-stranded of all sequences is diluted to 600 μM (final concentration of stock solution) adding NH_4OAc in a final concentration of 150 mM. The single strand d(T_6) is added in each stock solution to serve as internal standard. All kinetics experiments are carried out with the sample at room temperature. Quadruplex formation is initiated by the addition of NH_4OAc (final concentration: 150 mM). We therefore assume that, once formed, all complexes formed resist the dilution step. The signal intensity of the reference is used to normalize the intensity variations of each signals, and to deduce their respective response factors.

We firstly studied the unmodified sequence **I**, in order to have a kinetic reference of G-quadruplex formed without 5'-end moiety. In **Figure 4** is reported as typical ESI-MS spectra, the spectra of d(TGGGAG) (**I**) recorded after 1 day. The monomer is detected mainly at charges state 2 $^-$ ($m/z=934.93$) with some sodium ions non-specifically bound, but no ammonium ions bound. Sodium is a common contamination in DNA samples. Dimer and trimer are also detected, like the monomer with a non-specific sodium adducts, issuing respectively at $m/z=1246.99$ and $m/z=1402.83$. A tetramer is unambiguously detected at the charge state 5 $^-$ ($m/z=1503.69$) and 4 $^-$ ($m/z=1884.16$). As shown in the spectra (**Figure 4**), G-quadruplexes capture different number of ammonium ions. The internal standard, d(T_6) ($m/z=880.36$) is detected only in the monomeric form as properly supposed. An unexpected result is the detection of an octameric specie predominantly at charge states 7 $^-$ ($m/z=2153.54$).

In these years, an increased number of papers has reported the existence of higher order DNA structures formed by multimerization of G-quadruplex units^{21,22}.

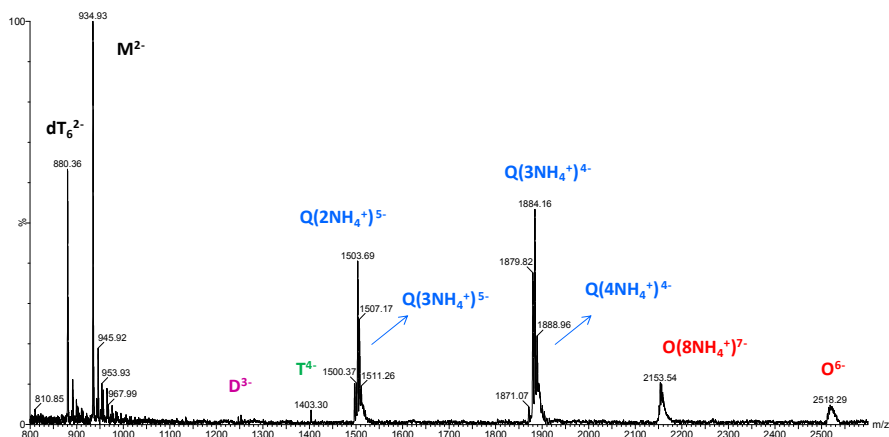


Figure 4. Electrospray mass spectra of d(TGGGAG) (20 μ M in 150 mM NH_4OAc) recorded after 1 day from ammonium acetate addition. M (single strand, **ss**) for monomer, D for dimer, T for trimer, Q for tetramer, O for octamer.

In particular, very recently, exactly for d(TGGGAG), it is observed by NMR data, the formation of high order than G-quadruplex structures²³ confirming the octamer detected by ESI-MS. In addition, in 2011, Borbone et al. described a novel dimerization pathway of two tetramolecular G-quadruplex subunits obtained by head-to-head stacking^{24,25}. This dimerization pathway stimulates many questions regarding the type of interaction involved in the formation of detected $[\text{d}(\text{TGGGAG})_4]_2$ and 5'-end $[\text{d}(\text{TGGGAG})_4]_2$ octamers. All modified sequences showed almost the same spectra profile of d(TGGGAG), in terms of type of complexes and relative charge states. By using a recent Gabelica's mathematical method¹⁸, the relative ESI-MS response of each component of the mixture can be determined and therefore the concentration relative to each complex.

Figure 5 shows the time evolution of the concentration (μM) of monomer, dimer, trimer, tetramer and octamer for sequences (I-IV), unfortunately two of these modified ODNs, V and VI, aggregated already at $600 \mu\text{M}$ in water solution, preventing to follow their kinetic association pathways.

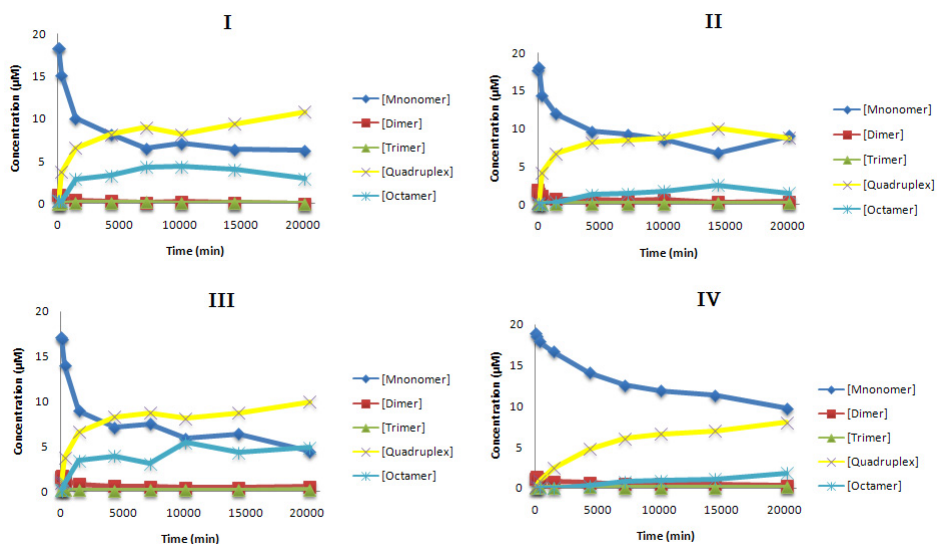


Figure 5. Time evolution of the concentration (μM) of monomer, dimer, trimer, tetramer and octamer for sequences I-IV.

From ESI-MS data, we observed that the single strand (M) is very quickly converted into a dimer (D), both tetramer (Q) and octamer (O) species began to form quite quickly (up to 1 day) and continued to increase up to 14 days reaching the plateau (**Figure 5**). The formation of octamer begins simultaneously to tetramer, but in any cases remains lower than that of tetramer. The detection of these complexes for long time scales confirmed that, once formed, they are stable to the dilution step ($600 \mu\text{M}$ to $20 \mu\text{M}$).

In **Figure 6** is reported the general trend of all G-quadruplex kinetics studied in 150 mM NH_4OAc .

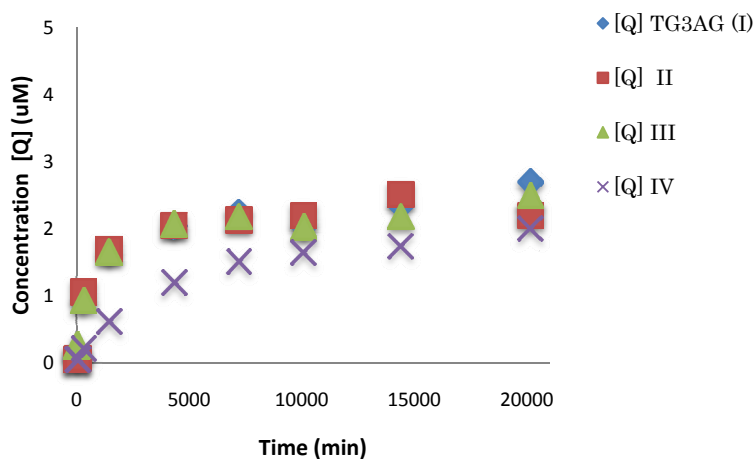


Figure 6. General trend of the kinetics of all G-quadruplex complexes (I–IV) studied at 600 μM in 150 mM NH_4OAc over 12 days.

The preliminary kinetic data obtained, suggest that the kinetic of G4 formation by unmodified d(TGGGAG) (I), no-active sequence, does not deviate too much from the kinetics of formation related to the active sequences II–IV, suggesting that also the kinetics of G4 folding are negligible for the anti-HIV activity. As shown in **Figure 6**, the kinetics of V are slower than others. Based on the spectra recorded in NH_4OAc (150 mM) and taking in account the number of ammonium ions incorporated in G-quadruplex structures, we conducted ESI-MS experiments for each ODN, using the TMAA/KCl mixture as buffer. The use of these new buffer aims to determine the number of potassium ions specifically coordinated to the structure and consequently, the number of G-quartets involved.

In all electrospray mass spectra (performed in 150 mM TMAA + 1 mM KCl) is observed the preferential presence of three K^+ for each charge state of G-quadruplex complex, and presumably, the formation of four G-quartets (no data shown).

4.3.1 Native PolyAcrylamide Gel Electrophoresis

In order to verify the formation of a higher order G-quadruplex structures for 5'-end modified d(TGGGAG) also in solution, we carried out native gel electrophoresis experiments. Aiming at observing the mobility of all complexes, all sequences (I–IV) are loaded on the gel, in both conditions: **ss** conditions (no potassium added, indicated by “–”) and **G4/G8** conditions (stock solution at 4.5 mM of oligo in 100 mM KCl, indicated by “+”).

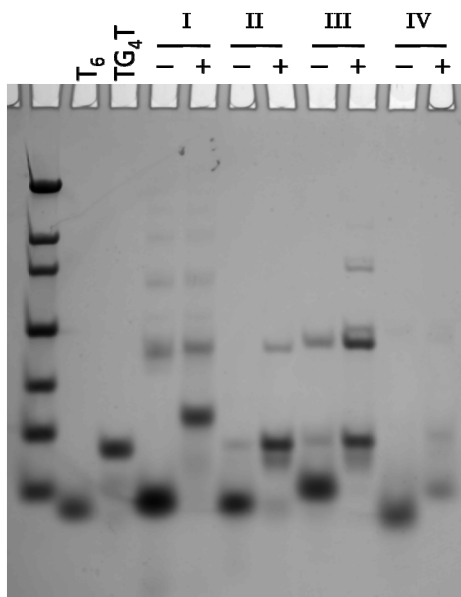


Figure 7. Native gel electrophoresis of I–IV sequences in both conditions (“–”, no potassium added, “+” in 100 mM KCl); 15% polyacrylamide gel supplemented with 100 mM KCl. The gel was run at 26°C at constant voltage (110 V) for 2.5 h.

Figure 7 shows PAGE experiments on the **I–IV** sequences loading in both conditions (“–” and “+”), **d(T₆)** is used as a single-stranded 6-mer marker and **d(TG₄T)** annealed in 0.1 M potassium buffer is used as a tetramolecular G-quadruplex marker, **[d(TG₄T)]₄**. For all ODNs loading in water condition (“–”), the more intense band is that related to the single strand (**ss**) in agreement with the fastest migration. For **I, II** and **III** (“+”), it is observed a retarded migration respect to the **[d(TG₄T)]₄** G4 reference. We therefore assigned the slow migrating PAGE bands to octameric self-assembly structures. The sequence **IV** showed an evident smearing in terms of intensity of band in agreement with the slow kinetic observed by ESI-MS (**Figure 7**).

4.3.2 Ion Mobility Spectrometry for the detection of high order structures

Ion Mobility Spectrometry (**IMS**) is a high resolution technique that provides indications on the tridimensional oligonucleotide structure of the studied ions. This technique allows to separate ions with identical mass-to-charge ratio due to their different mobility in the drift tube. The mobility of ions is the quantity that describes how quickly the ion moves through a drift cell filled with a high pressure of buffer gas under the influence of a weak electric field²⁶. Interestingly, the use of **IMS** allows to have information about the shape of species detected depending on the their drift time²⁷. In the drift tube, complexes with compact conformation such as G-quadruplexes travel more quickly and with small collision cross sections (CCS) than large extended ions, like single-strand, that drift slowly and with large CCS (**Figure 8**). The collision cross sections are a measure of the surface of the ion that is exposed to collision with the bath gas.

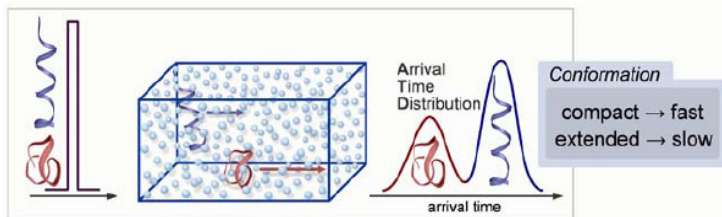


Figure 8. Representation of the ions in the drift tube in function of their different shape.

- **Preliminary experiments on IMS**

In order to confirm the molecularity and to determine the compactness of detected complexes, we tested all sequences on **IMS**, paying attention to octamer complexes. In **Figure 9** is reported a representative example of the Driftscope spectrum characterized by a 2D-graph with the mass spectrum (top of panel) and the drift time in the ion mobility (bottom of panel).

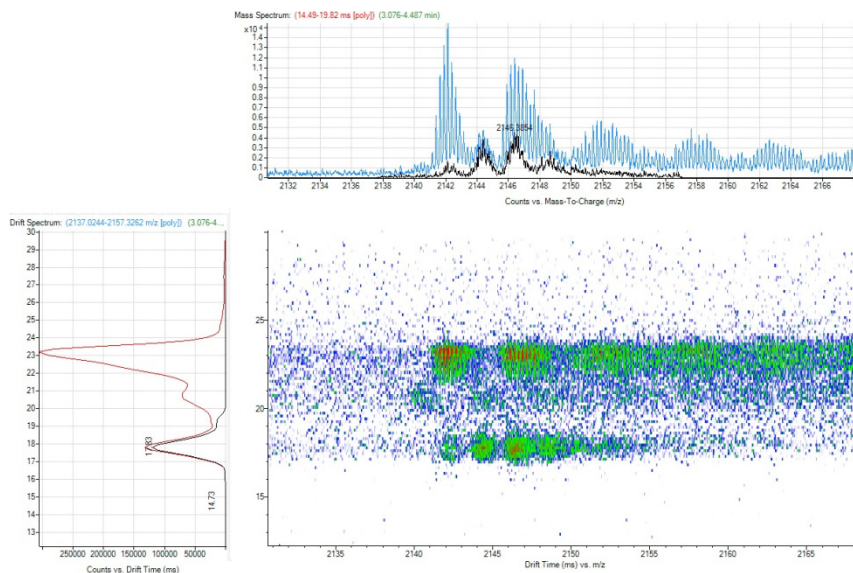


Figure 9. Representation of the contribution of O^8 in comparison with that of Q^4 in the Driftscope spectrum.

As described, at each ion detected by ESI-MS corresponds an unique drift time. Particular attention, it has been addressed on octamer signals, thanks to **IMS** it has been possible to distinguish the octamer at the charge state 8⁺ from the more abundant tetramer at the charge state 4⁺, even if they have the same m/z ratio. In **Figure 9**, it is reported the contribute of octamer respect to that more abundant of tetramer. From preliminary results obtained, we observed for all sequences (**I–IV**) the same distribution of complexes seen by ESI-MS (*LCT mass spectrometer*) but an additional consistent amount of octamer.

4.4 Conclusions and Perspective

The kinetic ESI-MS studies on modified d(TGGGAG), confirmed the formation of some intermediates as earlier reported for unmodified tetramolecular G-quadruplexes^{2,28}. The association pathway of G-quadruplex folding, based on modified d(TGGGAG), revealed a pre-equilibrium between single-strand, dimer and trimer that occurs before the G4 formation, in agreement with the mechanism for tetramer formation reported by Gabelica in 2010⁷.

From preliminary kinetic results obtained by ESI-MS in 150 mM NH₄OAc, it seems that the kinetics of all modified sequences do not deviate from that of unmodified d(TGGGAG), suggesting that the aromatic moieties at 5'-end of d(TGGGAG) do not improve the kinetics of G4 formation. Moreover it has been observed that all sequences, including unmodified sequence, already at 600 μM in NH₄OAc formed simultaneously to G-quadruplex complex also a high order G4 structures identified as octamers. In addition, by Ion Mobility Spectrometry experiments conducted in the same experimental conditions of *LCT-Waters* (kinetic ESI-MS

experiments), it has been observed that the amount of octamer formed is not insignificant and thereby it is very interesting.

These findings open the door to future studies that aim to the understanding of the dimerization phenomenon (how happen and if is relevant for therapeutic activity), especially for 5'-end modified sequences endowed with high anti-HIV activity. Finally, by using of a new sample preparation method (TMAA/KCl mixture), we detected the number of potassium ions specifically coordinated to the G-quadplexes formed by all sequences ($3K^+$), and presumably, the number of quartets involved (4 quartets).

In light of recent **IMS** studies performed on all 5'-modified d(TGGGAG) (**Figure 3**), comparison studies between the experimental data (CCS) obtained by **IMS** and CCS developed by theory models are in progress.

4.5 Experiment Session

Preparation of samples. Stock solutions were prepared at 1 mM in water and stored at -20°C . The stock concentrations were determined by UV absorbance at 260 nm measured on an Agilent Cary 100 UV spectrophotometer. Water was nuclease-free grade from Ambion (Applied Biosystems, Lennik, Belgium). Ammonium acetate (NH_4OAc , Ultra for Molecular Biology, Fluka), trimethylammonium acetate (TMAA, Ultra for UPLC, Fluka) and potassium (KCl, 999.999%, Sigma) were purchased from Sigma-Aldrich (Saint-Quentin Fallavier, France). Annealing experiments were performed at 80°C heating for 5 min and then a fast cooling to 20°C were carried out. Stock solutions of 600 μM of each ODN were obtained by dilution of the samples in 150 mM NH_4OAc or 150 mM TMAA and 1 mM KCl

buffers. For all kinetics experiments, 50 μM $\text{d}(\text{T}_6)$ (monoisotopic mass 1762.318 Da) was added to each stock solution in order to follow the intensities of the reactant (single strand, ss), and the complexes (dimer, trimer, tetramer and octamer) relative to that of the reference. The solutions were stored at 20°C for MS measurements performed in 14 days. The samples are agitated, loaded into the syringe and the spray is initiated in few minutes.

Electrospray Mass Spectrometry. Native ESI-MS spectra were obtained using a *LCT Premier mass spectrometer* (Waters, Manchester, U.K.). The electrospray ion source was operated in negative ion mode and the voltage is set to 2200 V. The desolvation temperature is 60°C, and the gas temperature is 40°C. In all experiments provided in NH_4OAc it have been recorded, three spectra at different voltage (50 V, 100 V, 200 V) to be sure of soft condition of analysis. The source pressure is increased to 45 mbar (measured by a Center Two probe, Oerlikon Leybold Vacuum, Cologne, Germany). The sample cone voltage in TMAA/KCl experiments is 200 V. At this voltage TMA adducts on the mass spectra are totally avoided, but the K^+ stoichiometry is not affected. The syringe injection rate is 200 $\mu\text{L}/\text{h}$. Shown MS spectra is the sum of 3 min accumulations (1 scan per 1.1 s). The voltage of spectra chosen to fit the kinetics, was that one for the best compromise to observe the single strand, tetramer and octamer. The spectra were smoothed (mean function, 2×15 channels), background-subtracted (polynomial order = 99, 0.1% below curve, tolerance 0.010), centroided (peak width 15 channels, reconstructed area of the top 80% of the peak), and recalibrated using the reference as a lock mass $[\text{d}(\text{T}_6)]^{2-}$ monoisotopic peak at $m/z = 880.153$.

Native PolyAcrylamide Gel Electrophoresis (PAGE). The molecular size of structures were probed using native polyacrylamide gel electrophoresis. ODN samples (50 μ M), obtained by diluting the annealed stock solutions just before the experiment, were loaded on a 15% polyacrylamide gel supplemented with 100 mM of KCl. Sucrose (10 %) was added just before loading. The gel was pre-run for about 30 min before loading samples. The gel was run at 26°C at constant voltage (110 V) for 2.5 h. The bands were visualized by UV shadowing and after 'Syber green' coloration.

Sample preparation. To achieve complete G4 formation, high concentrations of samples are necessary. After heating at 80°C for 5 min, to the water stock solution of samples were added 100 mM KCl (4.5 mM final concentration of oligos). In parallel, the samples in single-stranded condition, are prepared only by annealing in pure water.

References

- (1) Lane, A. N., Chaires, J. B., Gray, R. D., and Trent, J. O. (2008) Stability and kinetics of G-quadruplex structures. *Nucleic acids research* *36*, 5482–515.
- (2) Mergny, J. L., De Cian, A., Ghelab, A., Saccà, B., and Lacroix, L. (2005) Kinetics of tetramolecular quadruplexes. *Nucleic Acids Research* *33*, 81–94.
- (3) Petraccone, L., Pagano, B., Esposito, V., Randazzo, A., Piccialli, G., Barone, G., Mattia, C. A., and Giancola, C. (2005) Thermodynamics and Kinetics of PNA - DNA Quadruplex-Forming Chimeras. *journal american chemical society* *127*, 16215–16223.
- (4) Zhou, J., Rosu, F., Amrane, S., Korkut, D. N., Gabelica, V., and Mergny, J. L. (2014) Assembly of chemically modified G-rich sequences into tetramolecular DNA G-quadruplexes and higher order structures. *Methods (San Diego, Calif.)* *67*, 159–68.
- (5) Wyatt, J. R., Davis, P. W., and Freier, S. M. (1996) Kinetics of G-quartet-mediated tetramer formation. *Biochemistry* *35*, 8002–8008.
- (6) Stefl, R., Cheatham, T. E., Spacková, N., Fadrná, E., Berger, I., Koca, J., and Sponer, J. (2003) Formation pathways of a guanine-quadruplex DNA revealed by molecular dynamics and thermodynamic analysis of the substates. *Biophysical journal* *85*, 1787–1804.
- (7) Rosu, F., Gabelica, V., Poncelet, H., and De Pauw, E. (2010) Tetramolecular G-quadruplex formation pathways studied by electrospray mass spectrometry. *Nucleic acids research* *38*, 5217–25.
- (8) Smargiasso, N., Rosu, F., Hsia, W., Colson, P., Baker, E. S., Bowers, M. T., De Pauw, E., and Gabelica, V. (2008) G-quadruplex DNA assemblies: Loop length, cation identity, and multimer formation. *Journal of the American Chemical Society* *130*, 10208–10216.
- (9) Gros, J., Rosu, F., Amrane, S., De Cian, A., Gabelica, V., Lacroix, L., and Mergny, J.-L. (2007) Guanines are a quartet's best friend: impact of base substitutions on the kinetics and stability of tetramolecular quadruplexes. *Nucleic acids research* *35*, 3064–75.
- (10) Marchand, A., and Gabelica, V. (2014) Native electrospray mass spectrometry of DNA G-quadruplexes in potassium solution. *Journal of the American Society for Mass Spectrometry* *25*, 1146–54.
- (11) Rosu, F., De Pauw, E., and Gabelica, V. (2008) Electrospray mass spectrometry to study drug-nucleic acids interactions. *Biochimie* *90*, 1074–87.
- (12) Marchand, A., Granzhan, A., Iida, K., Tsushima, Y., Ma, Y., Nagasawa, K., Teulade-Fichou, M.-P., and Gabelica, V. (2015) Ligand-Induced Conformational

Changes with Cation Ejection upon Binding to Human Telomeric DNA G-Quadruplexes. *Journal of the American Chemical Society* 137, 750–756.

(13) Chemistry, P. (2014) *Nucleic Acids in the Gas Phase* (Gabelica, V., Ed.). Springer Berlin Heidelberg, Berlin, Heidelberg.

(14) Abi-Ghanem, J., and Gabelica, V. (2014) Nucleic acid ion structures in the gas phase. *Physical chemistry chemical physics* 16, 21204–18.

(15) Ganem, B., Li, Y.-T., and Henion, J. D. (1993) Detection of oligonucleotide duplex forms by ion-spray mass spectrometry. *Tetrahedron Letters* 34, 1445–1448.

(16) Galefn, D. C., and Smithcor, R. D. (1995) Characterization of noncovalent complexes formed between minor groove binding molecules and duplex DNA by electrospray ionization-mass spectrometry. *Journal of the American Society for Mass Spectrometry* 6, 1154–64.

(17) Goodlett, D. R., Camp, D. G., Hardin, C. C., Corregan, M., and Smith, R. D. (1993) Direct observation of a DNA quadruplex by electrospray ionization mass spectrometry. *Biological mass spectrometry* 22, 181–3.

(18) Gabelica, V., Rosu, F., and De Pauw, E. (2009) A simple method to determine electrospray response factors of noncovalent complexes. *Analytical chemistry* 81, 6708–15.

(19) Wyttenbach, T., Kemper, P. R., and Bowers, M. T. (2001) Design of a new electrospray ion mobility mass spectrometer. *International Journal of Mass Spectrometry* 212, 13–23.

(20) Gabelica, V., Galic, N., Rosu, F., Houssier, C., and De Pauw, E. (2003) Influence of response factors on determining equilibrium association constants of non-covalent complexes by electrospray ionization mass spectrometry. *Journal of mass spectrometry* □: *JMS* 38, 491–501.

(21) Krishnan-Ghosh, Y., Liu, D., and Balasubramanian, S. (2004) Formation of an interlocked quadruplex dimer by d(GGGT). *Journal of the American Chemical Society* 126, 11009–16.

(22) Pedersen, E. B., Nielsen, J. T., Nielsen, C., and Filichev, V. V. (2011) Enhanced anti-HIV-1 activity of G-quadruplexes comprising locked nucleic acids and intercalating nucleic acids. *Nucleic acids research* 39, 2470–81.

(23) Virgilio, A., Esposito, V., Citarella, G., Mayol, L., and Galeone, A. (2012) Structural investigations on the anti-HIV G-quadruplex-forming oligonucleotide TGGGAG and its analogues: evidence for the presence of an A-tetrad. *Chembiochem* □: *a European journal of chemical biology* 13, 2219–24.

(24) Borbone, N., Amato, J., Oliviero, G., D'Atri, V., Gabelica, V., De Pauw, E., Piccialli, G., and Mayol, L. (2011) d(CG GTGGT) forms an octameric parallel G-

quadruplex via stacking of unusual G(:C):G(:C):G(:C):G(:C) octads. *Nucleic acids research* 39, 7848–57.

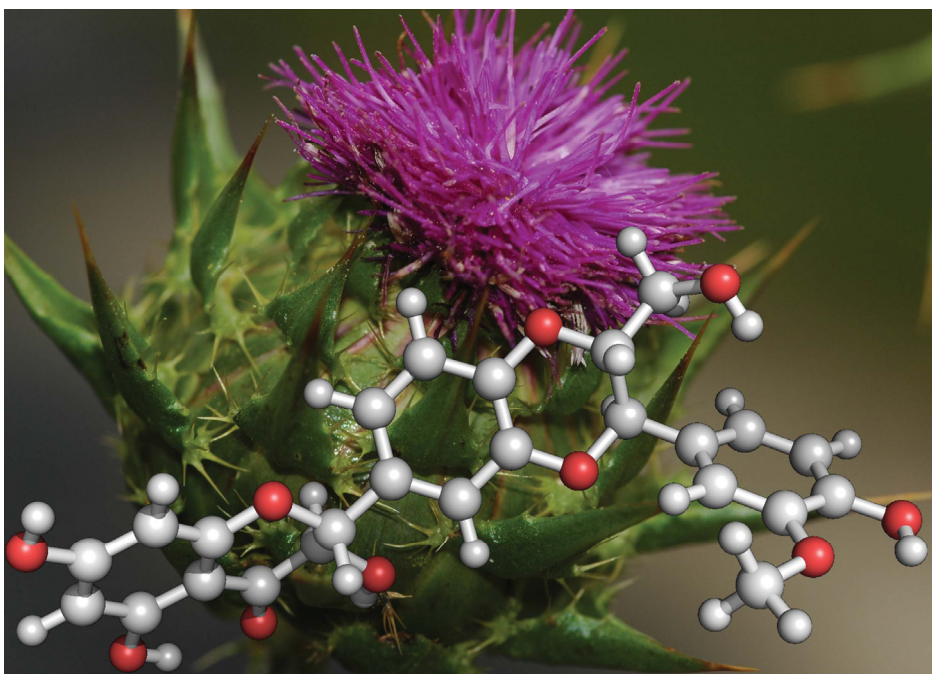
(25) D'Atri, V., Borbone, N., Amato, J., Gabelica, V., D'Errico, S., Piccialli, G., Mayol, L., and Oliviero, G. (2014) DNA-based nanostructures: The effect of the base sequence on octamer formation from d(XGGYGGT) tetramolecular G-quadruplexes. *Biochimie* 99, 119–128.

(26) Bowers, M. T. (2014) Ion mobility spectrometry: A personal view of its development at UCSB. *International Journal of Mass Spectrometry* 370, 75–95.

(27) Von Helden, G., Hsu, M.-T., Kemper, P. R., and Bowers, M. T. (1991) Structures of carbon cluster ions from 3 to 60 atoms: Linears to rings to fullerenes. *The Journal of Chemical Physics* 95, 3835.

(28) Bardin, C., and Leroy, J. L. (2008) The formation pathway of tetramolecular G-quadruplexes. *Nucleic Acids Research* 36, 477–488.

Silibinin



CHAPTER 5

Silibinin: biomolecule as potential G-quadruplex-ligand

Nucleic acid G-quadruplexes are non canonical secondary structures formed in particular G-rich sequences in presence of monovalent cations¹. G-quadruplex structures have been identified in telomeric DNA and RNA sequences²⁻⁴ as well as in the promoter regions of many proto-oncogenes such as *c-myc*⁵, Bcl-2⁶, VEGF⁷, KRAS⁸, *c-kit*^{9,10} and *RET*^{11,12}.

The formation of G-quadruplex structures can have important consequences at the cellular level and particularly, in the inhibition of telomere extension by the telomerase enzyme, which is up-regulated in cancer cells¹¹. These findings have stimulated the study of G-quadruplexes as important targets for cancer drug discovery. A general consensus is that G-quadruplex-ligands stabilizing G-quadruplex structures could pave the way for the discovery of novel anti-cancer agents¹³. In this frame, the number of known G-quadruplex-ligands has grown rapidly over the past few years. The binding between G4 and ligands can occur in many ways and it is not yet clear how can be regulated. In most cases, the quadruplex-stabilization occurs, via π - π stacking and electrostatic interactions resulting in the binding of the ligand (usually a flat aromatic molecule) with G-quartets¹⁴.

Many molecules with these characteristics have been reported as telomerase inhibitors: anthraquinones¹⁵, 3,6-disubstituted acridines¹⁶, trisubstituted acridines¹⁷, porphyrins¹⁸, and triazines¹⁹.

One of the most promising compounds of this series is represented by **BRACO-19**, a 3,6,9-trisubstituted acridine²⁰ (**Figure 1**).

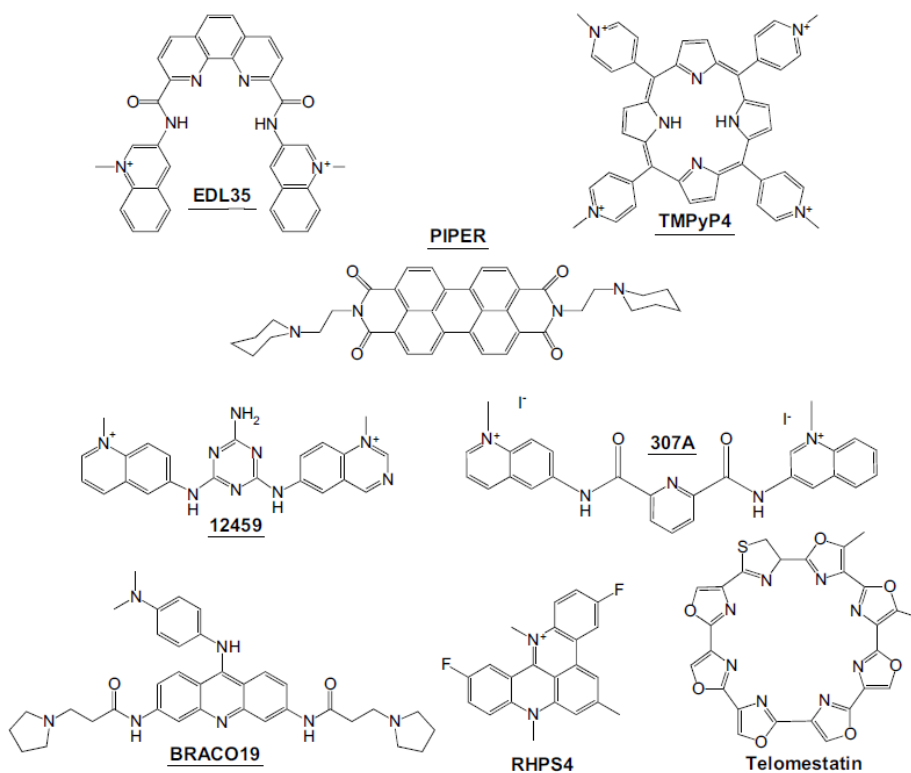


Figure 1. Some structures of G-quadruplex ligands.

In these years, numerous natural compounds have been found to inhibit telomerase, which among berberine²¹ and **Telomestatin**²² (**Figure 1**), and some flavonoids (**Quercetin**, **Genistein** and **Apigenin**; **Figure 2**)^{23,24}. Flavonoids have been known for a long time to exert multiple biological effects (bioflavonoids), ranging from their famous antioxidant properties to anti-inflammatory, anti-microbial and anti-cancer properties²⁵.

Relevant examples of telomerase inhibitors within the flavonoid family, are two soluble derivatives of **Quercetin** reported by Kerr²⁶

and D'Alarcao²⁷. In particular **QC12**, synthesized by Kerr has been subjected to phase I of clinical trials.

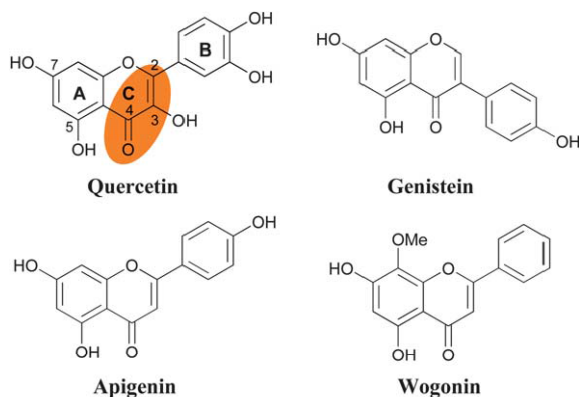


Figure 2. Flavonoids exhibiting anti-telomerase activity.

Among these anti-telomerase flavonoids, is included the activity of **silibinin**²⁸ a flavolignan found in silymarin, isolated from the fruits of the milk thistle *Silybum marianum* (L.) Gaertn. (*Carduus marianus* L., Asteraceae; milk thistle)^{29,30}. This metabolite is present in nature as diastereoisomeric mixture of two flavonolignans, namely **silybin A** and **silybin B** in a ratio of approximately 1:1, hardly separable³¹ (**Figure 3**).

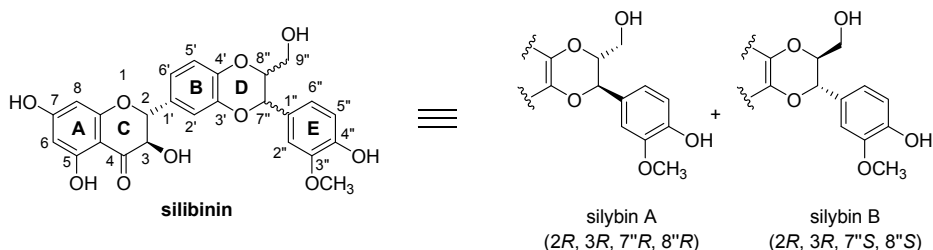


Figure 3. Silibinin and its two diastereoisomers (silybin A and B).

Over the years different modes of numbering for silibinin have been proposed³⁰. In this thesis we used a systematic numbering as

shown in **Figure 3**. Silibinin is the major biologically active constituent of silymarin, exhibiting multiple biological activities. Unfortunately, the pharmacological use *in vivo* of silibinin is dramatically limited for its content in nature as diastereoisomeric mixture hardly separable, and for its low water solubility³². In recent years, many efforts have been made to overcome these limitations, in particular, two water soluble derivatives of silibinin, well-known as **Flavobion™** and **Legalon™**, endowed with high hepatoprotective activities are used in chronic liver diseases caused by oxidative stress³³ (such as alcoholic and non-alcoholic fatty liver diseases or drug- and chemically-induced hepatic toxicity).

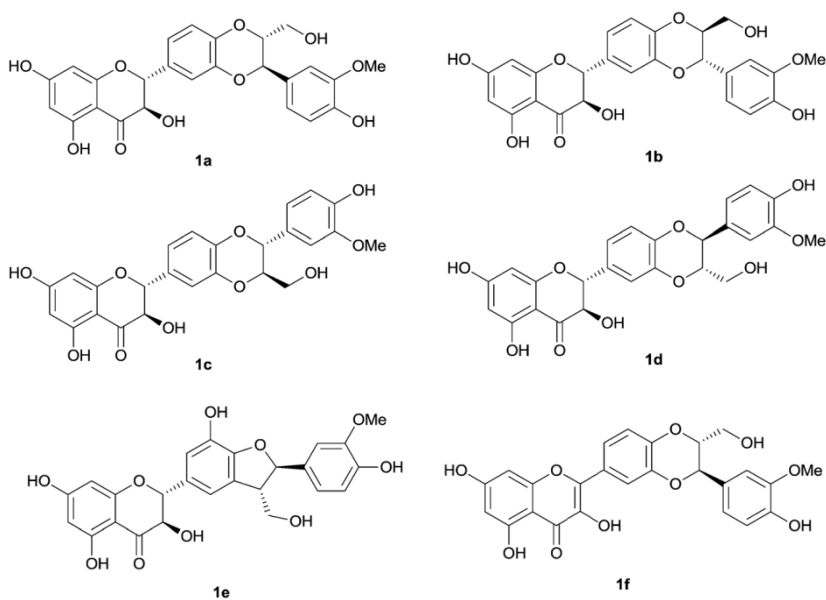


Figure 4. Chemical structures of natural components of silymarin complex.

In addition, in the '90s in order to maximize oral bioavailability of silibinin, the formulation most commonly employed in pharmacokinetic trials has been changed with a mixture of silibinin

and phosphatidylcholine sold by Indena SpA (Milan, Italy) as **Siliphos®**, or IdB 1016. Barzaghi and co-workers, reported pharmacokinetic studies on silybin-phosphatidylcholine complex³⁴.

Silibinin has received attention also thanks to its alternative beneficial activities, which mostly include anticancer and chemopreventive actions³⁵ as well as hepatoprotective³⁶, neuroprotective³⁷ and antiviral activities³⁸. Based upon these promising results, silibinin has been tested in human cancer patients in phase I-II of clinical trials³⁹. In this frame, in addition to silibinin, other constituents of silymarin such as isosilybin (**1c**, **1d**), silychristin (**1e**) and 2,3-dehydrosilybin (**1f**) (**Figure 4**), have shown attractive pharmacological properties. In particular, the oxidized form of silibinin, the 2,3-dehydrosilybin (DHS), displays major antioxidant⁴⁰ and anticancer properties than silibinin suggesting that DHS may be useful therapeutically⁴¹. Unfortunately, the use of DHS as therapeutic agent is rather restricted by its low content in silymarin complex, too low to study the biological activities.

5.1 Aim of research work

In order to better understand the G-quadruplex molecular recognition and further enhance the drug design, detailed information about quadruplex-ligand complexes are crucial. Because the specificity of the interactions between ligands and G-quadruplexes (involved in gene regulation), is a main concern in the determination of biological activity of these compounds, in my PhD project we focused our attention on the study of silibinin and its derivatives as potential new selective ligands for G-quadruplex structures. Silibinin is a diastereoisomeric mixture of two flavonolignans, namely silybin A and silybin B in an approximately 1:1 ratio. The stereochemistry of this

metabolite plays an extremely important role in its pharmacological activities with interesting structural implications.

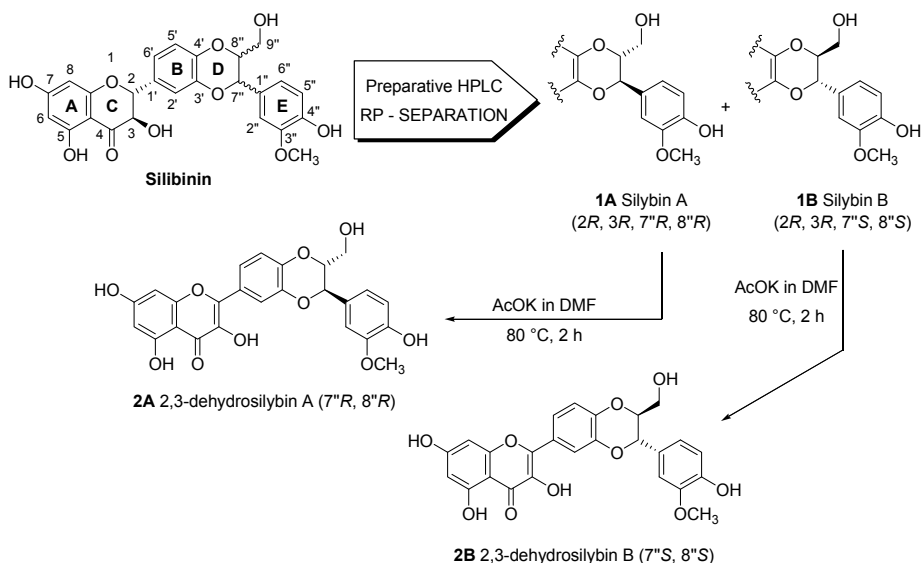
New data on the pharmacological activity related to the pure flavonolignans have reported that two silybin diastereomers (A and B) exhibit different biological activities most likely regulated by stereospecific mechanism of action^{42,43}.

Based on this structural limitation of silibinin (diastereoisomeric mixture) and aiming to investigate its ability to bind G-quadruplex structures, we developed a new, simple and fast HPLC method to obtain the two diastereoisomers of silibinin, silybin A and B in pure form and in great amount⁴⁴. In addition, in order to test also the ability of DHS to bind G-quadruplex structures, we carried out a base-catalyzed oxidation of silybin A and B promoted by microwave (MW), obtaining the pure enantiomers DHS A and B, in very brief times and with high yields⁴⁵. The potentialities of these pure compounds(silybin A and B, DHS A and B), will be analyzed in the near future.

While remaining within of chemistry of silibinin, we also dealt with the low water solubility of silibinin that dramatically limits its pharmacological use⁴⁶. In this frame, we developed a synthetic strategy to obtain new silibinin derivatives linking suitable chemical modifications able to improve its applications in biomedicine and biochemistry⁴⁷⁻⁴⁹.

5.2 A rapid and simple chromatographic separation of diastereomers of silibinin and their oxidation to produce 2,3-dehydrosilybin enantiomers in an optically pure form.

A major problem hampering studies of optically pure silibinin is the extremely complicated separation of its diastereoisomers. This problem has been approached over the years by several research groups through the use of HPLC methods. Recently, a preparative HPLC method for the separation of silybin A, silybin B and other silymarin congeners in larger quantities was described^{50,51}. A multifaceted approach has been proposed by Kren et al. in which the chromatographic separation is performed on the mixture of the two diastereoisomers suitably modified by chemical or enzymatic methods^{52,53}. Generally, these methods require special expertise in both organic synthesis and enzymatic kinetic resolutions. By a careful analysis of the studies cited, it is evident that a rapid and less laborious method for the separation of silibinin is still required.



Scheme 1. Separation of two diastereoisomers of silibinin (**1A** and **1B**) and their oxidation to 2,3-dehydrosilybin A (**2A**) and 2,3-dehydrosilybin B (**2B**).

Initially we developed a rapid and preparative separation (gram-scale amounts) of the diastereoisomers of silibinin using preparative HPLC (**Scheme 1**) and their oxidation to produce enantiomers of 2,3-dehydrosilybin in a very pure form using our optimised procedure⁵⁴. Previous investigations have shown that the solubility of silibinin in THF at 25°C (greater than 140–150 mg/mL) is considerably greater than in H₂O or MeOH (0.05–1.5 mg/mL)⁵¹, allowing for the injection of large quantities of analyte. The key point of our approach is dissolving the sample in THF, an alternative solvent to H₂O or MeOH in which silibinin has a very low solubility. Various types of HPLC conditions (columns, flow and mobile phases) were evaluated; the optimum chromatographic conditions for the separation of both silybin A and B were characterized by using a Phenomenex Gemini C18-110A preparative column (10- μ m particle size, 250 mm \times 21.2 mm.i.d.), as a mobile phase a ternary mixture of H₂O/MeOH/MeCN (60:35:5, v/v/v) and 0.1% TFA. In preliminary studies, we also used DMSO, to better dissolve the silibinin, but it resulted in poor resolution under all the conditions tested. To attain the highest quantity of pure silybin A and silybin B and to avoid poor resolution due to the expansion of their chromatographic peaks, 500 μ L injections containing 70 mg of silibinin were used. Better resolution was observed in all injections performed dissolving the sample in THF and then mixing with an equal volume of the eluent solution (**Figure 5**). The resolution of silybin A and silybin B was high enough to obtain pooled fractions containing practically pure single isomers. Using groups of 10 injections each time, fractions of silybin A (t_R = 67.5 min) and silybin B (t_R = 74.5 min) were collected, and after removal of the mobile phase under reduced pressure, amorphous

colourless powders of silybin A (300 mg) and silybin B (315 mg) were obtained by drying under vacuum.

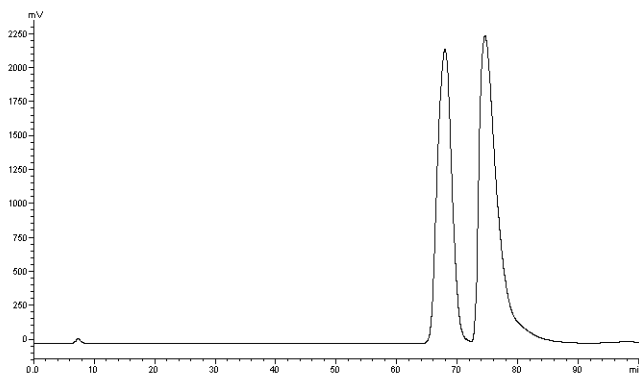


Figure 5. Prep-HPLC profile of the silybinin. Silybin A (**1A**, $t_R = 67.5$ min) and silybin B (**1B**, $t_R = 74.5$ min). Conditions: Phenomenex Gemini C18-110A preparative column (10 μm particle size, 250 mm \times 21.2 mm i.d.), eluted with $\text{H}_2\text{O}/\text{MeOH}/\text{MeCN}$ (60:35:5, v/v/v) containing 0.1% of TFA; flow 12 mL/min, monitored at 288 nm. 500 μL aliquot of 140 mg/mL of the silybinin solution was mixed with 500 μL of the eluent solution and then injected.

To make the procedure quicker and to maximise the functionality of our instruments, we carried out the injections in sequence every 40 min (**Figure 6**).

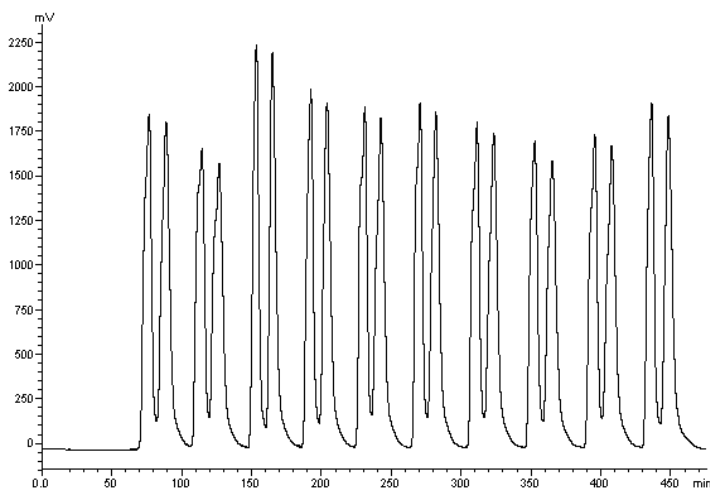


Figure 6. HPLC profile of sequential injections.

Thus, we were able to obtain approximately 1 g for both diastereoisomers in a very pure form in less than a week. The purified products, whose HPLC purity was higher than 98%, were fully characterised by NMR (^1H , ^{13}C) (tables in Experimental Session), CD (**Figure 7a** in Experimental Session), ESI MS and $[\alpha]_{\text{D}}$. The confirmation of two specific structures was also obtained by comparing the NMR and CD data with those published in the literature^{55,56}.

Afterwards, diastereoisomers **1A** and **1B** were treated with potassium acetate (AcOK) in DMF at 80°C to produce **2A** and **2B** (**Scheme 1**). In our procedure, a 0.1 M solution of pure silybin A (**1A**) or silybin B (**1B**) was treated with anhydrous AcOK in DMF at 80°C for 2 h. The crude mixture was purified by chromatography on a silica gel column (eluent: $\text{CHCl}_3/\text{acetone}$, 80:20, v/v) to yield **2A** and **2B** in good yields, and the HPLC purity was greater than 98%. The purified products were fully characterised by NMR (^1H , ^{13}C) (tables in Experimental Session), CD (**Figure 7b** in Experimental Session), ESI MS and $[\alpha]_{\text{D}}$. The obtained data were compared with those published in the literature⁵⁷.

5.2.1 Experimental Session

The preparative HPLC method was performed with a Shimadzu LC-8A PLC system equipped with a Shimadzu SCL-10A VP System control and Shimadzu SPD-10A VP UV-VIS Detector. A Phenomenex Gemini C18-110A preparative column (10- μm particle size, 250 mm \times 21.2 mm.i.d.) was used, and the mobile phase of $\text{H}_2\text{O}/\text{MeOH}/\text{MeCN}$ (60:35:5, v/v/v), containing 0.1% of TFA, was delivered isocratically at 12 mL/min. The chromatograms were monitored at 288 nm. The HPLC system was controlled by LC Real Time Analysis software

(Shimadzu Corporation). The silibinin solution was prepared by dissolving and sonicating the accurately weighed compound in THF. The obtained solution (ca 140 mg/mL) was then applied to Nylon filters (pore size = 0.45 μm). A 500 μL volume of the silibinin solution was mixed with 500 μL of the mobile phase and then applied to the chromatographic system. Silybin A and silybin B peaks were collected manually.

The analysis was performed with a Waters 1525 HPLC equipped with a binary gradient pump and a Waters 2996 Photodiode Array Detector using a RP18 column Phenomenex LUNA (5- μm particle size, 10.0 mm \times 250 mm i.d.). The mobile phase of $\text{H}_2\text{O}/\text{MeOH}$, containing 0.01% acetic acid (50:50, v/v), was delivered isocratically at 0.8 mL/min. The chromatograms were monitored at 288 nm. Standard solutions of silybin A, silybin B, 2,3-dehydrosilybin A and 2,3-dehydrosilybin B were prepared by dissolving the accurately weighed standard compounds in THF to yield final concentrations of 5 mg/mL. A 25- μL volume of each analyte was applied to the chromatographic system for the determination of purity.

(2R,3R)-3,5,7-trihydroxy-2-[(2R,3R)-3-(4-hydroxy-3-methoxyphenyl)-2-(hydroxymethyl)-2,3-dihydrobenzo[b][1,4]dioxin-6-yl]chroman-4-one
(*Silybin A*, **1A**): colourless, amorphous powder; mp. 161–162; $[\alpha]^{25}_{\text{D}}$ +14.5 (*c* 0.20, acetone); CD spectra see **Figure 7a**; ESI MS (negative ions) *m/z* 481.51 (calcd for $\text{C}_{25}\text{H}_{21}\text{NO}_{10}$ 481.11).

(2R,3R)-3,5,7-trihydroxy-2-[(2S,3S)-3-(4-hydroxy-3-methoxyphenyl)-2-(hydroxymethyl)-2,3-dihydrobenzo[b][1,4]dioxin-6-yl]chroman-4-one
(*Silybin B*, **1B**): colourless, amorphous powder; mp. 157–159; $[\alpha]^{25}_{\text{D}}$ –

11.2 (*c* 0.24, acetone); CD spectra see **Figure 7a**. ESI MS (negative ions) *m/z* 481.17 (calcd for C₂₅H₂₁NO₁₀ 481.11).

*3,5,7-trihydroxy-2-[(2R,3R)-3-(4-hydroxy-3-methoxyphenyl)-2-(hydroxymethyl)-2,3-dihydrobenzo[*b*][1,4]dioxin-6-yl]chroman-4-one* (*2,3-dehydrosilybin A*, **2A**): mp. decompose at 200 °C (decomp.); [α]²⁵_D -22.8 (*c* 0.18, MeOH); CD analysis see **Figure 7b**. ESI MS (negative ions) *m/z* 479.23 (calcd for C₂₅H₁₉NO₁₀ 479.10).

*3,5,7-trihydroxy-2-[(2S,3S)-3-(4-hydroxy-3-methoxyphenyl)-2-(hydroxymethyl)-2,3-dihydrobenzo[*b*][1,4]dioxin-6-yl]chroman-4-one* (*2,3-dehydrosilybin B*, **2B**): [α]²⁵_D +23.0 (*c* = 0.14, MeOH); CD analysis see **Figure 7b**. ESI MS (negative ions) *m/z* 479.41 (calcd for C₂₅H₁₉NO₁₀ 479.10).

Table: ¹H NMR data of silybin A (**1A**), silybin B (**1B**) and 2,3-dehydrosilybin (**2**)

<i>position</i>	1A	1B	2
H-2	5.06 d (11.3)	5.06 d (11.3)	–
H-3	4.60 d (11.1)	4.59 d (11.0)	–
OH-3	<i>not obs.</i>	<i>not obs.</i>	9.54 s
OH-5	11.88 s	11.70 s	12.7 s
H-6	5.89 d (1.8)	5.90 d (2.1)	6.20 d (2.0)
OH-7	10.84 s	10.30 s	<i>not obs.</i>
H-8	5.84 d (1.8)	5.86 d (2.0)	6.46 d (2.0)
H-2'	7.07 d (1.4)	7.07 d (1.8)	7.66 d (2.2)
H-5'	6.96 d (8.3)	6.96 d (8.3)	7.12 d (8.8)
H-6'	7.01 dd (8.4, 1.6)	7.07 dd (8.1, 1.6)	7.76 dd (8.8, 2.2)
H-2''	6.99 d (1.5)	7.06 d (1.5)	7.06 d (2.1)
OH-4''	9.15 s	9.10 s	9.15 s
H-5''	6.79 d (8.1)	6.79 d (8.0)	6.85 d (8.1)
H-6''	6.85 dd (8.1, 1.4)	6.84 dd (8.4, 1.7)	6.88 dd (8.0, 2.0)
H-7''	4.89 d (7.9)	4.90 d (7.9)	4.97 d (8.0)
H-8''	4.16 ddd (6.9, 3.9, 2.7)	4.15 ddd (6.8, 3.9, 2.5)	4.27 ddd (8.0, 4.3, 2.5)
H-9'' _a	3.52 dd (12.3, 2.4)	3.52 dd (12.0, 2.4)	3.56 ddd (12.3, 4.9, 2.5)
H-9'' _b	3.33 dd (12.3, 3.9)	3.33 dd (12.0, 3.9)	3.37 ddd (12.3, 5.0, 4.5)
OH-9''	<i>not obs.</i>	<i>not obs.</i>	<i>not obs.</i>
OCH ₃	3.76 s	3.77 s	3.80 s

NMR spectra were recorded in DMSO-d₆, on Bruker WM-400Table: ¹³C NMR data of silybin A (**1A**), silybin B (**1B**) and 2,3-dehydrosilybin (**2**)

<i>position</i>	<i>type</i>	1A	1B	2
C-2	CH	82.6	82.5	145.8
C-3	CH	71.4	71.5	136.3
C-4	C	197.6	197.7	176.0
C-4a	C	100.4	100.4	103.1
C-5	C	163.3	163.3	160.7
C-6	CH	96.1	96.1	98.3
C-7	C	167.1	166.9	164.1
C-8	CH	95.1	95.1	93.6
C-8a	C	162.5	162.5	156.3
C-1'	C	130.1	130.1	123.8
C-2'	CH	116.5	116.6	116.2
C-3'	C	143.3	143.2	143.4
C-4'	C	143.7	143.6	145.1
C-5'	CH	116.3	116.3	116.8
C-6'	CH	121.3	121.1	121.3
C-1''	C	127.5	127.5	127.3
C-2''	CH	111.8	111.7	111.9
C-3''	C	147.6	147.7	147.3
C-4''	C	147.0	147.0	147.1
C-5''	CH	115.3	115.3	115.4
C-6''	CH	120.5	120.5	120.2

C-7"	CH	75.9	75.9	75.9
C-8"	CH	78.1	78.1	78.6
C-9"	CH ₂	60.2	60.2	60.1
OCH ₃	CH ₃	55.7	55.7	55.8

NMR spectra were recorded in DMSO-d₆, on Bruker WM-400

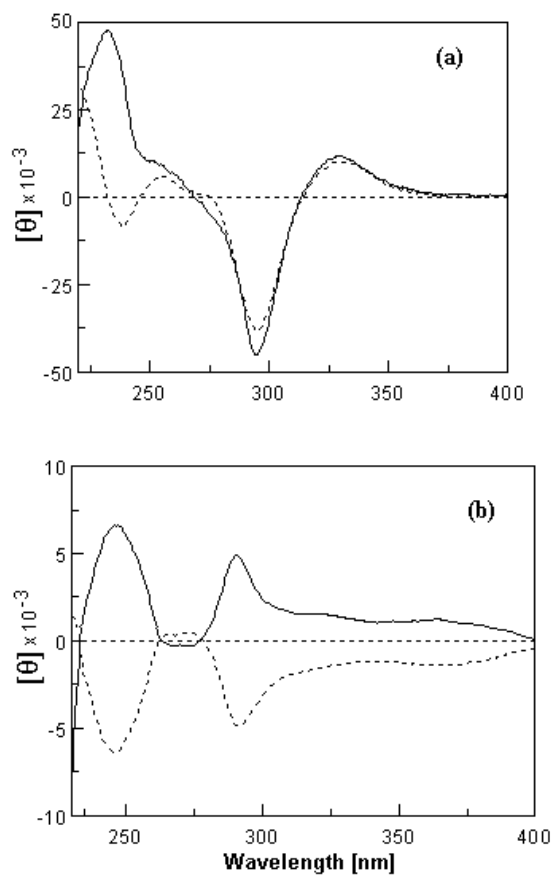


Figure 7. (a) CD spectra at 25°C of the silybin A (*bold line*) and silybin B (*dotted line*) at 21 μM in MeOH; (b) CD spectra at 25°C of the 2,3-dehydrosilybin A (*dotted line*) and 2,3-dehydrosilybin B (*bold line*) at 19.3 μM in MeOH.

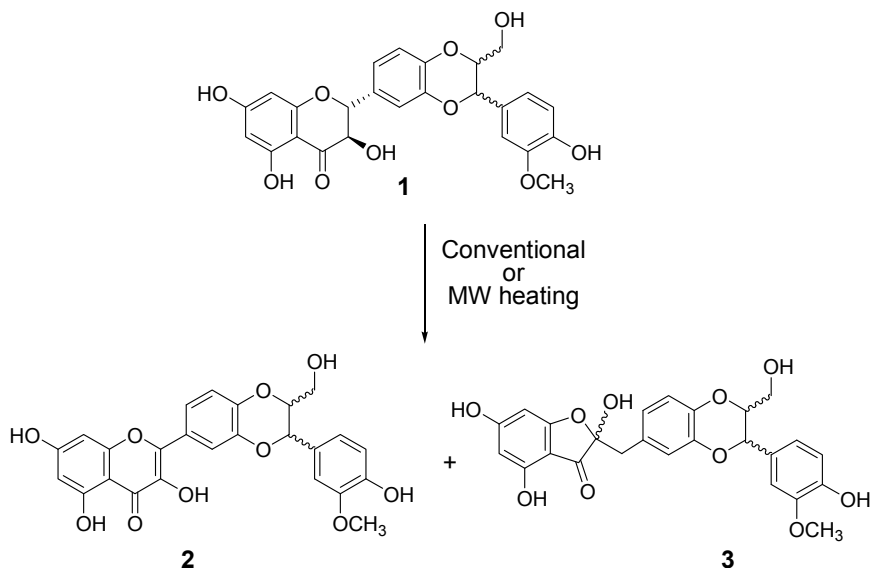
5.3 Microwave-assisted oxidation of Silibinin: a simple and preparative method for the synthesis of improved radical scavengers

Recently it has been reported that, the 2,3-dehydrosilybin, (oxidation product of silibinin) present in traces in silymarin extract, shows more potent antioxidant activity than its parent compound. This compound also appeared to be more effective than silibinin in biological assays comparing their antitumour and antiproliferative potencies⁴⁰, and shown also positive effects against some skin diseases (*e.g.*, psoriasis and atopic eczema)⁵⁸.

Years ago, the biological activity of 2,3-dehydrosilybin was basically related to the biological activity of silibinin and silymarin because of its difficult isolation. Therefore, many methods to synthesize 2,3-dehydrosilybin are reported in literature, including treatment with H₂O₂ in a solution of NaHCO₃⁵⁹ or with N-methylglucamine⁵⁷. Very recently, my research group reported this oxidation using pyridine at reflux⁵⁴, attended by an alternate approach described by Křen and co-worker employed potassium acetate in DMF at 50°C⁶⁰. In this paper, they reported also the formation of an interesting byproduct, obtained from alkaline treatment of silibinin, the hemiacetal **3** (**Scheme 2**).

This compound was first isolated and characterised by Křen, *et al.* and was found to be a more potent antioxidant than either silibinin or 2,3-dehydrosilibin. Nevertheless, little is known about its biological properties, as to date it has been obtained only as an undesired side product. All methods just described for 2,3-dehydrosilybin preparation, provide at most the 50% yield. A new preparative oxidation of silibinin and silybin is developed, exploring the use of microwave heating (MW) that enhances reaction rates and in many

cases improves product yield⁶¹. We have also developed a preparative purification method to isolate 2,3-dehydrosilibin **2** and hemiacetal **3**, compounds with remarkable antioxidant activity that continue to spark much interest.



Scheme 2. Base-catalysed oxidation of silibinin1.

Firstly, it was examined the effect of several solvents in our procedure, 1,4-dioxane, THF, MeOH, pyridine and DMF, exploring also the utility of their mixtures. Progressively, it was investigated the effect of two bases, AcOK and TEA (potassium acetate and triethylamine). Reactions were monitored by RP-HPLC (**Figure 8**) and quenched by removing the solvent under reduced pressure. The strength of the bases chosen is significant because exposure to strong bases, such as alkali metal hydroxides, leads to the rapid decomposition of silybin. Reaction yields were calculated by weighing the products obtained after chromatographic purification over a pre-packed RP-18 column. Products were eluted with a ternary mixture of

CH₃OH/CH₃CN/H₂O containing increasing proportions of CH₃CN. The formation of product **3** was not observed under conventional heating. The best reaction yields were obtained when the solvent was DMF (78%), consistent with previous reports. Yields from reactions in other solvents never exceeded 60% (**Table 1**).

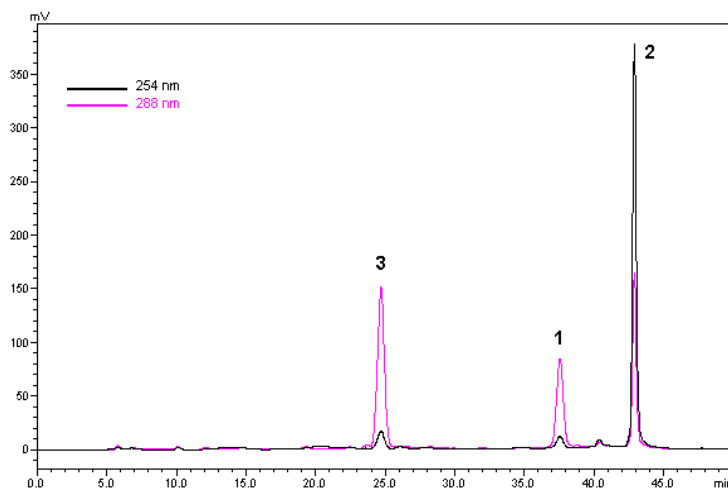


Figure 8. A typical HPLC profile of a reaction under MW heating: analytical Phenomenex LUNA RP-18 column (5 μ m particle size, 10.0 mm \times 250 mm i.d.), eluting with H₂O/CH₃CN (10 to 100% in 50 min), flow rate 1.0 mL/min, monitored at 254 and 288 nm.

The purified product **2** was fully characterised by NMR (¹H, ¹³C) and ESI-MS analysis, and these data were compared with published results to confirm the structure. The purity of **2** was greater than 97% in all cases, as determined by analytical HPLC.

The base-catalysed oxidation of silibinin was subsequently carried out under microwave heating. We varied several conditions (solvent, temperature, time) and all reactions were carried out in a minimum volume of solvent. As expected, reaction yields (**Table 1**) were very low

in slightly polar solvents with low dielectric constants, such as THF and 1,4-dioxane (yields $\leq 25\%$).

Similar results were obtained using solvent mixtures (see **Table 2**) composed of CH₃OH and H₂O, which have high dielectric constants.

Table 1. Base catalyzed oxidation of silibinin exploiting the classical heating method (oil bath).

Base (3 equiv.)	Solvent	Temperature (°C)	Time (hours)	Yield (%)	
				[2]	[3]
KOAc	THF	reflux	24	25	--
KOAc	THF	reflux	48	40	--
TEA	THF	reflux	24	25	--
TEA	THF	reflux	48	40	--
KOAc	dioxane	reflux	24	25	--
KOAc	dioxane	reflux	48	50	--
TEA	dioxane	reflux	24	25	--
TEA	dioxane	reflux	48	45	--
KOAc	DMF	80	0.5	78	--
--	pyridine	95	100	60 (51)	--(<10)

n.r.= no reaction, was observed degradation of the reaction mixture.

In some cases the harsh reaction conditions led to rapid and substantial decomposition of starting material and the formation of a brown and insoluble residue. When the reaction was conducted in 1,4-dioxane:MeOH (8:2, v/v) at 80°C in the presence of AcOK, we observed partial degradation of silibinin and the formation of pitchy and insoluble brown material (ca. 40 wt. %). Reactions in DMF or pyridine gave very interesting results. Conducting the reaction in DMF at 50°C led to the formation of **2** and **3** in 70% and 15% yield, respectively, within 30 minutes. When the reaction was carried out in pyridine, **2** and **3** were formed in variable yields depending on the reaction temperature. At 110°C, the product distribution favoured

formation of **3** (62%) over **2** (32%). At a slightly lower temperature (100°C), formation of product **2** (28%) predominated over **3** (18%).

All reactions were monitored by RP-HPLC (**Figure 8**) and were quenched by removing the solvent under reduced pressure. In all cases, the yield of **3** (15–62%) was improved over previously reported yields⁵⁷. We subjected pure silybins A and B to the MW oxidation conditions. Heating in DMF at 50°C gave 2,3-dehydrosilybins A and B in average yields of 72%.

Table 2. Base catalyzed oxidation of silibinin exploiting the heating promoted by microwave (MW).

Base (3 equiv.)	Solvent	Temperature (° C)	Time (hour)	Yield (%)	
				[2]	[3]
KOAc	THF	50	1.5	15	--
KOAc	THF/H ₂ O (9:1, v/v)	50	1.5	18	--
--	THF/TEA (2:1, v/v)	60	2.5	25	--
--	THF/TEA (1:1, v/v)	60	2.5	25	--
KOAc	dioxane/CH ₃ OH (8:2, v/v)	110	0.5	n.r.	
KOAc	dioxane/CH ₃ OH (8:2, v/v)	90	0.5	n.r.	
KOAc	dioxane/ CH ₃ OH (8:2, v/v)	80	0.5	20	5
TEA	dioxane/ CH ₃ OH (8:2, v/v)	80	0.5	20	5
KOAc	dioxane/ CH ₃ OH (8:2, v/v)	50	10	35	--
KOAc	DMF	50	0.16	70	15
--	pyridine	150	1.5	n.r.	
--	pyridine	110	3.5	32	62
--	pyridine	100	3.5	28	18

n.r.= no reaction, was observed degradation of the reaction mixture.

Conducting the MW oxidation in pyridine at 110 °C gave good yields of the corresponding hemiacetals. Crude products were purified on a pre-packed RP-18 column, eluting with a ternary mixture of CH₃OH/CH₃CN/H₂O containing increasing proportions of CH₃CN.

The purified products **2** and **3** were fully characterised by NMR (^1H , ^{13}C) and ESI MS analysis, and these data were compared with published results to confirm the structures⁵⁷. The purity of products was greater than 97% in all cases, as determined by analytical HPLC.

5.3.1 Experimental Session

General procedure for HPLC analysis: HPLC analysis was performed using a Waters 1525 HPLC equipped with a binary gradient pump and a Waters 2996 Photodiode Array Detector using a Phenomenex LUNA RP18 column (5- μm particle size, 10.0 mm \times 250 mm i.d.). The column was eluted with $\text{H}_2\text{O}/\text{CH}_3\text{CN}$ (10 to 100% in 50 min), flow rate 1.5 mL/min, monitored at 254 and 288 nm.

General purification procedure: The crude material (1 g) was purified by chromatography over a pre-packed column RP-18 (Biotage® KP-C-18-HS 25 g) on a Biotage® Isolera Spektra one eluting with a ternary mixture of $\text{CH}_3\text{OH}/\text{CH}_3\text{CN}/\text{H}_2\text{O}$ containing increasing proportions of CH_3CN (from 4:1:5 to 4:3:3, v/v/v). The flow rate was 25 mL/min.

General procedure for oxidation under conventional heating: A solution of silibinin1 (1.0 g, 2.1 mmol) and base (KOAc or TEA, 6.22 mmol) in an appropriate solvent (15 mL for 1,4-dioxane, THF or their mixture; 8 mL for DMF; 6 mL for pyridine) was heated to reflux. The reaction mixture was quenched by removal of the solvent *in vacuo*. The crude product was purified by chromatography over a pre-packed RP-18 column.

General procedure for oxidation under MW heating: All irradiation experiments were carried out in a dedicated CEM-Explorer and CEM Discover monomode microwave apparatus, operating at a frequency of

2.45 GHz with continuous irradiation power from 0 to 300 W using the standard maximum power absorbance level of 300 W. A solution of silibinin **1** (1.0 g, 2.1 mmol) and base (6.22 mmol) in an appropriate solvent (8 mL for THF, THF/H₂O, 1,4-dioxane/MeOH and 4 mL for pyridine and DMF) was placed in a 10 mL glass tube. The tube was sealed with a Teflon septum, placed in the microwave cavity and irradiated. Initial microwave irradiation used the minimum wattage required to ramp the temperature from room temperature to the desired temperature. The reaction mixture was held at this temperature for the required time. After the irradiation period, the reaction vessel was cooled rapidly to ambient temperature by gas jet cooling.

5.4 Conclusions and Perspective

In conclusion, we have reported a simple and robust purification HPLC method to obtain two diastereoisomers of silibinin in a very pure form. The described preparative HPLC method is effective in obtaining gram-scale amounts of the standards silybin A and silybin B in short times and with minimal effort. In addition in order to test the biological activity of DHS, we have developed an efficient new preparative base-catalysed oxidation of silibinin. The oxidation is carried out under conventional heating in comparison with microwave (MW). The MW procedure gave a rapid access to good yields of 2,3-dehydrosilybin **2** and hemiacetal **3** in minimum solvent volumes (**Table 2**). The optimised conditions were then used to oxidize optically pure silybin A and B to 2,3-dehydrosilybin A and B, respectively. All purified products were fully characterised by NMR (¹H, ¹³C), CD, [α]_D and ESI MS analyses. Access to significant quantities of these compounds will facilitate the evaluation of their specific

pharmacological properties, that was not possible before. Thanks to the optimization of oxidation conditions promoted by microwave (MW) heating, we intend to extend this method to obtain modified DHS starting from the synthesis of water soluble silybin analogues.

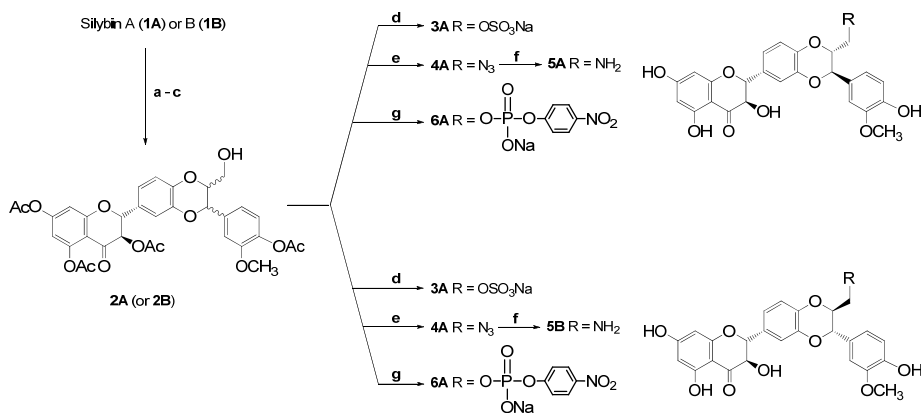
5.5 New silibinin analogues with improved bioavailability

As previously alluded, the therapeutic efficiency of silibinin is rather limited by its low bioavailability and water solubility. Typically, silibinin is administered orally and this method of administration, limits the efficacy of the natural product because of its poor absorption and short half-life in the body⁶². In order to reach their target tissues, cells, and organelles for their desired therapeutic effects a number of physical and chemical approaches by which accomplish these difficult challenges have been proposed⁶³. The most important is **Siliphos®** (IdB 1016), a silybin-phosphatidylcholine complex³⁴ developed in 1990 by Indena SpA (Milan, Italy).

Only a few modifications have been introduced in these years; these most simply alter the chemical and physicochemical properties of the natural metabolite enhancing its biological efficacy, *in vivo* stability, low bioavailability and overall uptake^{33,52,54,64–67}. Generally tissue- and cell- specific drug targeting can only be achieved by employing carrier-drug complexes or conjugates that contain a ligand recognized by a receptor on the target cell. Carbohydrate-based conjugates allow targeting of a certain class of cell membrane receptors that are referred to as lectins that recognize a specific carbohydrate motif and internalize their ligands by endocytosis⁶⁸.

5.5.1 Synthesis of new silybins and evaluation of their antioxidant properties

Aiming to exploit a readily available natural product as a scaffold for chemical diversification, we considered silybin A and B as versatile starting materials. Starting from a pure form of silybin A and B easily obtained by HPLC method described before (see Paragraph 5.2), it was developed a successful synthetic strategy to obtain a variety of silybin derivatives bearing different substituents, including some of charged groups at the C(9'') position. The antioxidant activity of these derivatives and also of silybin A and B were evaluated *in vitro* assays. We chose to insert the modifications at the C(9''), because it has been reported that this functional position is not responsible for antioxidant and antiradical action of this metabolite^{54,69}. By modifying this position for both diastereoisomers of silibinin (silybin A and B), we generated a series of new and more polar analogues that could be useful models for chemical diversification (**Scheme 3**).



Scheme 3. Reagents and conditions: **a)** DMTCl, pyridine, 50°C, overnight. **b)** Ac₂O, pyridine, 25°C, overnight. **c)** 5% formic acid in CH₂Cl₂, 25°C, 30 min. **d)** SO₃·Et₃N, DMF, 25°, 30 min.; NH₄OH/MeOH, 25°C, 30 min. **e)** TPP, DPPA, THF, 25°C, 5h; 0.1M HCl/EtOH 1 : 4, 50°C, 20 min. **f)** H₂, C/Pd, MeOH, 25°C, overnight. **g)** 4-nitrophenyl dichlorophosphate, pyridine, 0°C, 40 min.; NH₄OH/MeOH, 25°C, 30 min.

The synthesis of the key silybin intermediates **2A** or **2B** starting from silybin A and B respectively (**Scheme 3**) provided using an efficient orthogonal protection strategy, protecting the HO-C(3,5,7,4'') functional groups with acetyl (Ac) while the HO-C(9'') with dimethoxytriphenylmethyl group (DMT). The modifications introduced at the C(9'') position included the sulfate, phosphodiester, amino, and azide functional groups. The phosphodiester and amino functionalities were chosen in order to prepare a useful silybin-based scaffold for generating a library of C(9'')-modified compounds, such as phosphodiesters, amides, urethanes, and sulfonamides.

Purified silybin A (**1A**) (**Scheme 3**) was first converted into C(9'')-ODMT ether by a reaction with 4,4'-dimethoxytriphenylmethylchloride (DMTCl) after the HO-C(3,5,7,4'') functionalities were completely acetylated. The successive treatment with 5% formic acid in CH₂Cl₂ allowed for the removal of the DMT protecting group, leading to **2A**. Starting from **2A**, the silybin analogues **3A**, **4A**, **5A**, and **6A** were obtained in a few steps with good overall yields. To introduce the sulfate group, compound **2A** was reacted with SO₃·Et₃N and then treated with concentrated aqueous ammonia in MeOH, allowing for the full deprotection of acetyl groups and leading to the desired compound **3A**. The silybin derivative **4A** was prepared starting from the key intermediate **2A**, which was first converted into the corresponding C(9'')-azido derivative by the Mitsunobu reaction after deacetylation. The derivative **5A** was obtained by catalytic hydrogenolysis of the C(9'')-azido functionality of **4A**. The reaction of **2A** with 4-nitrophenyl dichlorophosphate in pyridine and subsequent deacetylation generated compound **6A**. In all cases, the intermediate compounds and final derivatives were purified by silica gel chromatography and then fully characterized by ¹H-NMR

(and also ^{31}P -NMR in the case of **6A**) and MALDI-MS. With the same pattern of reactions, compounds **3B–6B** were obtained from silybin B (**1B**) via the intermediate **2B**, which corresponds to compound **2A**. The antioxidant activity of each substance was assessed using the 2,2-diphenyl-1-picryl-hydrazyl-hydrate (DPPH) free radical assay. The DPPH free radical method is an antioxidant assay based on electron transfer that produces a violet solution in ethanol⁷⁰. This free radical, which is stable at room temperature, is reduced in the presence of an antioxidant molecule, giving rise to a colorless ethanol solution. The use of the DPPH assay provides an easy and rapid way to evaluate antioxidant activity of a variety of molecules by spectrophotometry⁷¹. The new compounds **3A–6A** and **3B–6B** were tested for their free radical scavenging ability in a comparison with their parent compounds **1A** and **1B** (**Table 3**), silibinin (mixture **1A/1B**, 1:1) and butylated hydroxyl anisole (BHA), which was used as standard antioxidant.

Table 3. Radical-Scavenging data of silibinin, silybin A and B, DHS A and B and their analogues.

Compound	DPPH IC ₅₀ (μM)
silibinin	392 ± 8
silybin A (1A)	425 ± 5
silybin B (1B)	446 ± 7
silybin A–9''- <i>O</i> -sulphate sodium salt (3A)	165 ± 8
silybin B–9''- <i>O</i> -sulphate sodium salt (3B)	189 ± 3
9''-Azide-silybin A (4A)	667 ± 26
9''-Azide-silybin B (4B)	657 ± 18
9''-Amine-silybin A (5A)	32 ± 2
9''-Amine-silybin A (5B)	33 ± 1
silybin A–9''- <i>O</i> -(4-nitrophenyl)-phosphate sodium salt (6A)	604 ± 15
silybin B–9''- <i>O</i> -(4-nitrophenyl)-phosphate sodium salt (6B)	591 ± 18
BHA	198 ± 4

Silybin A and B showed antioxidant activities that were absolutely comparable to each other (425 and 446 μM , respectively) slightly higher than that of the 1:1 mixture (Silibinin, 392 μM), and more than double than that of the BHA standard (198 μM). *Foti et al.* recently have reported kinetic measurements by DPPH assay to demonstrate that the reaction between phenols and DPPH occurs in alcohols by electron transfer from the phenoxide anions to DPPH⁷².

The presence of oxidized groups in the molecules reduces their ability to donate electrons or hydrogen atoms and thus their reactivity toward the radical. According to these studies, the oxidation of C(9") of silybin to azide derivatives (**4A** and **4B**, with IC_{50} values of 667 and 657 μM , respectively) or to *p*-nitrophosphate derivatives (**6A** and **6B**, with IC_{50} values of 604 and 591 μM , respectively) further reduced their radical scavenging properties. Significant improvement of this property compared to silibinin and BHA was observed for both sulphate derivatives **3A** and **3B** (IC_{50} values of 165 and 189 μM , respectively) and, especially for in both amine derivatives **5A** and **5B** (IC_{50} values of 32 and 33 μM , respectively, **Table 3**). Upon reaction with DPPH, silybin derivatives gave a very complex reaction mixture composed mostly of insoluble brownish precipitates. These are probably polymers (radical-initiated polymerization) and non-identified products of lower molecular weight.

5.5.1.1 Experimental Session

All the reagents were of the highest quality of those commercially available and they were used as received. Anal. TLC was performed on precoated alumina plates with *Merck* Silica Gel 60 F₂₅₄ as the adsorbent. Reaction products were visualized on TLC plates by UV

light followed by treatment with 5% H₂SO₄ ethanolic solution and then by heating to 130°C. For column chromatography, silica gel from *Merck (Kieselgel 40, 0.063–0.200 mm)* was used. NMR spectra were recorded on *Varian INOVA-500 FT NMR spectrometer* (at 499.710 and 125.663 MHz for ¹H and ¹³C, resp.), at 25°C; δ in ppm, J in Hz. Peak assignments have been carried out on the basis of standard ¹H-¹H COSY, HMBC, and HSQC experiments. ³¹P-NMR spectra were recorded on a *Bruker WM-400 spectrometer* (at 161.98 MHz, using 85% H₃PO₄ as external standard). For the ESI-MS analyses, a *Waters Micromass ZQ Instrument*, equipped with an electrospray source, was used. MALDI TOF mass spectrometric analyses were performed on a *PerSeptive Biosystems Voyager–De Pro MALDI mass spectrometer*.

General procedure for the preparation of 3,5,7,4''-O-tetra-acetyl-silybin A (2A) and 3,5,7,4''-O-tetra-acetyl-silybin B (2B). Purified silybin A (**1A**, 350 mg, 700 μ mol) was evaporated several times with anhydrous THF and dissolved in anhydrous pyridine (3 ml) before reaction with DMTCl (450 mg, 133 μ mol). The reaction mixture was left at 50°C overnight under stirring and was then diluted with MeOH and concentrated under reduced pressure. The basic ingredient in its natural state was next purified on a silica gel column and eluted with CHCl₃ containing increasing amounts of MeOH (from 0 to 5%) in the presence of a few drops of TEA, affording pure 9''-O-(4,4'-dimethoxytriphenylmethyl)-silybin A as an amorphous solid (0.45 g, 600 μ mol) in 88% yield. R_f = 0.5 (CHCl₃/MeOH 90 : 10).

9''-O-(4,4'-dimethoxytriphenylmethyl)-silybin A (0.38 g, 470 μ mol), was dissolved in anhydrous pyridine (2.2 ml) and reacted with acetic anhydride (1 ml, 11 mmol). The mixture was left under stirring at room temperature overnight and then concentrated under reduced

pressure. The basic ingredient was then diluted with CHCl_3 , transferred into a separatory funnel, washed three times with a saturated NaHCO_3 aqueous solution, and washed then twice with H_2O . The organic phase was dried over anhydrous Na_2SO_4 , filtered and concentrated under reduced pressure to produce pure 3,5,7,4''-*O*-tetra-acetyl-9''-*O*-(4,4'-dimethoxytriphenylmethyl)-silybin A as a pale amorphous solid (0.42 g, 426 μmol) in 91% yield. $R_f = 0.5$ (hexane/AcOEt 90 : 10). To a solution of 3,5,7,4''-*O*-tetra-acetyl-9''-*O*-(4,4'-dimethoxytriphenylmethyl)-silybin A (0.42 g, 426 μmol) in CH_2Cl_2 (5 ml), 5% formic acid in CH_2Cl_2 (8 ml) was added. The mixture was stirred for 30 min before the mixture was extracted with CHCl_3 (25 ml), washed with 10% NaHCO_3 solution, dried over Na_2SO_4 , and then concentrated *in vacuo*. The basic material was next purified on a silica gel column and eluting with hexane containing increasing amounts of AcOEt (from 50 to 70%) to afford pure 3,5,7,4''-*O*-tetra-acetyl-silybin A (**2A**) (220 mg, 340 μmol) as a pale amorphous solid in 80% yield.

Compound 2A: $R_f = 0.6$ ($\text{CHCl}_3/\text{CH}_3\text{OH}$, 90:10, v/v). The ^1H NMR (500 MHz, CDCl_3 , room temperature) δ 7.09-6.96 (6H, overlapped signals, H-2', H-6', H-5', H-2'', H-5'', H-6''), 6.74 (1H, s, H-8), 6.56 (1H, s, H-6), 5.66 (1H, d, $J = 12.5$ Hz, H-3), 5.32 (1H, d, $J = 12.5$ Hz, H-2), 4.99 (1H, d, $J = 8.0$ Hz, H-7''), 3.99 (1H, m, H-8''), 3.80-3.77 (4H, complex signals, OCH_3 , H-9''a), 3.49 (1H, dd, $J = 2.0$ Hz, $J = 9.5$ Hz, H-9''b), 2.32, 2.26, 2.23, 1.98 (12H, s, CH_3 of the acetyl groups) ppm. ESI-MS: 649.18 ($[\text{M} - \text{H}]^+$, $\text{C}_{33}\text{H}_{30}\text{O}_{14}$; 650.16).

The same procedure was used to obtain **2B** starting from silybin B (**1B**).

Compound 2B: $R_f = 0.6$ ($\text{CHCl}_3/\text{CH}_3\text{OH}$, 90:10, v/v). The ^1H NMR (500 MHz, CDCl_3 , room temperature) δ 7.04-6.93 (6H, overlapped

signals, H-2', H-6', H-5', H-2'', H-5'', H-6''), 6.76 (1H, s, H-8), 6.55 (1H, s, H-6), 5.64 (1H, d, J= 12.5 Hz, H-3), 5.30 (1H, d, J= 12.5 Hz, H-2), 4.97 (1H, d, J= 8.0 Hz, H-7''), 3.99 (1H, m, H-8''), 3.80-3.77 (4H, complex signals, OCH₃, H-9''a), 3.49 (1H, dd, J= 2.0 Hz, J= 9.5 Hz, H-9''b), 2.34, 2.24, 2.22, 1.99 (12H, s, CH₃ of the acetyl groups) ppm. ESI-MS: 649.21 ([M - H]⁺, C₃₃H₃₀O₁₄; 650.16).

General procedures for the preparation of silybin analogues 3A, 4A, 5A, 6A and respective isomers (3B, 4B, 5B, 6B).

Synthesis of silybin A-9''-O-sulphate sodium salt (3A). Compound **2A** (20 mg, 31 μmol) was dissolved in anhydrous DMF (200 μl) and reacted a sulphur trioxide triethylamine complex (6 mg, 33 μmol). After 30 min, the reaction mixture was quenched with H₂O and then concentrated under reduced pressure. The crude extract was next purified on a silica gel column using with CHCl₃/MeOH 97 : 3 as the eluent to afford pure 3,5,7,4''-O-tetra-acetyl-9''-O-sulphate silybin A (17 mg, 24 μmol) in 78% yield. 3,5,7,4''-O-tetra-acetyl-9''-O-sulphate silybin A was successively treated with 0.4 ml conc. aq. ammonia in MeOH 50:50 at 25°C for 30 min. The concentrated mixture was purified on a silica gel column and eluted with CHCl₃/MeOH 80:20, and then the compound was converted into the corresponding sodium salt (**3A**) by cation exchange on a DOWEX (Na⁺ form) resin to afford a homogeneous sample (10 mg, 17 μmol) in 70% yield. R_f = 0.5 (CHCl₃/MeOH 70 : 30). ESI-MS: 583.05 ([M - H]⁻, C₂₅H₂₁NaO₁₃S; 584.06). The same procedure was used to obtain the silybin B-9''-O-sulphate isomer as a sodium salt (**3B**).

Compound 3A: R_f = 0.5 (CHCl₃/MeOH 70 : 30). ESI-MS: 583.07 ([M - H]⁻, C₂₅H₂₁NaO₁₃S; 584.06). The ¹H NMR (500 MHz, CDCl₃, room temperature) δ 7.10 (1H, *br s*, H-2'), 7.04 (m, 1H, H-2''), 7.03 (1H, m,

H-5'), 6.96 (1H, m, H-6'), 6.90 (1H, m, H-6''), 6.83 (1H, m, H-5''), 5.92 (1H, s, H-8), 5.89 (1H, s, H-6), 4.95 (1H, d, $J = 12.4$ Hz, H-2), 4.78 (1H, d, $J = 7.9$ Hz, H-7''), 4.49 (1H, d, $J = 12.4$ Hz, H-3), 4.24 (1H, m, H-8''), 4.16 (1H, m, H-9''a), 3.90 (1H, m, H-9''b), 3.87 (3H, s, OCH₃).ESI-MS: 583.05 ($[M - H]^-$, C₂₅H₂₁NaO₁₃S; 584.06).

Compound 3B: $R_f = 0.5$ (CHCl₃/CH₃OH, 70:30, v/v). The ¹H NMR (500 MHz, CDCl₃, room temperature) δ 7.12 (1H, *br s*, H-2'), 7.04 (1H, m, H-2''), 7.02 (1H, m, H-5'), 6.96 (1H, m, H-6'), 6.91 (1H, m, H-6''), 6.83 (1H, m, H-5''), 5.92 (1H, s, H-8), 5.89 (1H, s, H-6), 4.95 (1H, d, $J = 12.5$ Hz, H-2), 4.78 (1H, d, $J = 8.0$ Hz, H-7''), 4.49 (1H, d, $J = 12.5$ Hz, H-3), 4.24 (1H, m, H-8''), 4.15 (1H, m, H-9''a), 3.91 (1H, m, H-9''b), 3.85 (3H, s, OCH₃).ESI-MS: 583.07 ($[M - H]^-$, C₂₅H₂₁NaO₁₃S; 584.06).

Synthesis of 9''-azide-silybin A (4A). 40 mg (60 μ mol) of **2A** and 15 mg (0.30 μ mol) of triphenylphosphine were dissolved in 0.8 ml of anhydrous THF at 0°C and then treated with a mixture of 15 μ L (7 μ mol) of DEAD and 15 μ L (8 μ mol) of diphenylphosphorylazide (DPPA) in anhydrous THF. After 10 min, the reaction temperature was raised to 25°C and the reaction was stirred for 5 h. The crude extract was concentrated under reduced pressure and purified by silica gel chromatography with hexane containing increasing amounts of AcOEt (from 40 to 50%), as the eluent to afford 30 mg (48 μ mol, 78%) of pure 3,5,7-*O*-three-acetyl-9''-azide-silybin. The obtained compound was treated with 0.8 ml of HCl conc./EtOH 10:40, at 50°C for 20 min. The crude mixture was diluted with AcOEt, transferred to a separatory funnel, washed with a saturated NaHCO₃ aqueous solution, and washed twice with H₂O. The organic phase was dried over anhydrous Na₂SO₄ and filtered prior to concentration under reduced pressure and purification using on TLC eluting with

CHCl₃/MeOH 92:8 was used as the eluent to pure **4A** (21 mg, 40 μmol) as a homogeneous solid in 84% yield.

Compound 4A: Rf = 0.4 (CHCl₃/MeOH 90 : 10). ¹H-NMR (500 MHz, CD₃OD): 6.95 (1H, *d*, *J* = 8.0, H-5), 6.94 (1H, *brs*, H-2'), 6.90 (1H, *d*, *J* = 8.5, H-5''), 6.89 (1H, *brs*, H-2''), 6.87 (1H, *brd*, *J* = 8.5, H-6''), 6.78 (1H, *brd*, *J* = 8.0, H-6'), 5.93 (1H, *brs*, H-8), 5.88 (1H, *brs*, H-6), 5.02 (1H, *d*, *J* = 12.5, H-2), 4.89 (1H, *brd*, *J* = 8.0, H-C7''), 4.56 (1H, *d*, *J* = 12.5, H-3), 4.13 – 4.15 (1H, *m*, H-C8''), 3.89 (3H, *s*, OCH₃), 3.54 (1H, *brd*, *J* = 13.0, CH_{2a}-9''); 3.13 (1H, *dd*, *J* = 4.0, *J* = 13.0, CH_{2b}-9''). ESI-MS: 530.49 [M + Na]⁺, 508.16 ([M + H]⁺, C₂₅H₂₁N₃O₉; calc. 507.13).

The same procedure was used to obtain the 9''-azide-silybin B (**4B**) isomer.

Compound 4B: Rf = 0.4 (CHCl₃/MeOH 90:10). ¹H-NMR (500 MHz, CD₃OD): 6.93 (1H, *d*, *J* = 8.0, H-5'), 6.91 (1H, *brs*, H-2'), 6.88 (1H, *d*, *J* = 8.5, H-5''), 6.85 (1H, *brs*, H-2''), 6.83 (1H, *brd*, *J* = 8.5, H-6''), 6.78 (1H, *brd*, *J* = 8.0, H-6'), 5.91 (1H, *brs*, H-8), 5.85 (1H, *brs*, H-6), 5.02 (1H, *d*, *J* = 12.5, H-2), 4.82 (1H, *brd*, *J* = 8.0, H-7''), 4.52 (1H, *d*, *J* = 12.5, H-3), 4.09 – 4.12 (1H, *m*, H-8''), 3.82 (3H, *s*, OCH₃), 3.51 (1H, *brd*, *J* = 13.0, CH_{2a}-9''), 3.15 (1H, *dd*, *J* = 4.0, *J* = 13.0, CH_{2b}-9''). ESI-MS: 530.37 [M + Na]⁺, 546.52 [M + K]⁺, 508.15 ([M + H]⁺, C₂₅H₂₁N₃O₉; calc. 507.13).

Synthesis of 9''-amine-silybin A (5A). The silybin derivative **4A** (30 mg, 54 μmol) was dissolved with stirring in MeOH (0.80 ml). 10% Pd/C (2.0 mg) was added as a catalyst, the flask was evacuated and an atmosphere of hydrogen was secured. The mixture was stirred overnight under hydrogen balloon pressure (reaction complete according to TLC). The mixture was filtered through a plug of silica and was washed with AcOEt, concentrated under reduced pressure and then purified using TLC with CHCl₃/MeOH 80:20 as the eluent to

pure **5A** (15 mg, 31 μmol) as a homogeneous solid in 62% yield. $R_f = 0.4$ ($\text{CHCl}_3/\text{MeOH}$ 80 : 20). ESI-MS (MALDI-TOF): 480.13 ($[\text{M} - \text{H}]^-$, $\text{C}_{25}\text{H}_{23}\text{NO}_9$; calc. 481.14). The same procedure was used to obtain the 9''-amine-silybin B (**5B**) isomer.

Compound 5A: $R_f = 0.4$ ($\text{CHCl}_3/\text{CH}_3\text{OH}$, 80:20, v/v). ^1H NMR (500 MHz, CDCl_3 , room temperature) δ 7.11 (1H, s, H-2'), 7.05 (1H, m, H-6'), 7.02 (1H, m, H-5'), 6.99 (1H, s, H-2''), 6.88 (1H, m, H-6''), 6.85 (1H, m, H-5''), 5.87 (1H, s, H-8), 5.84 (1H, s, H-6), 4.94 (1H, d, $J = 12.5$ Hz, H-2), 4.74 (1H, d, $J = 8.1$ Hz, H-7''), 4.47 (1H, d, $J = 12.5$ Hz, H-3), 4.13 (1H, d, $J = 8.1$ Hz, H-8''), 3.86 (3H, s, OCH_3), 2.83, 2.68 (1H, m, H-9''a, H-9''b). ESI-MS: 482.12 ($[\text{M} - \text{H}]^+$, $\text{C}_{25}\text{H}_{23}\text{NO}_9$; calc. 481.14).

Compound 5B: $R_f = 0.4$ ($\text{CHCl}_3/\text{CH}_3\text{OH}$, 80:20, v/v). ^1H NMR (500 MHz, CDCl_3 , room temperature) δ 7.11 (1H, s, H-2'), 7.05 (1H, m, H-6'), 7.02 (1H, m, H-5'), 6.99 (1H, s, H-2''), 6.88 (1H, m, H-6''), 6.85 (1H, m, H-5''), 5.87 (1H, s, H-8), 5.84 (s1H,, H-6), 4.94 (1H, d, $J = 12.4$ Hz, H-2), 4.74 (1H, d, $J = 8.0$ Hz, H-7''), 4.47 (1H, d, $J = 12.4$ Hz, H-3), 4.13 (1H, d, $J = 8.0$ Hz, H-8''), 3.86 (3H, s, OCH_3), 2.83, 2.68 (2H, m, H-9''a, H-9''b). ESI-MS: 480.13 $[\text{M} - \text{H}]^-$, $\text{C}_{25}\text{H}_{23}\text{NO}_9$; calc. 481.14.

Synthesis of silybin A-9''-O-(4-nitrophenyl)-phosphate sodium salt (6A). Compound **2A** (25 mg, 39 μmol) was dissolved in anhydrous pyridine (0.5 ml) and reacted with 4-nitrophenyl dichlorophosphate (10 mg, 4.2 μmol). The reaction was left under stirring at 0°C for 40 min and monitored by TLC using $\text{CHCl}_3/\text{MeOH}$ 90:10. The reaction mixture was quenched with H_2O , stirred at 0°C for 20 min, then concentrated under reduced pressure, and finally purified using TLC eluting with $\text{CHCl}_3/\text{MeOH}$ 95:5 as the eluent to pure (3,5,7,4''-O-tetraacetyl)-silybin A-9''-O-(4-nitrophenyl)-phosphate (25 mg, 30 μmol) in 80% yield. The NMR spectra of this compound showed dramatic line

broadening, which is diagnostic of slow equilibrium on the NMR time scale. This could suggest a strong propensity toward aggregation in CDCl₃. The obtained compound was treated with 0.5 ml conc. aq. ammonia in MeOH (1:1) at 25°C for 30 min. The reaction mixture was concentrated under reduced pressure and then purified on TLC eluting with CHCl₃/MeOH 70:30 as the eluent to afford pure **6A** (14 mg, 21 μmol) in 67% yield. Compound **6A** was converted into the corresponding sodium salt by cation exchange on a DOWEX (Na⁺ form) resin to obtain a homogeneous sample.

Compound 6A: Rf = 0.4 (CHCl₃/MeOH 70 : 30). ¹H-NMR (500 MHz, CDCl₃): 8.00 – 8.02 (2H, *m*, *m*-protons of 4-nitrophenyl moiety), 7.52 – 7.55 (1H, *m*, H-6'), 7.58 – 7.62 (1H, *m*, H-6''), 7.40 – 7.42 (2H, *m*, *o*-protons of 4-nitrophenyl moiety), 6.95 (1H, *s*, H-2'), 6.78 – 6.81 (1H, *m*, H-5'), 6.76 – 6.79 (1H, *m*, H-2''), 6.72 – 6.76 (1H, *m*, H-5''), 6.51 (1H, *s*, H-8), 6.24 (1H, *s*, H-6), 4.91 (1H, *d*, *J* = 8.0, H-7''), 4.19 (1H, *d*, *J* = 8.0, H-8''), 4.20 – 4.22 (1H, *m*, CH_{2a}-9''), 3.84 (3H, *s*, OCH₃), 3.76 – 3.79 (1H, *m*, CH_{2b}-9''). ³¹P-NMR (CD₃OD, 161 MHz): -4.8. ESI-MS: 682.13 ([M - H]⁻, C₃₁H₂₆NO₁₅P; calc. 683.10).

The same procedure was used to obtain the silybin B-9''-*O*-(4-nitrophenyl)-phosphate isomer as a sodium salt (**6B**).

Compound 6B: Rf = 0.4 (CHCl₃/MeOH 70 : 30). ¹H-NMR (500 MHz, CDCl₃): 8.08 (2H, complex signals, *m*-protons of 4-nitrophenyl moiety), 7.53 – 7.54 (1H, *m*, H-6'), 7.58 – 7.62 (1H, *m*, H-C6''), 7.40 (2H, complex signals, *o*-protons of 4-nitrophenyl moiety), 6.95 (1H, *s*, H-2'), 6.78 – 6.81 (1H, *m*, H-5'), 6.78 (1H, *s*, H-2''), 6.72 – 6.75 (1H, *m*, H-5''), 6.51 (1H, *s*, H-8), 6.24 (1H, *s*, H-6), 4.91 (1H, *d*, *J* = 8.0, H-7''), 4.19 (1H, *d*, *J* = 8.0, H-8''), 4.20 – 4.23 (1H, *m*, CH_{2a}-9''), 3.84 (3H, *s*, OCH₃), 3.75 – 3.80 (1H, *m*, CH_{2b}-9''). ³¹P-NMR (CD₃OD, 161 MHz): -4.8. ESI-MS: 682.11 ([M - H]⁻, C₃₁H₂₆NO₁₅P; calc. 683.10).

Assessing free radical scavenging activity using the DPPH method.

The measurement of the DPPH radical scavenging activity was performed according to methodology described by *Brand-Williams et al.*⁷⁰. Briefly, the antioxidant in methanol (0.1 ml) was added to 2.4 ml of methanolic DPPH solution (25 mg/L). The reaction mixture was covered and left in the dark at room temperature. The absorbance at 517 nm was recorded spectrophotometrically (*HP 8452A, Hewlett-Packard GmbH*) after 0.5, 1, 3, 15, 30, and 60 min and thereafter every hour until the steady state was achieved. Each antioxidant was prepared in duplicate for each of at least three concentrations and averaged. Butylated hydroxyl anisole (BHA) was used as a standard antioxidant. The amount of sample required to decrease the initial DPPH concentration by 50% (EC_{50}) was calculated by linear regression of the remaining DPPH (%) vs the sample concentration. When DPPH reacts with an antioxidant compound, which can donate hydrogen, it is reduced. The changes in color (from deep violet to light yellow) were read [Absorbance (Abs)] at 517 nm after 100 min of reaction using a UV-VIS spectrophotometer (DU 800; Beckman Coulter, Fullerton, CA, USA). The mixture of ethanol (3.3 ml) and the sample (0.5 ml) served as blanks. The control solution was prepared by mixing ethanol (3.5 ml) and DPPH radical solution (0.3 ml).

The percentage of scavenging activity (AA%) was determined according to *Mensor et al.*⁷³:

$$AA\% = 100 - (Abs_{sample} - Abs_{blank}) \times 100 / Abs_{control}$$

Statistical analysis. The experiments for each substance were done in triplicate. The results were expressed as decrease in percentage relative to control values and compared by one-way ANOVA and *Tukey's test*.

Differences were considered statistically significant if $p < 0.05$. The poor superoxide radical scavenging capacity of silybin was previously reported⁶⁹.

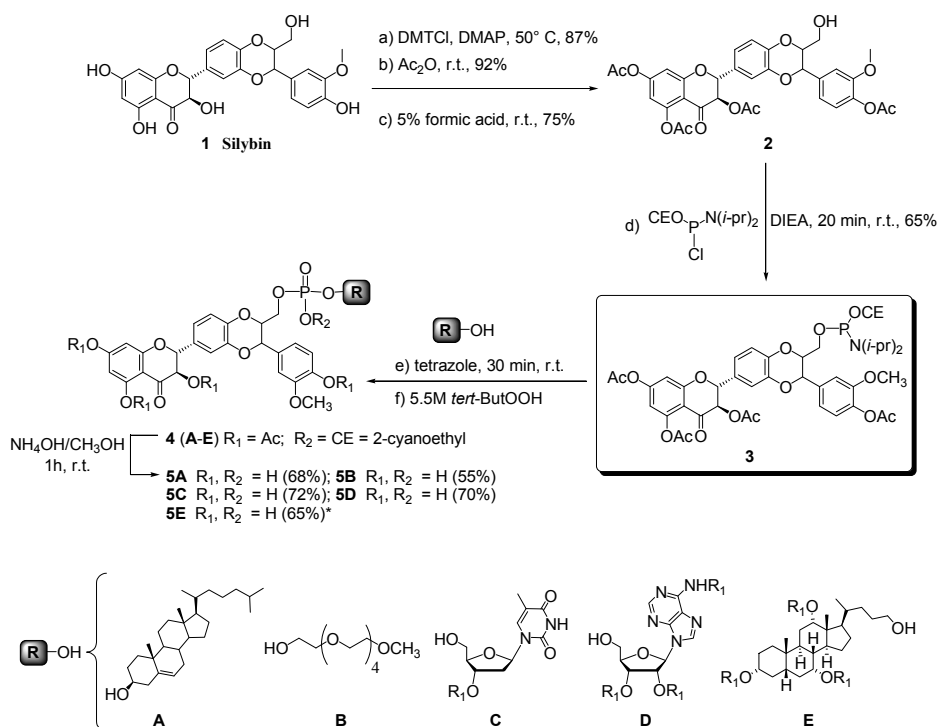
5.5.2 New silibinin scaffold for chemical diversification: synthesis of novel 9"-silibinin conjugates

Aiming to improve the bioavailability, the delivery as well as the biological activity of silibinin, we developed an efficient synthetic procedure to obtain new 9"-silibinin conjugates with different labels. Particularly, we have selected some molecules known for their ability as molecular carriers (steroids, bile acids)^{74,75}, radical scavengers (nucleosides)^{76,77}, and capable to improve water solubility (as polyether)^{78,79}. The introduction of these labels occur through a phosphate group that confers also great pharmaceutical and pharmacokinetic benefits to the molecule. Therefore we chose to start from the new 9"-phosphoramidite building block **3** (**Scheme 4**) which could be transformed into a series of conjugates using a solution-phase parallel array protocol and exploiting standard and reliable phosphoramidite chemistry⁸⁰. We initially converted silibinin **1** into 9"-ODMT intermediate **2**, using a synthetic approach described in the previous section (see Paragraph 5.5.1), then this compound **2** has been converted into the corresponding phosphoramidite derivatives **3**.

Thus intermediate **3**, whose synthesis has recently been optimized by my research group⁵⁴; was obtained using 2-cyanoethyl-N,N-diisopropylamino-chlorophosphoramidite reagent with DIEA (N,N-diisopropylethylamine) in anhydrous DCM (dichloromethane). In these preliminary studies, silibinin used as starting material was a mixture of its diastereoisomers, the derivatives **3** were obtained as a mixture of two diastereoisomers, not separable by chromatography,

and the ^1H and ^{31}P NMR spectra appeared like those of a single compound.

After purification the identity of compounds **3**, obtained in good yields (65%), was confirmed by NMR (^1H , ^{13}C and ^{31}P) and HRMS-ESI data⁸¹. Afterwards the group of molecules chosen for their peculiar properties have been selected also because having a free hydroxyl group (**A-E**, Scheme 4) that provides an easily coupling with the key intermediate **3**.



Scheme 4. Synthesis of 9''-phosphodiester silibinin conjugates **5 (A-E)**. *yields calculated from starting product **3**.

While **A**, **B** and **C** are commercially available, **D** and **E** were efficiently obtained starting from 2'-deoxyadenosine and 3 α ,7 α ,12 α ,24-tetrahydroxycholane, respectively. Exploiting the different reactivity of hydroxyl groups we used the *tert*butyldimethylsilyl group

(TBDMS) for the transient protection of the primary OH moiety while all other groups were protected with acetyl (Ac). 2'-deoxyguanosine and 3 α ,7 α ,12 α ,24-tetrahydroxycholesterol were protected by reactions with TBDMS-chloride (TBDMSCl) and DMTCl respectively^{82,83}. The products were acetylated by acetic anhydride to yield fully protected products. Finally, the TBDMS group was cleaved by triethylaminetrihydrofluoride (Et₃N·3HF) and dichloroacetic acid (DCA) to yield N²-acetyl-2',3'-*O*-di-acetyl-deoxyguanosine (**D**) and 3 α ,7 α ,12 α -*O*-tri-acetyl-24-hydroxycholesterol (**E**) in overall yields of 80 and 75% respectively. The coupling of **3** with **A-E** (**Scheme 4**) was carried out by using the classic coupling reagent (0.1M tetrazole in acetonitrile) subsequently, the treatment with 5.5M *tert*-butyl hydroperoxide solution in decane, led to phosphotriesters **4** (**A-E**). After purification by flash chromatography, the derivatives **4** were treated with conc. aq. ammonia and MeOH (1:1, v:v) at room temperature, allowing the full deprotection from acetyl and cyanoethyl groups and generating the desired phosphodiester derivatives **5** (**A-E**) in good yields (**Scheme 4**). All final derivatives **5** (**A-E**) were purified by flash chromatography and then characterized by NMR (¹H and ³¹P) and MS analyses. All the intermediates and final derivatives were obtained as a mixture of two diastereoisomers, that we failed to separate by chromatography, and the NMR spectra of many of them appeared like those of a single compound.

5.5.2.2 Experimental Session

General procedure for the preparation of phosphoramidite 3: To 240.0 mg (0.37 mmol) of 3,5,7,4"-*O*-tetra-acetyl-silibinin (**2**) dissolved in anhydrous dichloromethane (5 mL), DIEA (390 μ L, 2.22 mmol) and 2-cyanoethyl-N,N-diisopropylamino-chlorophosphoramidite (107 μ L, 0.48 mmol) were added under argon. After 30 min the solution was

diluted with AcOEt and the organic phase was washed twice with brine and then concentrated. Silica gel chromatography of the residue (eluent *n*-hexane:ethyl acetate, 3:7, v:v, in the presence of 1% of triethylamine), afforded desired compound **3** (205.0 mg, 0.24 mmol) in a 65% yield. R_f = 0.8 (*n*-hexane:ethyl acetate, 3:7, v:v).

Compound 3 ¹H NMR (CDCl₃, 500 MHz, room temperature, mixture of diastereoisomers): δ 7.11-6.90 (6H, overlapped signals, H-2', H-6', H-5', H-2'', H-5'', H-6''), 6.81 (1H, s, H-8), 6.58 (1H, s, H-6), 5.66 (1H, d, *J* = 11.6 Hz, H-3), 5.37 (1H, d, *J* = 11.6 Hz, H-2), 5.03 (1H, d, *J* = 7.6 Hz, H-7''), 4.13 (1H, m, H-8''), 3.90-3.60 (9H, complex signals, OCH₃, H-9'', OCH₂CH₂CN, N[CH(CH₃)₂]₂), 2.65 (2H, complex signals, OCH₂CH₂CN), 2.37, 2.32, 2.29, 2.04 (12H, s for each, CH₃ of acetyl groups) 1.25-1.15 (12H, complex signals, N[CH(CH₃)₂]₂) ppm. ¹³C NMR (CDCl₃, 125 MHz, room temperature, mixture of diastereoisomers): δ 185.3 (C-4), 169.1 (C-7), 168.7, 167.8 (CO of acetyl groups), 162.5 (C-5), 156.3 (C-8a), 151.4 (C-3''), 144.3 (C-4''), 143.6 (C-4'), 140.2 (C-3'), 134.8 (C-1'), 123.0 (C-1''), 120.8 (C-6'), 119.9 (C-6''), 119.8, 117.6, 117.2 (C-2', C-5', OCH₂CH₂CN), 116.2 (C-5''), 111.4, 111.2, 110.6, 108.9 (C-6, C-8, C-2'', C-4a), 81.0 (C-2), 76.2 (C-8''), 75.8 (C-7''), 73.3, 73.1 (C-3), 62.6, 62.2 (C-9''), 58.8, 58.5 (OCH₂CH₂CN), 56.0 (OCH₃), 43.3, 43.1 (N[CH(CH₃)₂]₂), 24.5 (N[CH(CH₃)₂]₂), 21.1, 20.9, 20.7, 20.4 (CH₃ of acetyl groups), 19.9 (OCH₂CH₂CN) ppm. ³¹P NMR (CDCl₃, 161.98 MHz): δ 152.9, 150.2 ppm. HRMS (ESI-MS - positive ions): *m/z* calcd for C₄₂H₄₇N₂O₁₅P = 850.2714; Found: [MH]⁺ = 851.2788; [MNa]⁺ = 873.2606.

General procedure for the synthesis of conjugates 5 (A-E): derivative **3** (150 mg, 0.22 mmol) and the select compound **A-E** (0.21 mmol, previously dried and kept under reduced pressure, were

reacted with a 0.45M tetrazole solution in anhydrous CH₃CN (1.0 mL, 0.45 mmol). The reaction was left under stirring at room temperature and monitored by TLC in the eluent system *n*-hexane: AcOEt, 1:1, v:v. After 1h, a 5.5M *tert*-butyl hydroperoxide (*t*-BuOOH) solution in decane (100 μ L) was added to the mixture and left under stirring at room temperature. After 30 minutes the reaction mixture was diluted with CHCl₃, transferred into a separatory funnel, washed three times with water, concentrated under reduced pressure, and purified by flash chromatography eluted with *n*-hexane: AcOEt, 7:3, v:v, affording pure **4 (A-E)** as yellow-brown amorphous powder. The next treatment with conc. aq. ammonia in CH₃OH (1:1, v:v) to 1h at room temperature, allowed full deprotection from acetyl and 2-cyanoethyl groups. The concentrated mixture was then purified on a silica gel column, eluted with CHCl₃/CH₃OH containing growing amounts of CH₃OH. Compounds thus obtained **5 (A-E)** were converted into the corresponding sodium salts by cation exchange on a DOWEX (Na⁺ form) resin to have a homogeneous samples in good yield (55-72%).

Compound 5A: NMR spectra of this compound showed dramatic line broadening, diagnostic of a slow equilibrium on the NMR time scale, which could suggest a strong propensity toward aggregation in CDCl₃. ¹H NMR (CDCl₃, 500 MHz, room temperature, mixture of diastereoisomers): δ 7.02-6.60 (6H, complex signals), 5.85 (2H, *br s*), 5.59 (1H, dd, $J = 11.9$ and 11.7 Hz), 5.11 (2H, complex signals), 4.78 (1H, *br s*), 4.04 (1H, *br signal*), 3.95-3.63 (6H, complex signals), 2.05 (2H, *br signal*), 1.92-0.99 (26H, complex signals), 0.85 (3H, *br s*), 0.79 (3H, d, $J = 4.8$ Hz), 0.74 (6H, *br s*), 0.55 (3H, s) ppm. ³¹P NMR (CDCl₃, 161.98 MHz): δ -0.83 ppm. HRMS (MALDI-TOF, negative ions) m/z calcd for C₅₂H₆₆O₁₃P = 929.4246, found 929.4246 [M - H]⁻.

Compound 5B: ^1H NMR (CD_3OD , 500 MHz, room temperature, mixture of diastereoisomers): δ 7.11-6.72 (6H, complex signals), 5.91 (1H, d, $J = 1.5$ Hz), 5.85 (1H, m), 4.98-4.75 (2H, complex signal), 4.41 (1H, d, $J = 11.5$ Hz), 4.21-4.05 (5H, m), 3.88-3.68 (24H, complex signals) ppm. ^{31}P NMR (CDCl_3 , 161.98 MHz): δ 3.1 ppm. HRMS (MALDI-TOF, negative ions) m/z calcd for $\text{C}_{36}\text{H}_{44}\text{O}_{18}\text{P} = 795.2271$, found 795.2271 $[\text{M} - \text{H}]^-$.

Compound 5C: ^1H NMR (CD_3OD , 500 MHz, room temperature, mixture of diastereoisomers): δ 7.79 (1H, s), 7.11-6.72 (6H, complex signals), 6.41 (1H, dd, $J = 6.8$ and 6.8 Hz), 5.91 (1H, d, $J = 1.5$ Hz), 5.85 (1H, m), 4.97-4.74 (2H, complex signal), 4.65 (1H, m), 4.41 (1H, d, $J = 11.5$ Hz), 4.22-4.10 (4H, m), 4.00-3.85 (5H, complex signals), 2.44 (2H, m), 1.99 (3H, s) ppm. ^{31}P NMR (CDCl_3 , 161.98 MHz): δ 3.3 ppm. HRMS (MALDI-TOF) m/z calcd for $\text{C}_{35}\text{H}_{34}\text{N}_2\text{O}_{17}\text{P} = 785.1600$, found 785.1602 $[\text{M} - \text{H}]^-$.

Compound 5D: ^1H NMR (CD_3OD , 500 MHz, room temperature, mixture of diastereoisomers): δ 8.56 (1H, s), 8.29 (1H, s), 7.11-6.72 (6H, complex signals), 6.05 (1H, d, $J = 6.0$ Hz), 5.91 (1H, d, $J = 1.5$ Hz), 5.85 (1H, m), 4.90 (2H, complex signals), 4.63 (1H, m), 4.54 (1H, m), 4.41 (1H, d, $J = 11.5$ Hz), 4.35 (1H, m), 4.20 (2H, m), 4.21-4.05 (3H, m), 3.88-3.68 (3H, s) ppm. ^{31}P NMR (CDCl_3 , 161.98 MHz): δ 3.1 ppm. HRMS (MALDI-TOF) m/z calcd for $\text{C}_{35}\text{H}_{33}\text{N}_5\text{O}_{16}\text{P} = 810.1665$ found 810.1666 $[\text{M} - \text{H}]^-$.

Compound 5E: ^1H NMR (CD_3OD , 500 MHz, room temperature, mixture of diastereoisomers): δ 7.08-6.81 (6H, complex signals), 5.95-5.89 (2H, m), 5.07 (1H, m), 4.97 (1H, m), 4.52 (2H, m), 4.24 (1H, m), 4.06 (1H, m), 3.95-3.68 (7H, complex signals), 3.30 (1H, m), 2.01-0.70

(33H, complex signals) ppm. ^{31}P NMR (CDCl_3 , 161.98 MHz): δ 4.3 ppm. ESI-MS (positive ions): m/z calcd for $\text{C}_{49}\text{H}_{63}\text{O}_{16}\text{P}$ = 938.39; Found: $[\text{MH}]^+$ = 939.48; $[\text{MNa}]^+$ = 961.37. HRMS (MALDI-TOF, negative ions) m/z calcd for $\text{C}_{49}\text{H}_{62}\text{O}_{16}\text{P}$ = 937.3781, found 937.3782 $[\text{M} - \text{H}]^-$.

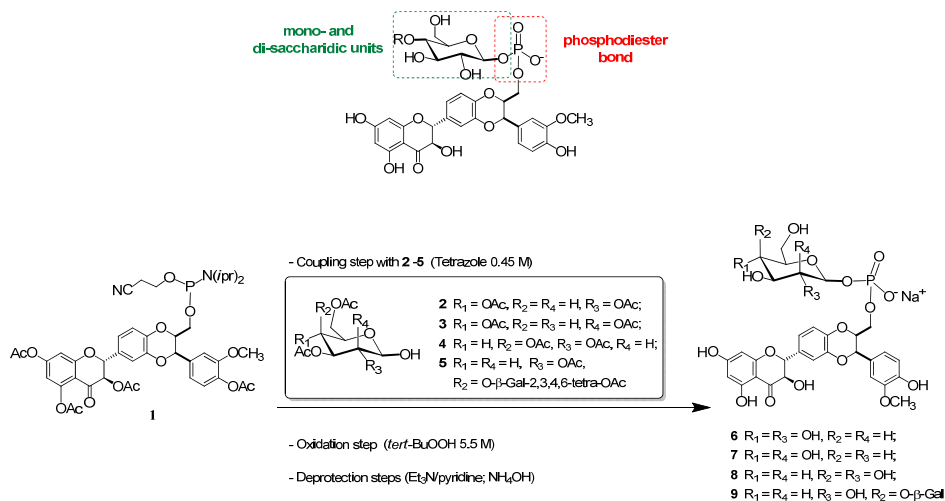
5.5.3 New silibinin glyco-conjugates: Synthesis and evaluation of antioxidant properties

As previously described, therapeutic efficiency of silibinin is rather limited by its low bioavailability that limited its affectivity³³. In this contest, it has been reported, for the quercetin, natural product endowed with potent antioxidant activity, that the therapeutic absorption of its modified quercetin glycoside, is more efficient than the quercetin aglycon, ascribing this benefit to the hydrophilic character of saccharide moieties that increase the water solubility of the aglycon, and enhance its bioavailability^{27,84,85}. Moreover, the presence of hydroxyl groups brings the possibility of *prodrug* approach making possible the improvement of its pharmaceutical, pharmacokinetic and/or pharmacodynamic properties⁸⁶.

Starting from these considerations, we synthesized and biologically characterized, new 9"-silibinin conjugates connecting the mono- and di-saccharide residues to hydroxyl anomeric position through phosphodiester bond (**Scheme 5**). In our approach 9"-phosphoramidite **1** (see Paragraph 5.5.2) has been used as silibinin substrate and 1-OH full protected mono- and di-saccharide derivatives (**2–5**, **Scheme 5**) chosen as sugar starting materials. We initially converted full acetylated mono and di-saccharides into 1-OH derivatives by a reaction with benzylamine in THF at room temperature^{87,88}.

Thus compounds **2–5** (**Scheme 5**) were coupled with derivative **1** using 0.45 M tetrazole in $\text{CH}_3\text{CN}/\text{DCM}$ (1:1, v:v). After the treatment

with 5.5 M *tert*-butyl hydroperoxide solution in decane and subsequently with conc. aq. Ammonia/MeOH (1:1, v:v) at room temperature, the phosphodiester derivatives **6–9** were obtained in good yields.



Scheme 5. General structures of new silibinin glyco-conjugates (top); synthesis of new 9''-glyco-silibinin analogues (bottom).

All compounds were then converted into the corresponding sodium salts by cation exchange on a DOWEX (Na⁺ form) resin to have crystalline samples. The crude materials were then subjected to the purification step, by reverse phase analysis (RP-18 HPLC), using a variety of columns and elution conditions, but unfortunately the mixture of diastereoisomers was too much complicated to be purified. In the end new silibinin analogues (**6–9**) were eluted onto Sep-Pak C18 cartridge and were obtained as a mixture of diastereoisomers, as observed ³¹P NMR analysis. The NMR analysis has proved very complex, in fact ¹H and ³¹P NMR spectra of all compound showed dramatic line broadening, already at 5.0 mg/mL (ca. 7.0 mM), diagnostic of a slow equilibrium on the NMR time scale, which could suggest a strong propensity toward aggregation in H₂O. This

drawback has not allowed a complete and detailed NMR characterization of the new derivatives. In this preliminary study we show the values of the ^{31}P NMR and ESI-MS mass spectra signals (see Experimental Session).

In order to evaluate their antioxidant activity, all silibinin derivatives were subjected to 2,2-diphenyl-1-picrylhydrazyl (DPPH) free radical scavenging assay⁸⁹ and the Xanthine oxidase (XO) inhibition models assay (**Table 4**).

Table 4. Free Radical Scavenging capacity (DPPH) and Xanthine Oxidase Inhibition (X – XO)

Samples	IC ₅₀ (μM) ^a	Cell viability (%) ^b	
			<i>after induction of oxidative stress</i>
silibinin-9"- phosphoryl-D-glucopyranoside (6)	301.7 ± 15.1	89.2 ± 3.1	42.7 ± 3.2
silibinin-9"- phosphoryl-D-mannopyranoside (7)	108.0 ± 3.2	89.5 ± 2.3	42.3 ± 4.2
silibinin-9"- phosphoryl-D-galactopyranoside (8)	233.0 ± 14.0	84.1 ± 2.4	42.8 ± 3.6
silibinin-9"- phosphoryl-D-lactopyranoside (9)	154.7 ± 6.2	91.8 ± 2.1	48.4 ± 3.8
silibinin	392.2 ± 7.8	45.3 ± 2.5	42.4 ± 2.9
2,3-dehydrosilybin	27.0 ± 0.8	-	-
quercetin	0.31 ± 0.01	-	-

^a IC₅₀ values (defined as concentrations that inhibites activity by 50%) were calculated using data obtained from at least three independent experiments.

^b (Mean ± SD from three separate experiments run in duplicate, at 10, 25, 50, 100, and 200 μM).

The DPPH test is a non-enzymatic method currently used to provide basic information on the scavenging potential of stable free radicals *in vitro*. On the other hand XO is considered to be the most important biological source of free radicals. Many references reveal cerebral microvascular injury resulting from XO production of superoxide free radicals⁹⁰. XO inhibition is thereby implicated as

useful approach in treating cerebrovascular pathological changes or Central Nervous System (CNS) diseases^{91,92}. From the DPPH assay shown in **Table 4**, we observed that introducing any sugar moieties in 9" position did not led to a significant reduction of quenching properties. For comparison purposes, the antioxidant activities of 2,3-dihydrosilybin and quercetin were evaluated as controls. In particular the new silibinin derivatives (**6–9**) showed DPPH radical scavenging activities similar to that of the silibinin **1**, confirming that the introduction in 9" of the sugar moiety did not influence the radical scavenging activity of this metabolite^{69,93}. In basal conditions, the pre-incubation of MKN28 cells with **6–9** and silibinin lead to two different results (**Table 4**). In fact, **6–9** analogues don't affect cell viability, while Silibinin induced a cell death of about 50%, also at the lower dose used. The evaluation of cell viability in MKN28 cultured cells after incubation with **6–9** and silibinin, and the subsequent induction of oxidative stress, have shown that these molecules protect from cell death under oxidative stress, at least as the silibinin.

5.5.3.1 Experimental Session

General procedure for the synthesis of conjugates (6–9): phosphoramidite **1** (150 mg, 0.18 mmol) and the select saccharide compound **2 - 5** (0.19 mmol, previously dried and kept under reduced pressure, were reacted with a 0.45 M tetrazole solution in anhydrous CH₃CN (1.0 mL, 0.45 mmol). The reaction was left under stirring at room temperature and monitored by TLC in the eluent system 1:2 *n*-hexane:AcOEt, (v:v). After 1h, a 5.5 M *tert*-butyl hydroperoxide (*tert*-BuOOH) solution in decane (70 μ L, 0.40 mmol) was added to the mixture and left under stirring at room temperature. After 30 minutes the reaction mixture was diluted with CHCl₃, transferred into a separatory funnel, washed three times with water and dried

under reduced pressure. The next treatment with TEA/pyridine (1:1, v/v) to 1 h at 50°C and then with aq. ammonia (28%)/CH₃OH (1:1, v:v) for 1 h at room temperature, allowed full deprotection from acetyl and 2-cyanoethyl groups. The dried mixtures were purified by a Sep-Pak C18 Cartridge and then converted into the corresponding sodium salts by cation exchange on a DOWEX (Na⁺ form) resin to have a homogeneous samples in good yield (60-72%).

Compound 6 (brown powder, 88.1 mg, 68%): ³¹P NMR (161.98 MHz, D₂O, room temperature, mixture of diastereoisomers) δ 2.9, 1.4, 0.8. HRMS (MALDI-TOF, negative ions) m/z calcd for C₃₁H₃₂O₁₈P = 723.1332, found 723.1332 [M – H]⁻.

Compound 7 (brown powder, 94.0 mg, 72%): ³¹P NMR (161.98 MHz, D₂O, room temperature, mixture of diastereoisomers) δ 1.3, 0.9, 0.7. HRMS (MALDI-TOF, negative ions) m/z calcd for C₃₁H₃₂O₁₈P = 723.1332, found 723.1333 [M – H]⁻.

Compound 8 (brown powder, 82.3 mg, 63%): ³¹P NMR (161.98 MHz, D₂O, room temperature, mixture of diastereoisomers) δ 2.4, 1.6, 1.1, 0.8. HRMS (MALDI-TOF, negative ions) m/z calcd for C₃₁H₃₂O₁₈P = 723.1332, found 723.1333 [M – H]⁻.

Compound 9 (brown powder, 104.8 mg, 60%): ³¹P NMR (161.98 MHz, D₂O, room temperature, mixture of diastereoisomers) δ 1.1, 0.8. HRMS (MALDI-TOF, negative ions) m/z calcd for C₃₇H₄₂O₂₃P = 885.1860, found 885.1859 [M – H]⁻.

DPPH radical scavenging activity assay. The antioxidant activities of the compounds was assessed by examining their abilities to scavenge the 1,1-diphenyl-2-picrylhydrazyl (DPPH) free radical. DPPH solution (20 mg/mL) was prepared in methanol. The compounds was dissolved in methanol to prepare the stock solution (1 mM). Freshly prepared DPPH solution was taken in test tubes and analogue solutions (1

mM–1 μ M) were added to every test tube so that the final volume was 2.25 mL and after 10 min, the absorbance was read at 515 nm. Quercetin and 2,3-dehydrosilybin were used as a reference standards and dissolved in methanol to make the stock solution with the same concentration (1 mM).

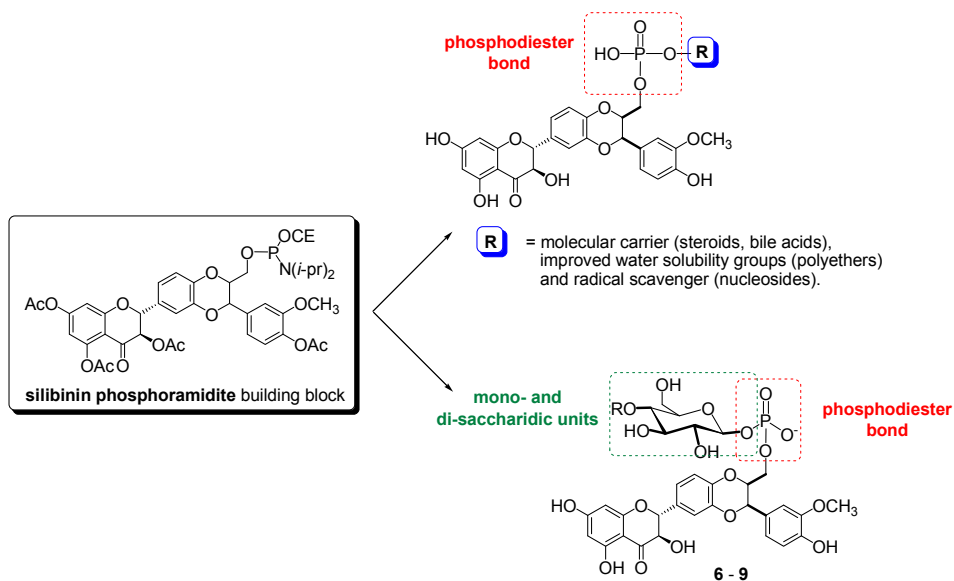
Xanthine Oxidase Inhibition Assay. Oxidative stress was induced by incubating MKN28 cells with XO (10-100 mU/mL) in the presence of its substrate xanthine (X) (1 mM) for periods of up to 3 h. We examined the effect of Silibinin and of our analogues (**6–9**) on X – XO induced cell damage. In particular, cells were incubated with serum free medium (control) for 1 - 48 h; with serum free medium for 1–48 h and then with X (1 mM) – XO (50 mM) for 2 h (X – XO control); with **6–9** and silibinin (10 – 200 μ M) for 1–48 h and then, after washing, with X (1 mM) – XO (50 mM) for 2 h. Subsequently, we determined cell viability by [3-(4,5-dimethylthiazol-2-yl)-2,5-diphenyl tetrazoliumbromide] MTT assay in MKN28 cultured cells.

5.5.4 General Conclusions

In conclusion in order to enhance water solubility and bioavailability of silibinin, we developed efficient protocols for the synthesis of new 9"-silibinin derivatives conjugated to a broad array of groups. Firstly, we generated a series of new and more polar analogues of silybin, useful models for chemical diversification (sulfate, phosphodiester, NH₂, and N₃ functional group) (Paragraph 5.5.1, **Scheme 3**). The antioxidant activities of these analogues were evaluated using the DPPH assay. The results revealed that the amino-derivatives of silybin A and B (**5A** and **5B**) are much more active than other derivatives and both sulfate derivatives (**3A** and **3B**)

exhibit significant improvement of antioxidant activity compared to that of silibinin and BHA (**Table 3**).

Subsequently, in the preceding paragraphs 5.5.2 and 5.5.3, it has been reported a simpler synthetic strategy that leads to a key building block of silibinin (**Scheme 6**), useful for a variety of modifications following a reliable and well-known phosphoramidite chemistry. Basically we synthesized new 9''-phosphodiester silibinin derivatives conjugating at the key intermediate, molecular carrier (steroids, bile acids), improved water solubility groups (polyethers), radical scavenger (nucleosides), and polar molecules as saccharides (**Scheme 6**).



Scheme 6. Graphical abstract of 9''-phosphodiester silibinin analogues starting from a phosphoramidite building block.

The antioxidant activity of new silibinin glyco-conjugates was evaluated by DDPH and Xanthine oxidase (XO) inhibition model

assays. DPPH assays showed that the scavenging activities of silibinin glyco-conjugates (6–9) were similar to that of the silibinin confirming that the introduction of the sugar moiety in 9"position, had little effect on radical scavenging activity of this metabolite.

From Xanthine oxidase (XO) assays in basal conditions, the pre-incubation of MKN28 cells with silibinin and its glyco-analogues, showed that silibinin induce a cell death of about 50% also at the lower dose used, in contrast with the analogues that have not affect on the cell viability. Indeed, from the evaluation of cell viability in MKN28 cultured cells after the induction of oxidative stress, it results that these glyco-conjugates (6–9), protect from cell death after induction of oxidative stress, at least as silibinin. Moreover the glyco-conjugates showed a water solubility well above that of silibinin, in fact it was possible to prepare solutions of about 70 mg/mL of analogues in water. These data encourage our future studies that are aimed to improve this synthetic strategy to realize libraries of optically pure glyco-conjugated silibinin and 2,3-dehydroxylibin derivatives.

References

- (1) Lea Spindler, W. F. (2012) Guanine Quartets (Spindler, L., and Fritzsche, W., Eds.). Royal Society of Chemistry, Cambridge.
- (2) Phan, A. T. (2010) Human telomeric G-quadruplex: structures of DNA and RNA sequences. *The FEBS journal* 277, 1107–17.
- (3) Petraccone, L., Malafronte, A., Amato, J., and Giancola, C. (2012) G-quadruplexes from human telomeric DNA: How many conformations in PEG containing solutions? *Journal of Physical Chemistry B*.
- (4) Xu, Y., and Komiyama, M. (2012) Structure, function and targeting of human telomere RNA. *Methods (San Diego, Calif.)* 57, 100–5.
- (5) Siddiqui-Jain, A., Grand, C. L., Bearss, D. J., and Hurley, L. H. (2002) Direct evidence for a G-quadruplex in a promoter region and its targeting with a small molecule to repress c-MYC transcription. *Proceedings of the National Academy of Sciences of the United States of America* 99, 11593–8.
- (6) Dai, J., Dexheimer, T. S., Chen, D., Carver, M., Ambrus, A., Jones, R. A., and Yang, D. (2006) An intramolecular G-quadruplex structure with mixed parallel/antiparallel G-strands formed in the human BCL-2 promoter region in solution. *Journal of the American Chemical Society* 128, 1096–8.
- (7) Sun, D., Guo, K., and Shin, Y.-J. (2011) Evidence of the formation of G-quadruplex structures in the promoter region of the human vascular endothelial growth factor gene. *Nucleic acids research* 39, 1256–65.
- (8) Cogoi, S., Paramasivam, M., Membrino, A., Yokoyama, K. K., and Xodo, L. E. (2010) The KRAS Promoter Responds to Myc-associated Zinc Finger and Poly(ADP-ribose) Polymerase 1 Proteins, Which Recognize a Critical Quadruplex-forming GA-element. *Journal of Biological Chemistry* 285, 22003–22016.
- (9) Phan, A. T., Kuryavyi, V., Burge, S., Neidle, S., and Patel, D. J. (2007) Structure of an unprecedented G-quadruplex scaffold in the human c-kit promoter. *Journal of the American Chemical Society* 129, 4386–4392.
- (10) Kuryavyi, V., Phan, A. T., and Patel, D. J. (2010) Solution structures of all parallel-stranded monomeric and dimeric G-quadruplex scaffolds of the human c-kit2 promoter. *Nucleic Acids Research* 38, 6757–6773.
- (11) Neidle, S. (2010) Human telomeric G-quadruplex: the current status of telomeric G-quadruplexes as therapeutic targets in human cancer. *The FEBS journal* 277, 1118–25.
- (12) Tong, X., Lan, W., Zhang, X., Wu, H., Liu, M., and Cao, C. (2011) Solution structure of all parallel G-quadruplex formed by the oncogene RET promoter sequence. *Nucleic acids research* 39, 6753–63.

- (13) De Cian, A., Lacroix, L., Douarre, C., Temime-Smaali, N., Trentesaux, C., Riou, J.-F., and Mergny, J.-L. (2008) Targeting telomeres and telomerase. *Biochimie* 90, 131–55.
- (14) Murat, P., Singh, Y., and Defrancq, E. (2011) Methods for investigating G-quadruplex DNA/ligand interactions. *Chemical Society reviews* 40, 5293–307.
- (15) Sun, D., Thompson, B., Cathers, B. E., Salazar, M., Kerwin, S. M., Trent, J. O., Jenkins, T. C., Neidle, S., and Hurley, L. H. (1997) Inhibition of Human Telomerase by a G-Quadruplex-Interactive Compound. *Journal of Medicinal Chemistry* 40, 2113–2116.
- (16) Read, M., Harrison, R. J., Romagnoli, B., Taniou, F. A., Gowan, S. H., Reszka, A. P., Wilson, W. D., Kelland, L. R., and Neidle, S. (2001) Structure-based design of selective and potent G quadruplex-mediated telomerase inhibitors. *Proceedings of the National Academy of Sciences of the United States of America* 98, 4844–9.
- (17) Harrison, R. J., Cuesta, J., Chessari, G., Read, M. a, Sanji, K., Reszka, A. P., Morrell, J., Gowan, S. M., Christopher, M., Taniou, F. a, Wilson, W. D., Kelland, L. R., and Neidle, S. (2003) Trisubstituted Acridine Derivatives as Potent and Selective Telomerase Inhibitors Trisubstituted Acridine Derivatives as Potent and Selective Telomerase. *Journal of Medicinal Chemistry* 4463–4476.
- (18) Seenisamy, J., Bashyam, S., Gokhale, V., Vankayalapati, H., Sun, D., Siddiqui-Jain, A., Streiner, N., Shin-Ya, K., White, E., Wilson, W. D., and Hurley, L. H. (2005) Design and synthesis of an expanded porphyrin that has selectivity for the c-MYC G-quadruplex structure. *Journal of the American Chemical Society* 127, 2944–59.
- (19) Riou, J. F., Guittat, L., Mailliet, P., Laoui, A., Renou, E., Petitgenet, O., Megnin-Chanet, F., Helene, C., and Mergny, J. L. (2002) Cell senescence and telomere shortening induced by a new series of specific G-quadruplex DNA ligands. *Proceedings of the National Academy of Sciences* 99, 2672–2677.
- (20) Gowan, S. M., Harrison, J. R., Patterson, L., Valenti, M., Read, M. A., Neidle, S., and Kelland, L. R. (2002) A G-Quadruplex-Interactive Potent Small-Molecule Inhibitor of Telomerase Exhibiting in Vitro and in Vivo Antitumor Activity. *molecular pharmacology* 61, 1154–1162.
- (21) Naasani, I., Seimiya, H., Yamori, T., and Tsuruo, T. (1999) FJ5002: A potent telomerase inhibitor identified by exploiting the disease-oriented screening program with COMPARE analysis. *Cancer Research* 59, 4004–4011.
- (22) Kim, M. Y., Vankayalapati, H., Shin-Ya, K., Wierzba, K., and Hurley, L. H. (2002) Telomestatin, a potent telomerase inhibitor that interacts quite specifically with the human telomeric intramolecular G-quadruplex. *Journal of the American Chemical Society* 124, 2098–2099.
- (23) Menichincheri, M., Ballinari, D., Bargiotti, A., Bonomini, L., Ceccarelli, W., D'Alessio, R., Fretta, A., Moll, J., Polucci, P., Soncini, C., Tibolla, M., Trosset, J. Y.,

and Vanotti, E. (2004) Catecholic flavonoids acting as telomerase inhibitors. *Journal of Medicinal Chemistry* 47, 6466–6475.

(24) Chen, J. L.-Y., Sperry, J., Ip, N. Y., and Brimble, M. a. (2011) Natural products targeting telomere maintenance. *Medicinal Chemistry Communications* 2, 229.

(25) Liu, X.-H., Liu, H.-F., Shen, X., Song, B.-A., Bhadury, P. S., Zhu, H.-L., Liu, J.-X., and Qi, X.-B. (2010) Synthesis and molecular docking studies of novel 2-chloropyridine derivatives containing flavone moieties as potential antitumor agents. *Bioorganic & medicinal chemistry letters* 20, 4163–4167.

(26) Mulholland, P. J., Ferry, D. R., Anderson, D., Hussain, S. A., Young, A. M., Cook, J. E., Hodgkin, E., Seymour, L. W., and Kerr, D. J. (2001) Pre-clinical and clinical study of QC12, a water-soluble, pro-drug of quercetin. *Ann. Onc.* 12, 245–248.

(27) Calias, P., Galanopoulos, T., Maxwell, M., Khayat, A., Graves, D., Antoniadis, H. N., and D'Alarcao, M. (1996) Synthesis of inositol 2-phosphate-quercetin conjugates. *Carbohydrate research* 292, 83–90.

(28) Thelen, P., Wuttke, W., Jarry, H., Grzmil, M., and Ringert, R.-H. (2004) Inhibition of telomerase activity and secretion of prostate specific antigen by silibinin in prostate cancer cells. *The Journal of urology* 171, 1934–1938.

(29) Pelter, A., and Hänsel, R. (1968) The structure of silybin (silybum substance E6), the first flavonolignan. *Tetrahedron Letters* 9, 2911–2916.

(30) Biedermann, D., Vavříková, E., Cvak, L., and Křen, V. (2014) Chemistry of silybin. *Natural product reports* 31, 1138–57.

(31) Lee, D. Y.-W., and Liu, Y. (2003) Molecular structure and stereochemistry of silybin A, silybin B, isosilybin A, and isosilybin B, Isolated from *Silybum marianum* (milk thistle). *Journal of natural products* 66, 1171–4.

(32) Theodosiou, E., Purchartová, K., Stamatidis, H., Kolisis, F., and Křen, V. (2013) Bioavailability of silymarin flavonolignans: Drug formulations and biotransformation. *Phytochemistry Reviews* 13, 1–18.

(33) Gazak, R., Walterova, D., and Kren, V. (2007, January) Silybin and Silymarin - New and Emerging Applications in Medicine. *Current Medicinal Chemistry*.

(34) Barzaghi, N., Crema, F., Gatti, G., Pifferi, G., and Perucca, E. (1990) Pharmacokinetic studies on IdB 1016, a silybin-phosphatidylcholine complex, in healthy human subjects. *European Journal of Drug Metabolism and Pharmacokinetics* 15, 333–338.

(35) Agarwal, C., Wadhwa, R., Deep, G., Biedermann, D., Gažák, R., Křen, V., and Agarwal, R. (2013) Anti-Cancer Efficacy of Silybin Derivatives - A Structure-Activity Relationship. *PLoS ONE* 8, e60074.

- (36) Loguercio, C., and Festi, D. (2011) Silybin and the liver: from basic research to clinical practice. *World journal of gastroenterology* 17, 2288–2301.
- (37) Marrazzo, G., Bosco, P., La Delia, F., Scapagnini, G., Di Giacomo, C., Malaguarnera, M., Galvano, F., Nicolosi, A., and Li Volti, G. (2011) Neuroprotective effect of silibinin in diabetic mice. *Neuroscience Letters* 504, 252–256.
- (38) Payer, B. A., Reiberger, T., Rutter, K., Beinhardt, S., Staettermayer, A. F., Peck-Radosavljevic, M., and Ferenci, P. (2010) Successful HCV eradication and inhibition of HIV replication by intravenous silibinin in an HIV-HCV coinfecting patient. *Journal of clinical virology* 49, 131–3.
- (39) Deep, G., and Agarwal, R. (2010) Antimetastatic efficacy of silibinin: molecular mechanisms and therapeutic potential against cancer. *Cancer metastasis reviews* 29, 447–63.
- (40) Huber, A., Thongphasuk, P., Erben, G., Lehmann, W. D., Tuma, S., Stremmel, W., and Chamulitrat, W. (2008) Significantly greater antioxidant anticancer activities of 2,3-dehydrosilybin than silybin. *Biochimica et Biophysica Acta* 1780, 837–847.
- (41) Zhan, T., Digel, M., KÜch, E.-M., Stremmel, W., and Füllekrug, J. (2011) Silybin and dehydrosilybin decrease glucose uptake by inhibiting GLUT proteins. *Journal of cellular biochemistry* 112, 849–59.
- (42) Plíšková, M., Vondráček, J., Křen, V., Gažák, R., Sedmera, P., Walterová, D., Psotová, J., Šimánek, V., and Machala, M. (2005) Effects of silymarin flavonolignans and synthetic silybin derivatives on estrogen and aryl hydrocarbon receptor activation. *Toxicology* 215, 80–89.
- (43) Monti, D., Gažák, R., Marhol, P., Biedermann, D., Purchartová, K., Fedrigo, M., Riva, S., and Křen, V. (2010) Enzymatic kinetic resolution of silybin diastereoisomers. *Journal of Natural Products* 73, 613–619.
- (44) Di Fabio, G., Romanucci, V., Di Marino, C., De Napoli, L., and Zarrelli, A. (2013) A rapid and simple chromatographic separation of diastereomers of silibinin and their oxidation to produce 2,3-dehydrosilybin enantiomers in an optically pure form. *Planta medica* 79, 1077–80.
- (45) Di Fabio, G., Romanucci, V., De Nisco, M., Pedatella, S., Di Marino, C., and Zarrelli, A. (2013) Microwave-assisted oxidation of silibinin: A simple and preparative method for the synthesis of improved radical scavengers. *Tetrahedron Letters* 54, 6279–6282.
- (46) Kroll, D. J., Shaw, H. S., and Oberlies, N. H. (2007) Milk thistle nomenclature: why it matters in cancer research and pharmacokinetic studies. *Integrative cancer therapies* 6, 110–119.

- (47) Zarrelli, A., Romanucci, V., Greca, M. Della, De Napoli, L., Previtiera, L., and Di Fabio, G. (2013) New silybin scaffold for chemical diversification: Synthesis of novel 23-phosphodiester silybin conjugates. *Synlett* 24, 45–48.
- (48) Zarrelli, A., Romanucci, V., Tuccillo, C., Federico, A., Loguercio, C., Gravante, R., and Di Fabio, G. (2014) New silibinin glyco-conjugates: Synthesis and evaluation of antioxidant properties. *Bioorganic & Medicinal Chemistry Letters* 24, 5147–5149.
- (49) Zarrelli, A., Romanucci, V., De Napoli, L., Previtiera, L., and Di Fabio, G. (2015) Synthesis of New Silybin Derivatives and Evaluation of Their Antioxidant Properties. *Helvetica Chimica Acta* 98, 399–409.
- (50) Graf, T. N., Wani, M. C., Agarwal, R., Kroll, D. J., and Oberlies, N. H. (2007) Gram-Scale Purification of Flavonolignan Diastereoisomers from *Silybum marianum* (Milk Thistle) Extract in Support of Preclinical in vivo Studies for Prostate Cancer Chemoprevention. *Planta Medica* 73, 1495–1501.
- (51) Li, W., Han, J., Li, Z., Li, X., Zhou, S., and Liu, C. (2008) Preparative chromatographic purification of diastereomers of silybin and their quantification in human plasma by liquid chromatography–tandem mass spectrometry. *Journal of Chromatography B* 862, 51–57.
- (52) Křen, V., Kubisch, J., Sedmera, P., Halada, P., Přikrylová, V., Jegorov, A., Cvak, L., Gebhardt, R., Ulrichová, J., and Šimánek, V. (1997) Glycosylation of silybin. *Journal of the Chemical Society, Perkin Transactions 1* 2467–2474.
- (53) Gažák, R., Marhol, P., Purchartová, K., Monti, D., Biedermann, D., Riva, S., Cvak, L., and Křen, V. (2010) Large-scale separation of silybin diastereoisomers using lipases. *Process Biochemistry* 45, 1657–1663.
- (54) Zarrelli, A., Sgambato, A., Petito, V., De Napoli, L., Previtiera, L., and Di Fabio, G. (2011) New C-23 modified of silybin and 2,3-dehydrosilybin: Synthesis and preliminary evaluation of antioxidant properties. *Bioorganic and Medicinal Chemistry Letters* 21, 4389–4392.
- (55) Kim, N.-C., Graf, T. N., Sparacino, C. M., Wani, M. C., and Wall, M. E. (2003) Complete isolation and characterization of silybins and isosilybins from milk thistle (*Silybum marianum*). *Organic & biomolecular chemistry* 1, 1684–1689.
- (56) Napolitano, J. G., Lankin, D. C., Graf, T. N., Brent Friesen, J., Chen, S. N., McAlpine, J. B., Oberlies, N. H., and Pauli, G. F. (2013) HiFSA fingerprinting applied to isomers with near-identical NMR Spectra: The silybin/isosilybin case. *Journal of Organic Chemistry* 78, 2827–2839.
- (57) Gažák, R., Svobodová, A., Psotová, J., Sedmera, P., Přikrylová, V., Walterová, D., and Křen, V. (2004) Oxidised derivatives of silybin and their antiradical and antioxidant activity. *Bioorganic and Medicinal Chemistry* 12, 5677–5687.

- (58) Dvorák, Z., Vrzal, R., and Ulrichová, J. (2006) Silybin and dehydrosilybin inhibit cytochrome P450 1A1 catalytic activity: a study in human keratinocytes and human hepatoma cells. *Cell biology and toxicology* 22, 81–90.
- (59) Halbach, G., and Trost, W. (1974) Chemistry and pharmacology of silymarin. Studies on various metabolites of silybin. *Arzneimittel-Forschung* 24, 866–867.
- (60) Gažák, R., Trouillas, P., Biedermann, D., Fuksová, K., Marhol, P., Kuzma, M., and Křen, V. (2013) Base-catalyzed oxidation of silybin and isosilybin into 2,3-dehydro derivatives. *Tetrahedron Letters* 54, 315–317.
- (61) Oliver Kappe, C. (2008) Microwave dielectric heating in synthetic organic chemistry. *Chemical Society reviews* 37, 1127–39.
- (62) Wen, Z., Dumas, T. E., Schrieber, S. J., Hawke, R. L., Fried, M. W., and Smith, P. C. (2008) Pharmacokinetics and metabolic profile of free, conjugated, and total silymarin flavonolignans in human plasma after oral administration of milk thistle extract. *Drug Metabolism and Disposition* 36, 65–72.
- (63) Ajazuddin, and Saraf, S. (2010) Applications of novel drug delivery system for herbal formulations. *Fitoterapia*.
- (64) Kosina, P., Kren, V., Gebhardt, R., Grambal, F., Ulrichová, J., and Walterová, D. (2002) Antioxidant properties of silybin glycosides. *Phytotherapy research* □: PTR 16 Suppl 1, S33–S39.
- (65) Maitrejean, M., Comte, G., Barron, D., El Kirat, K., Conseil, G., and Di Pietro, a. (2000) The flavanolignan silybin and its hemisynthetic derivatives, a novel series of potential modulators of P-glycoprotein. *Bioorganic & medicinal chemistry letters* 10, 157–160.
- (66) Wang, F., Huang, K., Yang, L., Gong, J., Tao, Q., Li, H., Zhao, Y., Zeng, S., Wu, X., Stöckigt, J., Li, X., and Qu, J. (2009) Preparation of C-23 esterified silybin derivatives and evaluation of their lipid peroxidation inhibitory and DNA protective properties. *Bioorganic and Medicinal Chemistry* 17, 6380–6389.
- (67) Gažák, R., Valentová, K., Fuksová, K., Marhol, P., Kuzma, M., Medina, M. Á., Oborná, I., Ulrichová, J., and Křen, V. (2011) Synthesis and antiangiogenic activity of new silybin galloyl esters. *Journal of Medicinal Chemistry* 54, 7397–7407.
- (68) Shukla, R. K., and Tiwari, A. (2011) Carbohydrate molecules: an expanding horizon in drug delivery and biomedicine. *Critical reviews in therapeutic drug carrier systems* 28, 255–292.
- (69) Gažák, R., Sedmera, P., Vrbacký, M., Vostálová, J., Drahota, Z., Marhol, P., Walterová, D., and Křen, V. (2009) Molecular mechanisms of silybin and 2,3-dehydrosilybin antiradical activity-role of individual hydroxyl groups. *Free Radical Biology and Medicine* 46, 745–758.

- (70) Brand-Williams, W., Cuvelier, M. E., and Berset, C. (1995) Use of a free radical method to evaluate antioxidant activity. *LWT - Food Science and Technology* 28, 25–30.
- (71) Alma, M. H., Mavi, A., Yildirim, A., Digrak, M., and Hirata, T. (2003) Screening chemical composition and in vitro antioxidant and antimicrobial activities of the essential oils from *Origanum syriacum* L. growing in Turkey. *Biological & pharmaceutical bulletin* 26, 1725–1729.
- (72) Foti, M. C., Sortino, S., and Ingold, K. U. (2005) New insight into solvent effects on the formal HOO. + HOO. reaction. *Chemistry (Weinheim an der Bergstrasse, Germany)* 11, 1942–8.
- (73) Ho, K. Y., Tsai, C. C., Chen, C. P., Huang, J. S., and Lin, C. C. (2001) Screening of Brazilian plant extracts for antioxidant activity by the use of DPPH free radical method. *Phytotherapy Research* 15, 127–130.
- (74) Swaan, P. W., Hillgren, K. M., Szoka, F. C., and Oie, S. (1997) Enhanced transepithelial transport of peptides by conjugation to cholic acid. *Bioconjugate chemistry* 8, 520–5.
- (75) Janout, V., Giorgio, C. Di, and Regen, S. L. (2000) Molecular Umbrella-Assisted Transport of a Hydrophilic Peptide Across a Phospholipid Membrane. *Journal of the American Chemical Society* 122, 2671–2672.
- (76) Kachur, A. V., Manevich, Y., and Biaglow, J. E. (1997) Effect of purine nucleoside phosphates on OH-radical generation by reaction of Fe²⁺ with oxygen. *Free radical research* 26, 399–408.
- (77) Richter, Y., and Fischer, B. (2006) Nucleotides and inorganic phosphates as potential antioxidants. *Journal of biological inorganic chemistry* 11, 1063–74.
- (78) Banerjee, S. S., Aher, N., Patil, R., and Khandare, J. (2012) Poly(ethylene glycol)-Prodrug Conjugates: Concept, Design, and Applications. *Journal of drug delivery* 2012, 103973.
- (79) Giorgi, M. E., Agusti, R., and de Lederkremer, R. M. (2014) Carbohydrate PEGylation, an approach to improve pharmacological potency. *Beilstein journal of organic chemistry* 10, 1433–44.
- (80) Ettmayer, P., Amidon, G. L., Clement, B., and Testa, B. (2004) Lessons Learned from Marketed and Investigational Prodrugs. *Journal of Medicinal Chemistry* 47, 2393–2404.
- (81) Venkatesan, N., Kim, S. J., and Kim, B. H. (2003) Novel phosphoramidite building blocks in synthesis and applications toward modified oligonucleotides. *Current medicinal chemistry* 10, 1973–1991.
- (82) Maier, M. a, Yannopoulos, C. G., Mohamed, N., Roland, A., Fritz, H., Mohan, V., Just, G., and Manoharan, M. (2003) Synthesis of antisense oligonucleotides

conjugated to a multivalent carbohydrate cluster for cellular targeting. *Bioconjugate chemistry* 14, 18–29.

(83) Wolf, S., Zismann, T., Lunau, N., and Meier, C. (2009) Reliable synthesis of various nucleoside diphosphate glycopyranoses. *Chemistry - A European Journal* 15, 7656–7664.

(84) Chang, Q., Zuo, Z., Chow, M. S. S., and Ho, W. K. K. (2005) Difference in absorption of the two structurally similar flavonoid glycosides, hyperoside and isoquercitrin, in rats. *European Journal of Pharmaceutics and Biopharmaceutics* 59, 549–555.

(85) Hirpara, K. V., Aggarwal, P., Mukherjee, A. J., Joshi, N., and Burman, A. C. (2009) Quercetin and its derivatives: synthesis, pharmacological uses with special emphasis on anti-tumor properties and prodrug with enhanced bio-availability. *Anti-cancer agents in medicinal chemistry* 9, 138–161.

(86) Morishita, M., and Park, K. (2009) Biodrug Delivery Systems: Fundamentals, Applications and Clinical Development, p 488. CRC Press.

(87) Cai, T. B., Lu, D., Tang, X., Zhang, Y., Landerholm, M., and Wang, P. G. (2005) New glycosidase activated nitric oxide donors: glucose and 3-morphorlinosydnonimine conjugates. *The Journal of organic chemistry* 70, 3518–24.

(88) Majumdar, D., Elsayed, G. A., Buskas, T., and Boons, G.-J. (2005) Synthesis of proteophosphoglycans of Leishmania major and Leishmania mexicana. *The Journal of organic chemistry* 70, 1691–7.

(89) Yang, L., Gong, J., Wang, F., Zhang, Y., Wang, Y., Hao, X., Wu, X., Bai, H., Stöckigt, J., and Zhao, Y. (2006) Synthesis and antioxidant evaluation of novel silybin analogues. *Journal of enzyme inhibition and medicinal chemistry* 21, 399–404.

(90) Beetsch, J. W., Park, T. S., Dugan, L. L., Shah, A. R., and Gidday, J. M. (1998) Xanthine oxidase-derived superoxide causes reoxygenation injury of ischemic cerebral endothelial cells. *Brain Research* 786, 89–95.

(91) Abramov, A. Y., Scorziello, A., and Duchen, M. R. (2007) Three distinct mechanisms generate oxygen free radicals in neurons and contribute to cell death during anoxia and reoxygenation. *The Journal of neuroscience* □: the official journal of the Society for Neuroscience 27, 1129–1138.

(92) Qin, C. X., Chen, X., Hughes, R. A., Williams, S. J., and Woodman, O. L. (2008) Understanding the cardioprotective effects of flavonols: discovery of relaxant flavonols without antioxidant activity. *Journal of medicinal chemistry* 51, 1874–84.

(93) Trouillas, P., Marsal, P., Svobodová, A., Vostálová, J., Gazák, R., Hrbác, J., Sedmera, P., Kren, V., Lazzaroni, R., Duroux, J.-L., and Walterová, D. (2008) Mechanism of the antioxidant action of silybin and 2,3-dehydrosilybin flavonolignans: a joint experimental and theoretical study. *The journal of physical chemistry. A* 112, 1054–1063.

Abbreviations

Ac: acetyl

Ac₂O: acetic anhydride

AcK: potassium acetate

AcOEt: ethyl acetate

AcOH: acetic acid

BHA: hydroxyl anisole

CCS: Collision Cross Section

CD: Circular Dicroism

AcCN: acetonitrile

CPG: Controlled Pore Glass

DBB: 3,4-dibenzyloxybenzyl

DCA: dichloroacetic acid

DCCI: N,N-dicyclohesylcarbodiimide

DCM: dichloromethane

DEAD: diethyl azodicarboxylate

DHS: 2,3-dehydrosilybin

DIEA: N,N-diisopropylethylamine

DMAP: 4-(dimethylamino)pyridine

DMF: N,N-dimethylformamide

DMSO: dimethylsulfoxide

DMT: 4,4-dimethoxy-triphenylmethyl

DPPA: diphenylphosphorylazide

DPPH: 2,2-diphenyl-1-picrylhydrazyl

DSC: Differential Scanning Calorimetry

EDTA: Ethylenediaminetetraacetic acid

ESI-MS: Electrospray Ionization Mass Spectrometry

Et₂O: ethyl etere

EtOH: ethanol
G4: G-quadruplex
HEG: hexaethylene glycol
HOBT: N-hydroxybenzotriazole
HPLC: High Performance Liquid Chromatography
HSA: Human Serum Albumin
IN: integrase
IMS: Ion Mobility Spectrometry
LC-MS: Liquid Chromatography-Mass Spectrometry
MALDI-TOF: Matrix Assisted Laser Desorption Ionization-Time of Flight
MeOH: methanol
MW: microwave
MSNT: 1-(2-mesitylsulfonyl)-3-nitro-1,2,4-triazole
NMI: N-methyl-imidazole
NMR: Nuclear Magnetic Resonance
ODNs: oligodeoxynucleotides
PAGE: PolyAcrylamide Gel Electrophoresis
Py: pyridine
RT: Reverse Transcriptase
RP-HPLC: Reverse Phase HPLC
RU: Response Unit
SELEX: systematic evolution of ligands by exponential enrichment
SPR: Surface Plasmon Resonance
TBDMS: *tert*-butyldimethylsilyl
TEA: triethylamine
TFA: trifluoroacetic acid
TG: tentagel
THF: tetrahydrofuran

TLC: Thin Layer Chromatography

T_m: Thermal Melting

TMAA: trimethylammonium acetate

TsCl: p-toluenesulfonyl chloride

XO: Xanthine Oxidase

